Enhancing the Performance of a Coagulometer through Optimization of Microfluidic Cartridge and Fiber Optic-Based Optomechanical Systems

by

Merve Kortel

A Dissertation Submitted to the
Graduate School of Sciences and Engineering
in Partial Fulfillment of the Requirements for
the Degree of

Master of Science

in

Biomedical Sciences and Engineering

February 5, 2024

Enhancing the Performance of a Coagulometer Through Optimization of Microfluidic Cartridge and Fiber Optic-Based Optomechanical Systems

Koç University

Graduate School of Sciences and Engineering

This is to certify that I have examined this copy of a master's thesis by

Merve Kortel

and have found that it is complete and satisfactory in all respects,

and that any and all revisions required by the final

examining committee have been made.

Committee Members:

Prof. Hakan Ürey

Prof. Özlem Yalçın

Assoc. Prof. Onur Ferhanoğlu

Date: 05.02.2024

ABSTRACT

Enhancing the Performance of a Coagulometer through Optimization of Microfluidic Cartridge and Fiber Optic-Based Optomechanical Systems

Master of Science in Biomedical Sciences and Engineering

February, 2024

More than 800 million clotting tests are performed each year in hospitals and clinical laboratories for emergencies, surgical operations, and periodic monitoring of patients. Monitoring of adequate anticoagulant dosage is essential to maintain the delicate balance between bleeding and thrombosis. The primary means of monitoring the response to warfarin (VKAs) is the Prothrombin Time (PT) test and the international normalized ratio (INR) while activated partial thrombosplastin time (aPTT) is used for heparin monitoring. Current clinical laboratory tests used to routinely measure blood coagulation still lack in rapidity and simplicity.

Whole-blood Point-of-Care (PoC) coagulation devices that respond to the exact needs of both clinicians and patients are still emerging in the field. Portable PoC and self-care PT/INR monitoring devices are gaining in popularity as they provide crucial advantages over traditional laboratory methods such as ease of use, instant results, rapid turnaround for timely anticoagulant dose adjustment and improved patient convenience by removing the need for routine hospital/laboratory visits and venipunctures. Moreover, PoC devices are using whole capillary blood usually from a finger prick while conventional laboratory methods utilize centrifuged plasma obtained from citrated venous blood.

This thesis presents several optimization activities that was performed on the disposable cartridge unit of an opto-mechanical-based Point-of-care and Self-care coagulometer. This study demonstrates several design optimization and validation activities undertaken during the product development stage in order to move the initial cartridge design into a commercializable product. Thus, this work focused of increasing the manufacturability and usability of the previous cartridge design developed by our group in terms of passive capillary flow/Microfluidics, biochemical functionalization, optical fiber assembly, and reagent optimization. Furthermore, the final cartridge design was used to conduct a proof-of-concept study in the topic of heparin monitoring and aPTT measurement on control plasma and blood samples, suggesting a reliable and rapid testing as a PoC device. A preclinical trial was conducted with an n=42 sample size to assess the correlation between our device and the standard hospital method, further validating its efficacy and potential for clinical use.

ÖZETÇE

Enhancing the Performance of a Coagulometer through Optimization of Microfluidic Cartridge and Fiber Optic-Based Optomechanical Systems

Biyomedikal Bilimleri ve Mühendisliği,

Yüksek Lisans

Şubat 2024

Hastanelerde ve klinik laboratuvarlarda her yıl 800 milyondan fazla pıhtılaşma testi, acil durumlar, cerrahi operasyonlar ve hastaların periyodik takibi amacıyla yapılır. Kanama ve tromboz arasındaki hassas dengeyi korumak için yeterli antikoagülan dozajının izlenmesi esastır. Varfarine verilen yanıtı (VKA'lar) izlemenin birincil yolu Protrombin Zamanı (PT) testi ve uluslararası normalleştirilmiş orandır (INR); heparin izleme için ise aktive edilmiş kısmi tromboplastin zamanı (aPTT) kullanılır. Kan pıhtılaşmasını rutin olarak ölçmek için kullanılan mevcut klinik laboratuvar testleri hâlâ hız ve basitlik açısından yetersizdir.

Hem klinisyenlerin hem de hastaların ihtiyaçlarına tam olarak yanıt veren Tam Kan Bakım Noktası (PoC) pıhtılaşma cihazları, bu alanda hâlâ ortaya çıkmaktadır. Taşınabilir PoC ve kişisel bakım PT/INR izleme cihazları, kullanım kolaylığı, anlık sonuçlar, zamanında antikoagülan doz ayarlaması için hızlı geri dönüş ve rutin ihtiyacını ortadan kaldırarak gelişmiş hasta rahatlığı gibi geleneksel laboratuvar yöntemlerine göre çok önemli avantajlar sağladıklarından popülerlik kazanmaktadır. Hastane/laboratuvar ziyaretleri ve damar delme işlemleri gibi sıkıntıları azaltmalarının yanı sıra, PoC cihazları genellikle parmak ucundan alınan tam kılcal kanı kullanırlar, bu da geleneksel laboratuvar metotlarına kıyasla daha kullanışlı bir yöntem sunar.

Bu tez, opto-mekanik tabanlı bir PoC koagülometresinin tek kullanımlık kartuş ünitesi üzerinde gerçekleştirilen çeşitli optimizasyon faaliyetlerini sunmaktadır. Bu çalışma, ilk kartuş tasarımını ticarileştirilebilir bir ürüne dönüştürmek için ürün geliştirme aşamasında gerçekleştirilen çeşitli tasarım optimizasyonu ve doğrulama faaliyetlerini göstermektedir. Dolayısıyla bu çalışma, grubumuz tarafından pasif kılcal akış/Mikroakışkanlar, biyokimyasal işlevselleştirme, optik fiber montajı ve reaktif optimizasyonu açısından geliştirilen önceki kartuş tasarımının üretilebilirliğini ve kullanılabilirliğini artırmaya odaklandı. Ayrıca son kartuş tasarımı, kontrol plazması ve kan örnekleri üzerinde heparin izleme ve aPTT ölçümü konusunda bir çalışma yürütmek için kullanıldı. Ayrıca klinik bir ön çalışma, cihazımızın standart hastane yöntemi ile olan korelasyonunu değerlendirmek için n=42 örneklem ile gerçekleştirildi, böylelikle etkililiğini ve klinik kullanım potansiyelini daha da doğrulayarak onayladı.

AKNOWLEDGEMENTS

These three years I spent at Koç have been some of the most challenging yet rewarding of my life. Having beloved ones beside me has been a blessing.

First and foremost, I would like to express my gratitude to my supervisor, Prof. Dr. Hakan Ürey, for giving me the opportunity to work on this project and enabling me to make meaningful contributions to this company, ultimately benefiting humanity, which was my initial goal.

Next, I'd like to thank Prof. Dr. Özlem Yalçın and Assoc. Prof. Onur Ferhanoğlu for agreeing to serve on my thesis defense committee and providing me with essential criticism and insight.

Secondly, I extend my heartfelt thanks to Dr. Sinan Müldür for being the "World's Best Boss" and consistently supporting me through the challenges of life, graduate school, and the business world.

Elif Esen, M.Sc., has been the best coworker and friend, always making our lives easier. Her contributions to our work are invaluable, and her ability to turn even the most disturbing conversations into something funny and tolerable is commendable.

I want to thank Asst. Prof. Ece Öztürk for her help through my master's degree and enabling me to follow my curiosity towards science. Prof. Mehmet Murat Özmen for his patience through the challenges I had.

There is no way that I could pass without thanking Prof. Dr. Zeynep Altıntaş for her incredible impact on my life that led me to this day without breaking. I appreciate everything she did for me in the past, as their echoes still reverberate.

Next, my appreciation goes to my two consecutive CEOs, Hasan Ürey and Esat Oğuz, for their meaningful contributions to the project and their constant kindness towards me.

I also want to thank Dr. Uğur Aygün for his guidance through tough times. Dr. Hadi Mirzajani and Dr. Parviz Zolfaghari are appreciated for their kind and positive attitudes in every situation.

I would like to specially thank Dr. Müge Gültekin Erzin for her thoughtful attitude towards my struggle to be a teaching assistant and supporting me through my thesis era.

Gamze Yılmaz for her help in everything I needed. A special shoutout goes to Selim Ölçer and Fırat Türkkal for their contributions to our project and the broad spectrum of their profession that expanded my knowledge.

Jeroen Hamers, M.Sc., has been an invaluable coworker for the short period I had a chance to work with. I also would like to thank Ali Mişe for his calm and able nature that always gave good vibes, and Demet Tümkaya for her contributions. I want to specially thank Emine Büyükdurmuş for her helpful attitudes towards me.

As a career-driven individual, I experienced a warm and cozy feeling of having lifelong friends who have faced similar challenges and navigated life together. The following acknowledgments will be in chronological order, representing the journey of meeting these wonderful people. First and foremost, I want to thank my dearest friend, Selay İrem Baştuğ, who has been by my side for 14 years. Life brings the right people beside you, thank you for reminding me all those good things we had and were. I express my gratitude to Hasan Bank, M.Sc., for everything he has done for me. I always believed in his pure intentions and kind heart. There is no way that I could easily express my gratitude towards you with these sentences, but simply know that you are an invaluable person in my life. I came to Koç with one of my dearest friends, Tahsin Emirhan Tekoğlu, and became friends with his friends—people I wouldn't have met otherwise. I thank him for introducing me to such good friends and for being a great friend himself. His honest opinions and support in crucial matters, accompanied by a smile, were invaluable. By never agreeing with me, he sparked meaningful arguments within our group. Umut Berkay Altıntaş, M.Sc., my dearest and weirdest friend, now living in a different time zone, has always been a source of joy and chaos. I am happy to have him in my life with his signature "Zirve" meetings. Having Elif Yapıcı, M.Sc., as one of the most sincere and nicest people on this journey was a blessing. I cherish the times we spent together, the mini concerts with songs from DKTT, and our shared motto of "Akışında." I want to thank my friend Seda Ergün for being beside me for a very long time now. I love you from Berlin to Istanbul. Ceydanur Altınışık has a special place in my heart with her incredibly pure intentions. I appreciate the time we spent together with Ayça Saymaz and Musa Dırak, simply being themselves throughout this journey has taught me a lot. My dearest hocam, Sepehr Madani, M.Sc., now annoys me with his friendship from another continent. Having such an honest person in my life is something I will always appreciate. Ece Özmen, M.Sc., one of my dearest friends, I enjoyed every moment we spent together. Your calm and mature character harmonized with the crazy and funny side of yours,

making the perfect combo for me to have fun. I always appreciated your perspectives, expanding my horizons.

Special thanks go to my roommates, Sevgi Sarıca and Kardelen Yangın, for being the kindest people to live with, and to Brandon Fasy for his incredible intrusion into our lives and getting along with me during our brief time as roommates. Aslı Dansık is now being thanked for her crazy side that enlightened me.

I extend my thanks to my lab mates, Arda Gülersoy, Koray Kavaklı, M.Sc., Mehrdad Khodapanahandeh, M.Sc., and Ozan Özhan for their friendship and stories that kept me laughing all the time.

The authors gratefully acknowledge the use of the services and facilities of the Koç University Research Center for Translational Medicine (KUTTAM), funded by the Presidency of Turkey, Head of Strategy and Budget.

I want to express my gratitude to the cast of "The Office" for making my life better in so many ways. Additionally, I shouldn't let my close friends' list on Instagram go unannounced, as they kept me sane towards the end of my thesis term.

Last but not least, I want to express my heartfelt thanks to my family for their infinite support of my craziest dreams. Having a mom who knows me to the fullest is one of the greatest blessings in life, and I am fortunate to have that. I appreciate her honesty, guiding me when I am in the wrong and the right place. She never lets me overload myself, always keeping me grounded, and warns me with her incredible vision that I could never think of having for myself. I want to thank my father for his support in everything I wanted to pursue and believing in me and seeing all the challenges I am having and supporting me in a kind way.

I also want to emphasize that I am grateful for everything I lived through these three years with its best and the worst that made me question everything that I thought I knew. Life is incredibly valuable, and trying to make it more meaningful is, I guess, why we all are living for as scientists.

In closing, let me draw inspiration from the profound words of Mustafa Kemal Atatürk, the visionary founder of Türkiye, who wisely stated, "*The most genuine guide in life is science*." These words echo with timeless truth, reminding us of the indispensable role of science as a beacon illuminating our path forward.

TABLE OF CONTENTS

LIST OF TABLES

LIST OF FIGURES

ABBREVIATIONS

ACT	Activated Clotting Time
aPTT	Activated Partial Thromboplastin Time
CRRT	Continuous Renal Replacement Therapy
DOS	Dioctyl Sulfosuccinate Sodium Salt
DVT	Deep Vein Thrombosis
ECMO	Extracorporeal Membrane Oxygenation
ICU	Intensive Care Unit
INR	International Normalized Ratio
MEMS	Microelectromechanical Systems
PE	Pulmonary Embolism
PT	Prothrombin Time
RF	Resonance Frequency
TF	Tissue Factor
TPA	Tissue Plasminogen Activator
TT	Thrombin Time
VKA	Vitamin K Antagonist

Chapter 1:
INTRODUCTION

1.1 Coagulation and Homeostasis

Homeostasis is a concept encapsulating the body's capacity to uphold a consistent internal environment amidst external fluctuations. This involves a network of automatic cellular mechanisms, neural and endocrine controls, and behavioral responses. Organisms operating in diverse external conditions often regulate numerous internal variables, showcasing intricate systems to manage crucial factors. For instance, mammals exhibit adaptable mechanisms for body temperature regulation, allowing them to function across a broad spectrum of external temperatures compared to reptiles. Negative feedback mechanisms predominantly underlie physiological homeostasis; signals related to regulated variables are sensed, prompting the system to react in ways that mitigate these signals. Homeostasis has a range of physiological processes, and blood clotting is just one of those contributing to the body's resilience in responding to and recovering from injuries [1]. Hemostasis, as a part of homeostasis, is an important aspect of health conditions. Any abnormalities related to the bleeding condition, whether inherited or acquired throughout life, demand significant attention, and require careful balancing. Excessive bleeding, referred to as hemorrhage, and inappropriate blood clot formation, known as thrombosis—with associated risks such as deep vein thrombosis (DVT) and pulmonary embolism (PE)—represent the two extremes. Anything within this spectrum requires careful attention and evaluation. The process of hemostasis, integral to an individual's overall health as part of homeostasis, occurs in three phases. These consist of the platelet phase of vascular bleeding, which maintains first hemostasis; a transformation that brings about clotting during the activation of coagulation cascade and; a number of inhibitors, which stop blood clot spreading and confine the activity of the coagulation cascade to the site where endothelial injury occurred [2]. Clotting factors are possibly the most important elements without which haemostasis would not be able to occur, because it is a physiological response to an injury in vascular endothelium. This response triggers a sequence of processes aimed at maintaining blood within the vascular system through clot formation. Hemostasis is classified into primary and secondary phases. Primary

hemostasis, leads to the creation of a pliable platelet plug, enables vasoconstriction, platelet adhesion, platelet activation, and platelet aggregation. Secondary hemostasis is then principally characterized by the making of fibrin from fibrinogen, ultimately transforming the soft platelet plug into a rigid, insoluble fibrin clot. Hence, three coagulation pathways are recognized as intrinsic, extrinsic, and common [3].

1.2 Extrinsic Pathway

It is a very fast process that takes a few seconds as it is more direct compared to the intrinsic ones. In traumatic injury, damage to the surrounding tissues arrests the extrinsic pathway. The initiation of coagulation is majorly by the extrinsic pathway that has tissue factor (TF) together with Factor VII. Tissue plasminogen activator (TPA) released from damaged endothelial cells converts plasminogen into plasmin thereby activating the extrinsic fibrinolytic pathway [4].

1.3 Intrinsic Pathway

On the contrary, the intrinsic pathway has a slower pace than the extrinsic one; it is set off by diverse things such as, platelets, only a little amount of thrombin from the extrinsic pathway, exposed subendothelium or damage to the vessel wall. The reactions in this pathway involve several key clotting factors like Factor VIII, Factor IX and Factor XI and their various biochemical reactions support coagulation once cascade has triggered thrombin generation. Additionally, activation of Factor XII through subendothelial collagen initiates the intrinsic pathway leading to conversion of plasminogen into plasmin and initiating intrinsic fibrinolytic pathway. Thrombin is then generated upon activation of coagulation cascade. Thrombin cleaves fibrinogen into fibrin which randomly form protofibril strands that undergo linear extension, branching and lateral association thus giving rise to three-dimensional network of fibrin fibers. At factor X activation level: This involved in meeting points between intrinsic/extrinsic pathways. Binding with cofactor factor Va activates prothrombin into thrombin Thrombin in turn catalyses Fibrin clots are formed when thrombin converts fibrinogen to fibrins thus completing the final two steps in common pathway blood coagulations [5], [6].

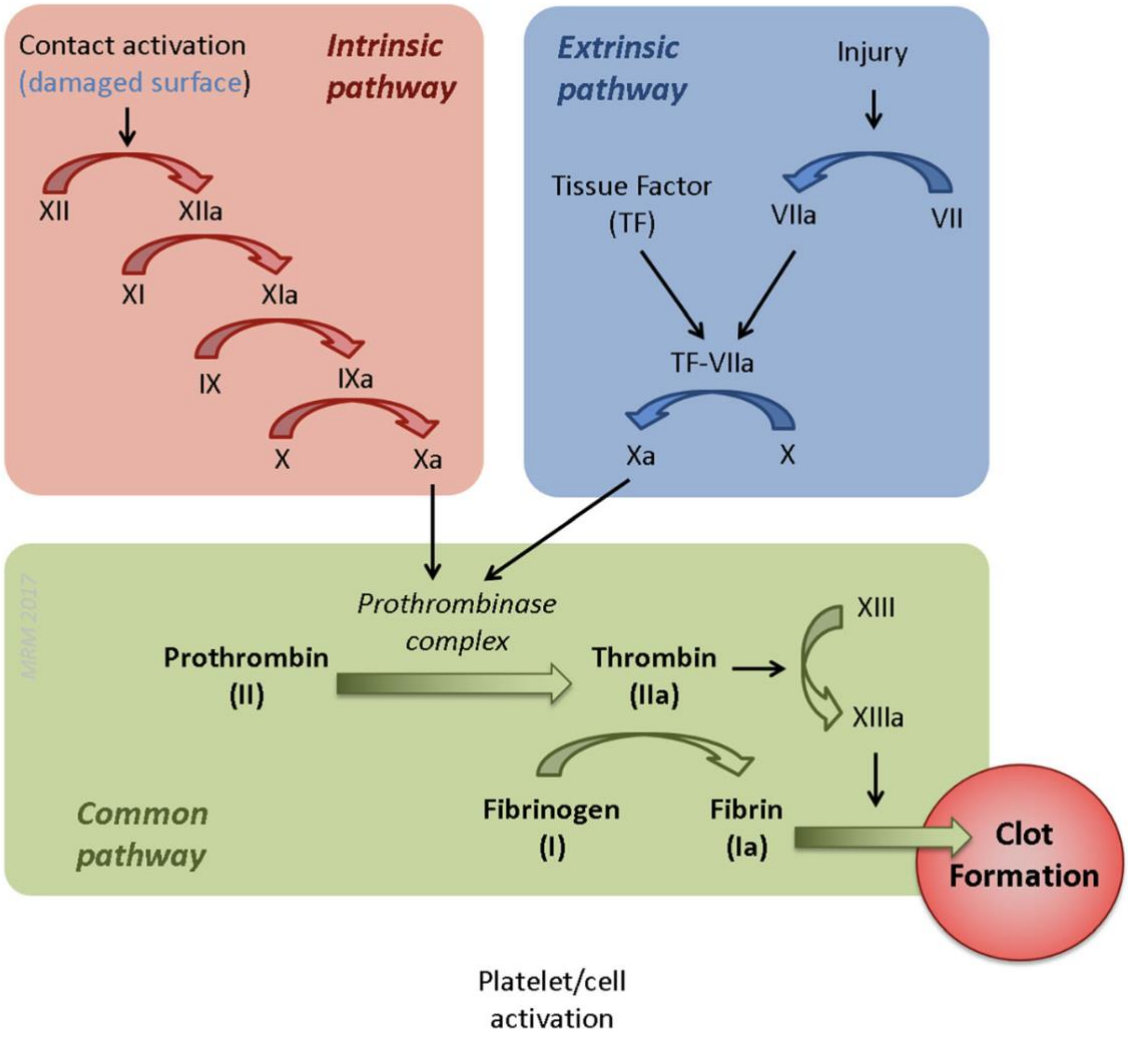

Figure 1: Intrinsic and extrinsic pathway of coagulation [6].

1.3.1 Coagulation Measurement

Bleeding Time is one of the methods used to assess the vascular platelet phase of hemostasis and how well a person's body can kick start primary hemostasis through vasoconstriction, platelet adhesion and aggregation. In this test, a small cut is made on the forearm and bleeding time is measured without applying external pressure. It serves as a screening test for the vascular platelet phase of hemostasis, to assess any vasospastic response and also platelet function. They might show up as purpura, mucosal bleeding or fundus hemorrhages sometimes accompanied by conditions like thrombocytopenia,

abnormal platelet functions, drug-induced platelet abnormalities and von Willebrand's disease [7].

Activated partial thromboplastin clotting time (aPTT) measures the time for fibrin generation through the intrinsic pathway. It is a screening test for inherited or acquired factor deficiencies, including disorders like hemophilia A and B. Prolonged aPTT can indicate reduced quantities of various coagulation factors or the presence of inhibitors. It helps differentiate factor deficiencies from inhibitors through mixing studies. The most common inhibitors include heparin and fibrin degradation products.

Thrombin time (TT) test measures the time for fibrinogen to fibrin conversion in the presence of thrombin. Abnormalities may indicate deficient fibrinogen, abnormal fibrinogen (dysfibrinogenemia), or inhibitors to the reaction. Acquired fibrinogen deficiency is linked to consumptive coagulopathy, while dysfibrinogenemia can be acquired or inherited. Common inhibitors include heparin and fibrin degradation products, detectable through specific reactions [7].

PT test is an assessment of the extrinsic and common pathways. It evaluates the formation of blood clots and the function of coagulation factors like Fibrinogen, Factor II (Prothrombin), Factor V, Factor VII, and Factor X, to gauge the overall capacity to form a clot within the expected timeframe. Tissue factor -thromboplastin- plays a key role in catalyzing the conversion of prothrombin to thrombin. However, it is essential to note that variations in reagents used and results obtained may occur between different laboratories and even within the same laboratory over time. To standardize PT results globally, the World Health Organization (WHO) has developed and recommended the use of the International Normalized Ratio (INR) [8]. The use of PT and INR is particularly relevant in the context of anticoagulant therapy. For instance, the monitoring of INR is crucial for the safety and efficacy of warfarin therapy in hospitalized patients, as achieving the first therapeutic target of warfarin within a specific timeframe is associated with improved safety outcomes [9]. Additionally, the attainment of a therapeutic INR has been significantly associated with a shorter length of stay following mechanical heart valve surgery, highlighting the clinical significance of INR monitoring in this context [10]. Furthermore, the PT and aPTT are screening tests used to assess the process of hemostasis in vivo, and their results are predictive of low prothrombin concentration and clinical outcomes in trauma patients [11], [12]. The PT test is also valuable in the context of various medical conditions. For example, in patients with

endometriosis, the PT, aPTT, and TT were significantly shortened, but fibrinogen significantly increased, indicating a hypercoagulable state in these individuals [13]. Moreover, PT has been shown to predict survival in several types of malignancies, including cholangiocarcinoma [14]. Additionally, coagulation parameters, including PT, have been associated with the prognosis of immunoglobulin A nephropathy, where shorter PT and aPTT were significantly associated with adverse outcomes [15]. In the realm of laboratory medicine, efforts have been made to optimize PT testing, including establishing and verifying normal reference intervals and assessing aPTT reagents for sensitivity to various factors, such as heparin and lupus coagulation inhibitor [16].

INR serves as a standardization measure for PT values, addressing issues in oral anticoagulant therapy arising from the variable sensitivity of different commercial sources and thromboplastin lots to blood coagulation Factor VII. The development of INR aimed to mitigate the inconsistencies in PT measurements by establishing a comparison between the responsiveness of thromboplastin and a reference thromboplastin from the World Health Organization (WHO), quantified as the international sensitivity index (ISI). The formula for calculating INR is $INR = (PT/MNPT)^{ISI}$ where MNPT represents the mean PT value. Widely adopted for patients on vitamin K antagonists (VKA), INR serves as a preferred test, offering insights into bleeding risk and the coagulation status of patients. Patients on oral anticoagulants regularly monitor INR to tailor VKA doses, which exhibit variations among individuals. INR is derived from the PT ratio, comparing the patient's PT to a control PT standardized with WHO's thromboplastin reagent. Measured in plasma, PT assesses the time it takes to form a clot in the presence of calcium and tissue thromboplastin, activating coagulation via the extrinsic pathway. INR values are dimensionless, typically ranging from a score of 2.0 to 3.0. Optimizing a patient's INR therapeutic range proves challenging due to the narrow therapeutic window associated with VKAs, influenced by patient characteristics, co-morbid conditions, diet, and other drug interactions. Monitoring occurs every 3–4 weeks at thrombosis centers, point-of-care clinics, or at home [17], [18].

Recent years have revealed that remote monitoring has potential of improving patients' lives. Accordingly, it was presented that remote patient monitoring has the potential to diminish the utilization of acute care, particularly in the realm of chronic conditions like cardiovascular disease and chronic obstructive pulmonary disease. In a study, roughly the half of the examined interventions demonstrated a correlation with a

decline in hospital admissions. This suggests that remote patient monitoring could play a role in lowering acute care usage by facilitating early detection, proactive management, and remote monitoring of patients dealing with chronic conditions [19]. Likewise, mobile health applications that run on smartphones or tablets, allows users to monitor vital signs, receive medication reminders, and communicate with healthcare providers remotely [20], [21]. The amalgamation of digital telemedicine instruments with commercial wearables signifies a move towards decentralized healthcare, emphasizing noninvasive remote monitoring [22]. Besides, in the context of gestational diabetes mellitus, it was suggested earlier that remote monitoring technologies, such as glucose monitors, play a crucial role. Portable devices for monitoring blood glucose levels, particularly important for individuals with diabetes, contribute significantly to better glycemic control [23]. On the other hand, a study with 85 adults on antihypertensive treatment highlighted the effectiveness of home blood pressure monitoring compared to clinic measurements. Differences, especially in the morning, suggested integrating home monitoring into hypertension management. A positive correlation between clinic and daytime home blood pressures emphasizes the broader applicability of home monitoring for informed treatment decisions and improved management [24], [25]. Electrocardiogram monitors that are portable and user-friendly, record the heart's electrical activity, with some models enabling at-home usage and data transmission to healthcare providers [26]. Additionally, remote monitoring implants, exemplified by cardiac monitors and neurostimulators, continuously track specific health parameters and wirelessly transmit data to healthcare professionals, contributing to comprehensive and proactive healthcare management [27]. In such case, it is plausible that the use of PoC devices enable such smooth transition from traditional medicine to telemedicine. Portable PoC devices play a pivotal role in advancing healthcare by offering convenient and efficient solutions, particularly in the context of remote patient monitoring and disease management.

1.3.2 PoC devices

More than 800 million clotting tests are performed each year in hospitals and clinical laboratories for emergencies, surgical operations, and periodic monitoring of patients [28]. The main attractive feature of PoC is that it is able to detect on-site and in real time without the need for extra peripheral devices. The success of PoC diagnostics is closely

linked with the continuing development of cheap, sensitive and reasonably accurate new medical technologies. Although PoC devices have many advantages, there have been concerns that transformation of lab-generated technologies into global health market is well-recognized within scientific and business arenas. Transition from laboratory prototypes to marketable products takes several years involving a great deal of technical work and significant investment in order to meet exacting demands required by the markets. This shift calls for strong partnership amongst scientists from various disciplines like chemistry, biochemistry, optics, engineering as well as health care providers or practitioners. A good start of such cooperation should be during the initial idea formulation stage hence bringing together diversified skills through out the whole design process of a device. Such collaboration seeks to avoid creating non-practicable devices which cannot work properly in actual clinical settings [29].

There have been several cases where PoC devices for coagulation measurement, stated as PT/INR and sometimes aPTT has become the second most common coagulation test due to the use of prescribed heparin. The commercially available PoC devices also do perform PT/INR and aPTT measurement and are dominating the market today. However, there are some challenges associated with PoC such as regulatory considerations, clinical need determinations, “miniaturized” assays accounting for interfering substances, and tests with multiplex platforms that must be simple enough. Furthermore, lack of current Clinical Laboratory Improvement Amendments (CLIA)-waived PoC coagulation and hematology devices with multiplexing capabilities is an obstacle that must be overcome to make point-of-care technologies more usable and effective in clinical settings [30].

Most significantly, the Covid-19 pandemic has increased the demand of rapid, easy and accurate portable PoC coagulation devices. Some significant actors in the point of care diagnostic market have reported increase in their revenue. The global point of care coagulation testing devices market size was 1.55 Billion USD in 2019. According to this analysis, a worldwide market growth of about 9.9% was seen in 2020. Over the 2020-2027 period, it is estimated that the market will increase from $1.9 billion to $2.76 billion at a CAGR of 7.2%. This was an increase from 1.9 billion dollars recorded in year 2020 since Covid-19 started [31]. The global impact of Covid-19 has been unprecedented in terms of these PoC coagulation testing devices witnessing a positive demand across all regions of the pandemic. This growth in demand is attributed to various medical

organizations recommending coagulation testing and monitoring for Covid-19 patients to prevent complications from clot formation.

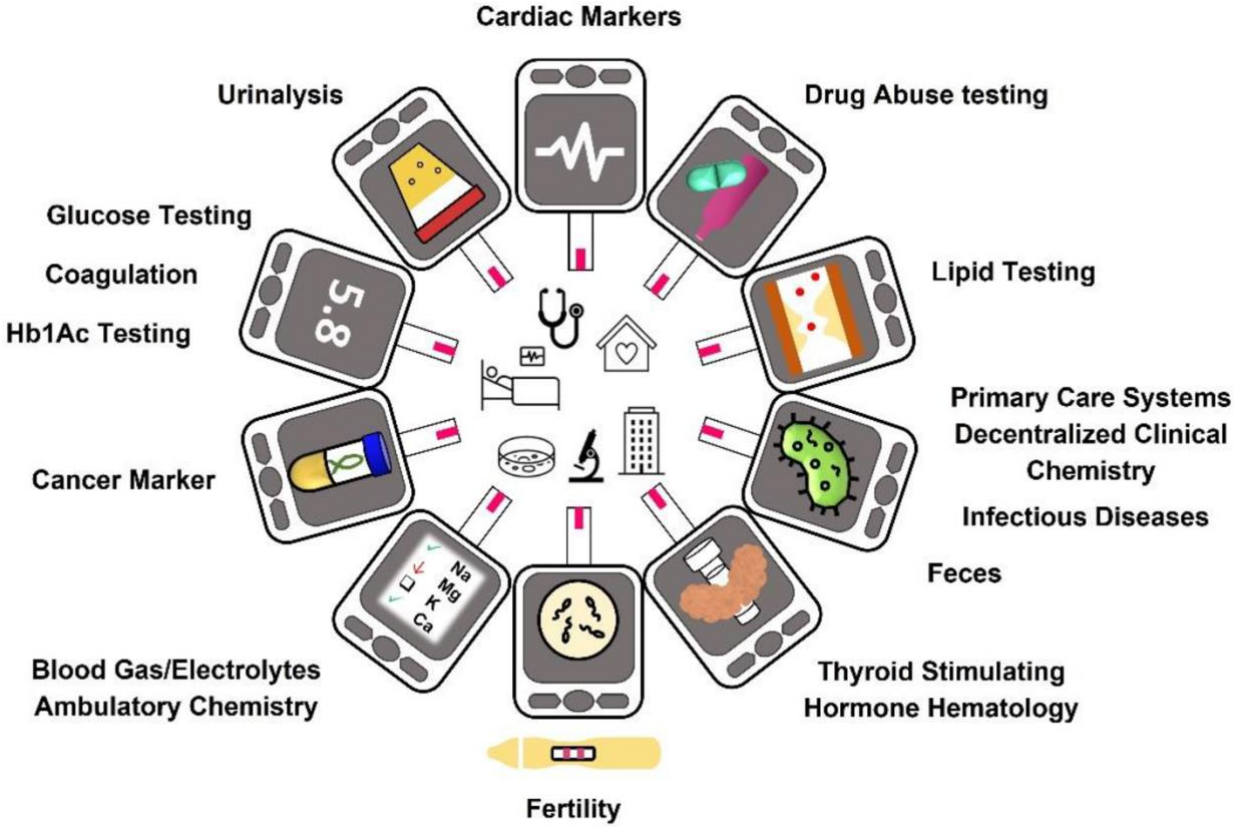

Figure 2: Biosensor types are depicted [29].

In intensive care units (ICU), prevalence of venous thromboembolism among patients with Covid-19 reported to be about 30% [32], while an infectious condition can also lead to a hyper-inflammatory state that entices prothrombotic events. In addition, in ICU; extracorporeal devices such as ECMO and CRRT can be used to support organ function recovery. Such techniques can cause thrombosis either suddenly or gradually since blood contacts with different non-physiological surfaces so causing an excessive activation of the coagulation system.

In response, several expert organizations, including the American Society of Hematology [33], International Society on Thrombosis and Haemostasis [34], CHEST Guideline and Expert Panel [35], and others [36] have recommended prophylactic anticoagulation for patients admitted with Covid-19, to reduce the risk of thromboembolism. Heparin based anticoagulants are commonly used in hospital settings. Given evidence that shows these drugs might also possess anti-inflammatory properties

[37], [38], heparin-based treatments might be particularly effective in patients with Covid-19 [39].

Monitoring of adequate heparin dosage is essential to maintain the delicate balance between bleeding and thrombosis. aPTT reflects the intrinsic coagulation pathway and is the most commonly used test to monitor heparin. Activated clotting time (ACT) and anti-Xa activity tests are performed as well [40], [41].

Venous thromboembolism has emerged as an important consideration in the management of hospitalized Covid-19 patients. Conventional coagulation measurement devices used in hospital are usually tabletop instruments which necessitate the transportation and processing of infected blood to be tested by being problematic given the risk of infecting non-Covid-19 hospitalized patients and hospital personnel.

To date, the development of PoC biosensors has been immensely studied by highlighting the advantages provided by these devices in terms of rapid testing time, cost-effectiveness, simplicity, and portability. Particularly, with the unexpected rise of Covid-19, the role of PoC devices became suddenly irreplaceable, and even provided a solid motivation to keep developing [42].

The total biosensor market size was estimated to be $10.8 billion dollars by 2007 [43] and has been steadily increasing since. Blood glucose monitors were estimated to reach $11.5 billion USD by 2012 [44]. The market for electrochemical biosensors is expected to extend at a compound annual growth rate of 9.7% and is projected to reach USD 23.7 billion by 2022, up from USD 12.8 billion in 2018 [45]. This remarkable extension of the market size underscores the potential augmentation of the anticipated growth of the biosensor market in following years.

The Roche Diagnostics CoaguChek® XS utilizes electrochemical detection with electrogenic substrates, particularly in the self-testing market for PT/INR measurements. This device provides results in terms of clotting time, enabling comparisons with standard clotting tests. Abbott Diagnostics' i-STAT® employs electrochemical detection for professional use, offering measurements of PT/INR and ACT. i-STAT® has shown positive outcomes in a pharmacist-managed anticoagulation clinic, improving safety, adherence, and cost, suggesting potential for broader implementation. Alere's INRatio®, formerly HemoSense, utilizes electrochemical impedance with screen-printed electrodes for self-testing PT/INR measurements. The device monitors coagulation by detecting changes in the resistance of coagulating blood. Microvisk Technologies' SmartStrip® is

highlighted as a device using MEMS-based resonant transducer technology for blood coagulation measurement. The device incorporates disposable strips with microcantilevers, enabling the measurement of changes in blood viscosity. The cost-effectiveness and single-use disposability are emphasized, but specific details regarding the device's performance were not provided. Accumetrics' VerifyNow® represents a form of miniaturized light transmission aggregometry, offering sensitivity to the level of aggregation and providing information on the impact of antiplatelet therapies. However, the text notes that such devices may not fully consider the complex nature of platelets and their interactions, potentially lacking full standardization and comprehensive comparison information with standard tests [46]. The issue of device and measurement bias associated with PoC devices, particularly in the context of different INR ranges was previously discussed by Faber et al. [47] suggesting that with the CoaguChek XS device, bias tends to increase as INR values rise, especially when the INR is greater than 3.0. On the other hand, the ProTime InRhythm device demonstrates the best agreement with CFX INR for values below 2.5, but the study did not assess its performance for INRs above 3.5. In comparing different devices, the Coag-Sense device showed better correlation with STAGO laboratory INR results compared to the CoaguChek XS, even at supratherapeutic INR levels. This underscores the importance for healthcare providers to be mindful of potential biases associated with PoC devices, particularly in different INR ranges, to ensure accurate and reliable measurement results.

Notable systems include the optical detection-based Hemochron Signature + and Signature Elite by ITC (USA), Cascade PoC by Helena Laboratories Point of care (USA), ProTime Microcoagulation System by ITC (USA), Coag-Sense PT/INR Monitoring System by CoaguSense Inc. (USA), GEMPCL Plus by Instrumentation Laboratory (USA), microINR by iLine Microsystems (Spain), Hepcon HMS Plus Hemostasis Management System by Medtronic Cardiac Surgery (USA), and Bio-AMD’s COAG by Bio-Alternative Medical Devices Ltd. (UK). These systems offer diverse functionalities, such as rapid results, user-friendly interfaces, and handheld/portable designs, catering to a range of testing scenarios. Systems like the Hepcon HMS Plus Hemostasis Management System and Bio-AMD’s COAG specifically address the needs of managing hemostasis in cardiac surgery settings. The electro-mechanical detection-based ACT Plus System by Medtronic Cardiac Surgery (USA), Hemochron Response by ITC (USA), Actalyke XL and Actalyke Mini II by Helena Laboratories Point of care (USA), Thrombotrack Select

2 and Thrombotrack Solo by Axis-Shield (Norway), and CoagLite & CoagMax by Microvisk Technologies (UK) add to the diversity in design and functionality. Additionally, the electro-chemical detection category includes the i-STAT by Abbott Point of care Inc. (USA), INRatio/INRatio2 PT INR Monitor by Alere (USA), and CoaguChek XS, CoaguChek XS Plus, and XS Pro PT Test System by Roche Diagnostics (USA). These systems, with their specific detection technologies, showcase the variety and advancements in hemostasis monitoring, making them suitable for different clinical applications and patient care scenarios. Various blood withdrawal methods and sample volumes associated with each system. These withdrawal methods range from fingerstick and venipuncture to specialized approaches like microcapillary cessation of flow. Sample volumes vary across the systems, with measurements specified in microliters (μL) and ranging from 2 μL to 3000 μL, highlighting the flexibility and adaptability of these hemostasis monitoring devices across different healthcare settings and patient needs [46].

Biosensors are presented with one or more biological component that require certain attention due to fragile nature of these particles compared to electronical and mechanical pieces. Compartmentalization of PoC devices has several steps to consider including mechanical integration, electrical integration, and biochemical stabilization to perform intended test. In cases where coagulation measurement is aimed with such devices, there is an emerging need for the desired coagulation measurement reagent depending on specific test. PT measurements are performed with PT reagents having tissue factor and/or thromboplastin whereas aPTT tests are performed with reagents having specific molecules. Hence, another important aspect to consider when developing a PoC device is the integration of reagents into the device. These reagents can be stored in liquid, solid/dry, or gel forms and released using mechanisms such as pressure/flow, dissolution, or in response to external stimuli. This provides diverse options for seamlessly incorporating reagents into PoC devices [48]. In this regard, we investigated several approaches to optimize reagent integration to the cartridge.

1.3.3 CoaRight Device

Previously, a biosensor platform designed for cost-effective PoC coagulation time measurements was engineered by our group. The methodology involved monitoring the vibrations of a mechanical structure, specifically a cantilever beam, immersed in a blood

sample—a technique closely resembling the gold standard of direct mechanical testing for coagulation time assessment. As blood coagulates, the increased viscosity induces changes in the resonance characteristics of the cantilever. This biosensor platform featured the creation of two distinct sensors leveraging the same underlying technology. The first sensor incorporated MEMS cantilevers, while the second sensor utilized an optical fiber as the mechanical cantilever. In both instances, remote actuation was achieved through an electro coil, with optical readout. The advantage of remote actuation and readout facilitated the development of a system with an independent reader unit and disposable cartridges. This innovative biosensor platform represented a notable advancement in PoC coagulation time measurements, combining the precision of direct mechanical testing with the practical benefits of remote actuation and optical readout in a previous research endeavor [49].

Our PoC device measures the coagulation status of blood using a cantilever-based opto-mechanical method sensitive to viscoelastic variation of blood during coagulation. The system consists of a reader unit that houses the electronics, light source, electromagnetic coil, heater and photodetectors and a disposable cartridge inserted in the reader unit. The blood sample is placed into a microfluidic channel through an inlet and flows by passive capillary motion into a cartridge where a resonant vibrating optical fiber (cantilever) and a pick-up optical fiber are aligned with a small gap in between. Near mechanical resonance of the vibrating fiber is achieved by magnetic actuation using a small nickel ring attached at the free end of the fiber. The key innovative feature of the system consists of a fluid stop region which separates blood interaction and measurement regions of the vibrating fiber [50]. The pick-up fiber collects a clear optical signal avoiding scattering and optical losses which results in high signal-to-noise ratio optical output. An initial frequency sweep in air determines at which frequency the signal amplitude is maximal. Once blood or plasma as the test subject is applied to the inlet, it flows into a measurement chamber that contains a dried PT reagent (RecombiPlasTin 2G, HemosIL) based on human recombinant thromboplastin. As blood starts to coagulate, both its viscosity and elasticity increases, leading to a decrease in fiber deflection (resonant frequency) and thus in a sharp decrease in the amplitude of the optical signal from which PT value is derived. The pick-up fiber collects a clear optical signal avoiding scattering and optical losses which results in high signal-to-noise ratio optical output. This signal is directly related to the coagulation time since during coagulation the viscoelastic

properties of blood change and thus change the fiber deflection. The device is designed for use by a diverse range of individuals, including untrained personnel, patients, and their relatives in home-use applications. Additionally, it caters to healthcare professionals such as nurses, physicians, and other medical staff for clinical applications. The application environments span healthcare facilities, PoC settings, and the convenience of patients' homes. This device is used with a polymer-based cartridge comprising all the elements mentioned above as shown in Figure 2. The cartridge comprises three main components. Firstly, the cartridge itself is composed of a microfluidic system featuring an inlet, main channel, and measurement chamber. Additionally, it includes a fluid stop-zone and V-grooves designed for placing the optical fibers. Secondly, the cartridge incorporates oscillating and pick-up optical fibers, specifically polyacrylic fibers without coating, each measuring 10 mm (1 cm) in length. Lastly, there is a nickel ring affixed to the inner extremity of the oscillating fiber through adhesive bonding. The cartridges are prepared by carving the PMMA plate in house with a CNC machine (Figure 3).

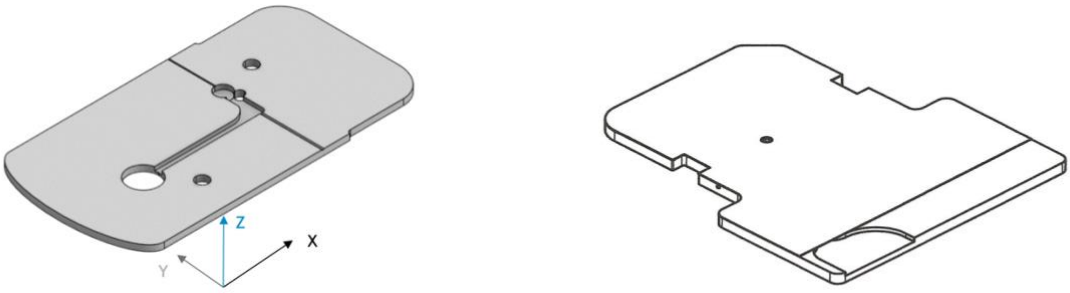

Figure 3: Evolution of the cartridge design. On the left older version of the cartridge can be seen. On the right, latest version of the cartridge is shown.

1.4 Contributions of the thesis

This thesis highlights a series of crucial design optimization and validation processes conducted during the product development phase, aiming to transition the initial cartridge design into a commercially viable product. The primary focus of these efforts was to enhance the manufacturability and usability of the original cartridge design, previously developed by our research group. My specific contribution involved planning and

executing verification and validation activities for the proposed design optimizations throughout the research and development (R&D) and product development stages. The key aspects addressed included optimizing capillary flow, refining functionalization techniques, and fine-tuning reagent composition. Notably, my substantial involvement in both idea conception, planning, and verification was most pronounced during the reagent integration study, which encompassed formulation and drying optimization activities.

Furthermore, the ultimate cartridge design was employed in a thorough proof-of-concept study, concentrating on the potential of heparin monitoring and activated partial thromboplastin time (aPTT) measurement, wherein I played a comprehensive role from inception to completion. My full contribution encompassed involvement in the planning, execution, and analysis of the study. The primary objectives included generating in-vitro heparin sensitivity curves by adding increasing amounts of heparin to aliquots of control plasmas, normal donors citrated plasma but also citrated blood. The main goal was to observe an increase of aPTT values when increasing the dose of heparin (indicative of performance validation) while also evaluating precision and repeatability of the measurements. My integral role in every phase of this study reinforced the credibility of the final cartridge design, emphasizing also its potential application in heparin monitoring and aPTT measurements in the near future.

Chapter 2: **CARTRIDGE DESIGN AND FABRICATION**

2.1 Working Principle of Our Technology

In this section, working principles of the sensor platform will be explained briefly. This section serves as a guide to the sensor platform and get the reader familiarize with it. The sensing platform consists of two essential units: a disposable cartridge and a reader unit. The cartridge integrates two optical fibers and microfluidic channels. Specifically, one optical fiber is situated within the microfluidic channel, while the other is firmly secured in the cartridge wall. Notably, the fluid stop region is larger than the remaining microfluidic network, acts as the convergence point for the end faces of the opposing fiber segments. This design enhances the stability of optical readout and minimizes noise by preventing the intrusion of blood into the light pathway. A nickel component is attached to the end of the suspended fiber within the sensor chamber and fluid stop region. The stationary fiber section functions as a receiver. The actuation of the fiber with the nickel component induces modulation in the light transmitted from the moving fiber to the receiving fiber. The resulting modulated light is then captured by the photodetector. The onset of blood or plasma coagulation causes a sudden change in viscosity due to clot formation.

Our methodology incorporates a movable optical fiber strategically placed across a microfluidic channel, enabling the direct mechanical assessment of coagulation time in disposable cartridges containing plasma or whole blood samples. The movement of the fiber is achieved through an electro coil, coupled with optical readout. This technological approach eliminates the requirement for electrical connections within the cartridge, making it an economically viable disposable solution.

In the realm of hydrodynamics, two primary force components contribute to loading as them being inertial and viscous forces. The inertial force is associated with the displacement of liquid mass caused by the vibrating structure. While the viscous force arises from the resistance of the liquid medium's viscous drag to the movement of the vibrating structure. Alterations in the viscosity of the liquid medium induce changes in the resonance characteristics of the system. Readers may refer to Sader's research [51], [52]. In instances of blood coagulation, an increase in system viscosity is observed. This heightened fluid viscosity leads to a reduction in the system's resonance frequency and

quality factor (Figure 4). The transformation in resonance characteristics can be effectively monitored by either maintaining a constant driving frequency and observing changes in phase and amplitude or by tracking the resonance frequency itself [53].

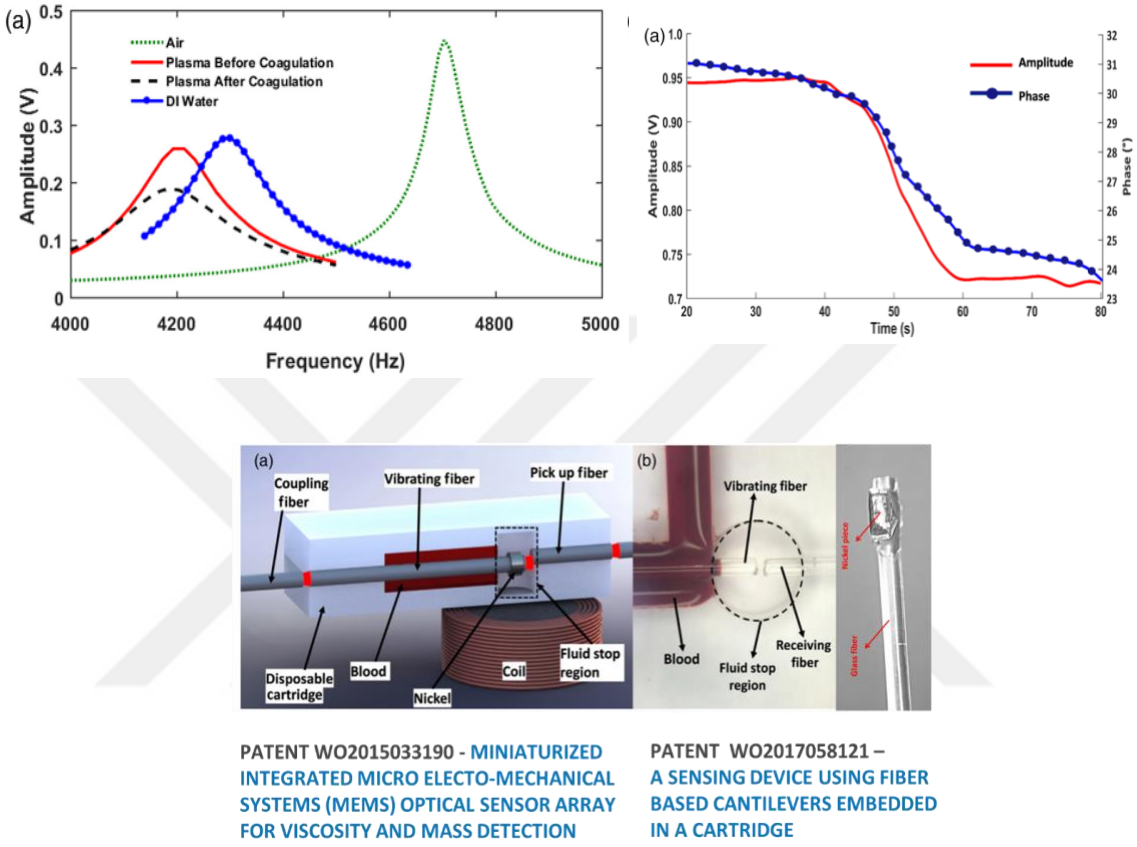

Figure 4: (a) Amplitude vs frequency graph is shown for different conditions, (b) amplitude over time graph is shown, (c) components of the cartridge described

2.1.1 Open Setup

In the context of cantilever-like systems working in viscous liquid environments, the resonance frequency and quality factor are affected by the viscosity of the immersed liquid. Hydrodynamic loading is fundamental to this dynamic in terms of encompassing inertial and viscous forces. The inertial force correlates with the mass of liquid displaced by the vibrating structure, while the viscous force originates from the resistance of the liquid medium to the movement of the vibrating structure. Variations in liquid viscosity result in corresponding adjustments to the system's resonance characteristics [49].

Sader's investigation [51], [52], [54] comprehensively explores hydrodynamic loading on cantilever-like structures vibrating in viscous mediums. Notably, during blood coagulation, there is a surge in the system's viscosity, leading to a concurrent reduction in the resonance frequency and quality factor. Monitoring these changes involves driving the system at a constant frequency while observing phase and amplitude changes or tracking the resonance frequency itself [55], [56].

The sensor platform further illustrates these principles, featuring a suspended fiber with a nickel part within the sensor chamber and fluid stop region. In this setup, the stationary fiber serves as a receiver, while the fiber with the nickel part is actuated, modulating the light between the moving and receiving fibers. The photo detector captures this modulated light. Importantly, when blood or plasma coagulates, there is a sudden increase in viscosity due to clot formation, underscoring the interplay between system dynamics and biological processes.

This section serves as a concise introduction to the sensor platform's operational principles, with more detailed discussions to follow in subsequent chapters. The measurement setup, depicted in Figure 5, comprises a disposable cartridge and a reader unit. The fluid stop region prevents blood leakage into the light pathway, ensuring a stable and low-noise optical readout. Further elaboration on these working principles will be presented in subsequent sections.

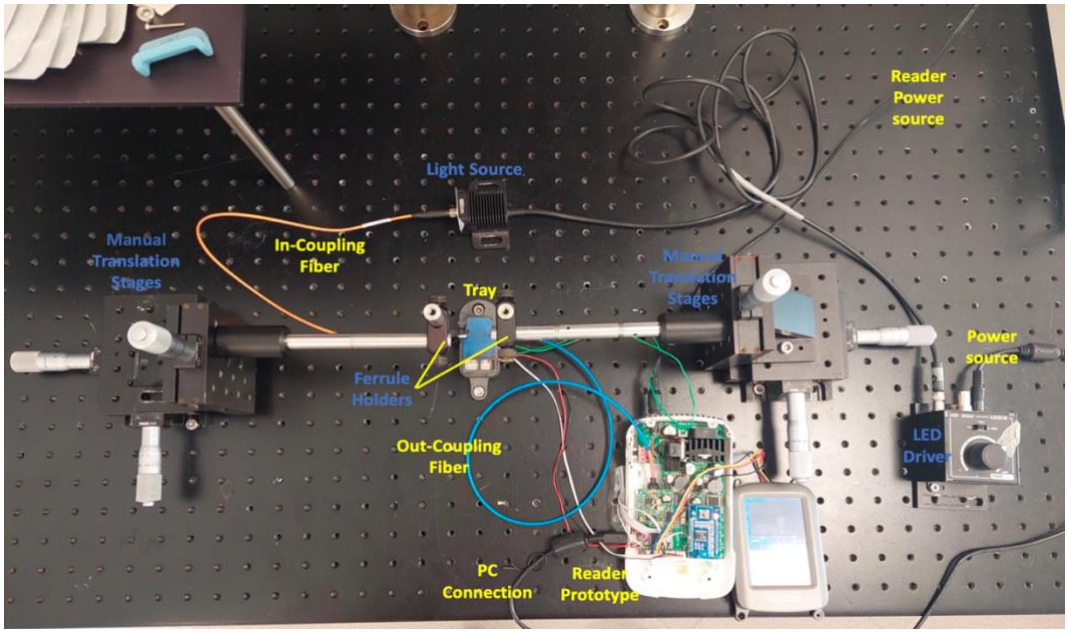

Figure 5: Open setup and its components.

2.1.2 Measurement Principle and Parameters

Coagulation is the complex physiological process by which blood forms clots, and understanding the dynamics of this process is crucial in various medical scenarios. In the exploration of time-dependent data analysis, three interconnected MATLAB functions have been developed, each serving a distinct purpose. The first function, denoted as find_peak_velocity, is designed to identify the time of peak velocity within a given dataset. Employing a systematic approach, the function calculates the first derivative of the input data, subsequently normalizes it, and then locates the time index corresponding to the minimum value of the normalized derivative as the peak velocity. Noteworthy is the incorporation of a try-catch block for robust error handling, ensuring the provision of NaN values in case of unexpected errors.

In the specific domain of coagulation data analysis, the provided MATLAB code takes on a heightened significance. Each function, namely `find_peak_velocity`, `find_peak_deceleration`, and `find_peak_acceleration`, plays a distinct role in delineating critical temporal points within the coagulation cascade. Moreover, a noteworthy parameter is introduced for each function, encapsulating crucial information about the coagulation process.

Finding TPV: `find_peak_velocity`

This function, tailored for coagulation data, identifies the time of peak velocity (TPV) during the coagulation cascade. In the coagulation context, TPV represents the moment when the rate of blood clot formation is at its zenith. This parameter becomes a pivotal indicator, potentially pinpointing the optimal time for the initiation of clot formation.

Finding TPD: `find_peak_deceleration`

In the coagulation scenario, this function determines the time of peak deceleration (TPD), signaling the point at which the coagulation process begins to slow down. TPD could be critical for understanding the latter stages of clot formation, providing insights into the deceleration phase of the coagulation cascade.

Finding TPA: `find_peak_acceleration`

Specific to coagulation data, this function calculates the time of peak acceleration (TPA), representing the phase where the coagulation process experiences the maximum acceleration. TPA might denote a crucial period in the initiation of clot formation,

offering valuable information about the rapid acceleration phase in the coagulation cascade.

In the context of coagulation data analysis, it has been determined that the most informative parameter for assessing coagulation time is TPV. The emphasis on TPV as a primary metric underscores its significance as a key temporal marker in the coagulation cascade. The results derived from TPA and TPD are considered supplementary, providing additional insights into acceleration and deceleration phases, respectively. This strategic approach to coagulation time determination, anchored by the TPV parameter, reflects a nuanced understanding of the coagulation process. It suggests that the moment of peak velocity serves as a robust indicator for characterizing the overall coagulation time, with complementary information derived from acceleration and deceleration phases contributing to a comprehensive analysis of coagulation dynamics.

2.1.3 Signal, Resonance Frequency and Amplitude

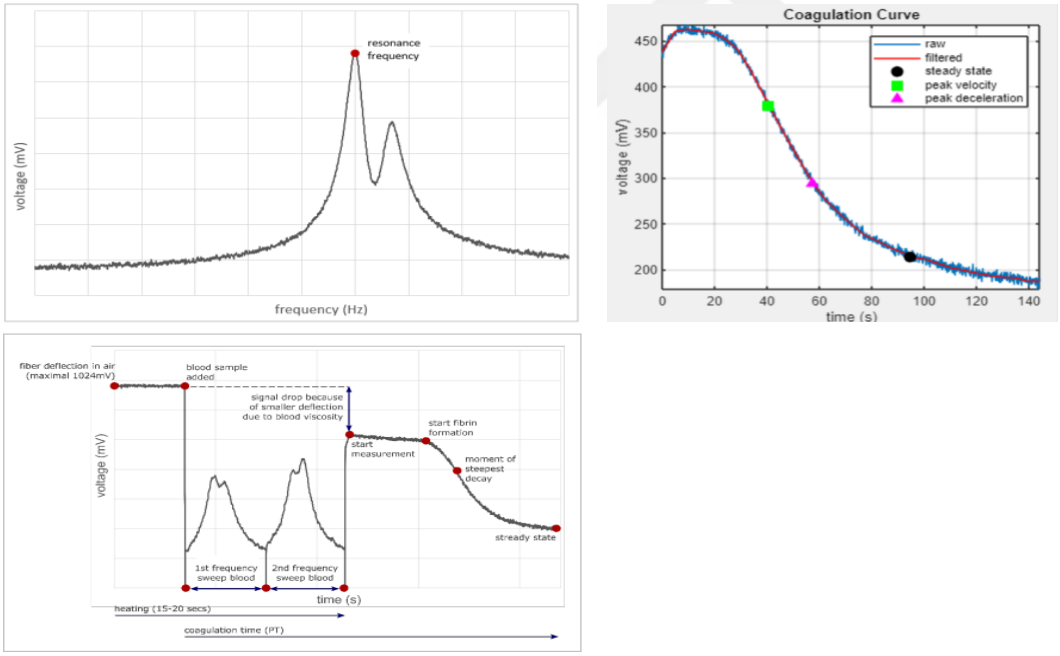

Figure 6: Exemplary Curves of Our Device: Exploring Performance and Characteristics

In Figure 6, an example of data produced by our device is shown in two graphs. The left plot displays the frequency voltage relation in air for a certain cartridge. The frequency where the voltage is maximal is marked as the resonance frequency. Initially, the alternating coil current frequency is set to that value. The next step is to inset the blood sample, find the resonance frequency in blood, set the coil current frequency to this new

value and measure the optical fiber deflection in time and finally relate that to the coagulation time. A typical measurement curve is shown on the right. Some important features of this curve are marked with red dots.

The measurement protocol is structured as follows: initially, the empty cartridge undergoes a resonance frequency (RF) test in an air environment. Subsequently, the cartridge is tested again, this time in the presence of DI water, with a known density of 0.9970 g/mL at 25 °C. Following the water exposure, the RF test in air is repeated to discern any differences. The protocol then progresses to testing with diluted glycerol (density: 1.252 g/mL at 25°C) [57]. Similar to the water testing, the cartridge undergoes the RF test, and the subsequent step involves removing the glycerol, followed by another RF test in air. The same sequence of steps is then repeated for testing with undiluted glycerol. This systematic testing procedure aims to evaluate the impact of varying fluid densities on the resonance characteristics of the system, providing insights into how the biosensor responds to different media and enabling a comprehensive understanding of its performance under diverse conditions.

Table 1: This table presents the resonance frequency in Hz and corresponding amplitude (mV) measurements for the biosensor in different environments, including air, DI water, diluted glycerol, and undiluted glycerol.

	Air		***DI Water***		***Air III***		***Diluted Glycerol***		***Air II***		***Glycerol***	
	Hz	***mV***	***Hz***	***mV***	***Hz***	***mV***	***Hz***	***mV***	***Hz***	***mV***	***Hz***	***mV***
09.07--10	*2108Hz*	*1023*	*1995Hz*	*355*	*2061Hz*	*1023*	*1862Hz*	*99*	*2073Hz*	*1023*	*2739Hz*	*71*
09.07--11	*2632Hz*	*1023*	*2511Hz*	*1023*	*2632Hz*	*1023*	*2435Hz*	*639*	*2630Hz*	*1023*	*2468Hz*	*220*
24.08--1	*3031Hz*	*1023*	*2831Hz*	*580*	*3131Hz*	*1023*	*2839Hz*	*219*	*3039Hz*	*1023*	*2722Hz*	*86*
24.08--2	*3019Hz*	*1023*	*2939Hz*	*1023*	*3030Hz*	*1014*	*2775Hz*	*93*	*3031Hz*	*971*	*2868Hz*	*54*
24.08--4	*3150Hz*	*1023*	*3000Hz*	*368*	*3092Hz*	*1023*	*2884Hz*	*153*	*3151Hz*	*1023*	*3057Hz*	*62*
24.08--5	*3295Hz*	*1018*	*3200Hz*	*229*	*3303Hz*	*1023*	*3169Hz*	*167*	*3306Hz*	*988*	*3052Hz*	*67*
24.08--6	*2984Hz*	*1023*	*2843Hz*	*999*	*2959Hz*	*1023*	*2779Hz*	*877*	*2970Hz*	*1023*	*2681Hz*	*265*
24.08--8	*3194Hz*	*1023*	*3062Hz*	*1023*	*3205Hz*	*1023*	*2937Hz*	*139*	*3221Hz*	*1023*	*2921Hz*	*107*
24.08--9	*3005Hz*	*1023*	*2935Hz*	*866*	*3013Hz*	*1015*	*2817Hz*	*95*	*3012Hz*	*1023*	*2613Hz*	*76*
24.08--10	*2970Hz*	*1005*	*2837Hz*	*236*	*2899Hz*	*1002*	*2732Hz*	*129*	*2975Hz*	*1023*	*2736Hz*	*75*

In our methodology, which utilizes a movable optical fiber within a microfluidic channel for coagulation time assessment, the trends observed in the table correlate with variations in fluid viscosity. The optical fiber's movement in this biosensor design is intricately linked to hydrodynamic forces within the microfluidic channel, where viscous forces play a pivotal role in coagulation time assessment. The inertial force is associated

with liquid mass displacement caused by the vibrating structure, while the viscous force arises from the liquid medium's viscous drag resistance to the vibrating structure's movement. As the biosensor interacts with fluids of different densities, such as plasma or whole blood samples, changes in the liquid medium's viscosity become prominent.

In instances of blood coagulation, system viscosity increases, leading to notable alterations in the system's resonance characteristics. The provided table affirms this pattern: transitioning from Air to DI Water to Diluted Glycerol to Glycerol results in a consistent decrease in resonance frequency (Hz) and amplitude (mV). This aligns with the anticipation that heightened fluid density corresponds to a reduction in the system's resonance frequency and amplitude.

The table, demonstrating changes in amplitude and resonance frequency with various fluids, aligns with the hydrodynamic principles governing the biosensor. An increase in fluid density, particularly due to heightened viscosity during blood coagulation, corresponds to a reduction in the system's resonance frequency and quality factor. This is in line with the general understanding that alterations in fluid viscosity influence the system's mechanical behavior.

In the biosensor applications, monitoring these transformations in resonance characteristics becomes crucial for detecting and assessing blood coagulation. The biosensor achieves this through optical readout techniques where the design eliminates the need for electrical connections within the disposable cartridge. In summary, the observed trends in the table align with the hydrodynamic principles governing the biosensor's operation. Changes in fluid viscosity, particularly during blood coagulation, influence the system's resonance characteristics, and the biosensor's capability to monitor these changes offers a promising avenue for real-time and disposable coagulation assessment in clinical settings.

2.1.4 Preparation of Cartridge and Optical Fiber to Perform Coagulation on the Device

The optical fiber preparation process involves several sequential steps to ensure the proper configuration and quality of the fibers for use in the cartridge assembly. First, a long fiber is cut from the bundle and its coating is stripped, using either a scalpel or Micro-Strip 0.010. Subsequently, the fiber is cleaved and polished, creating a vibrating fiber (1

cm) and a pick-up fiber (1 cm) using a diamond cutter (Thorlabs S90R). These fibers are then placed into a holder (Thorlabs BFT1), leaving the tips exposed, and are polished with various polishing pads until a straight cut edge is achieved.

Figure 7: Jonard JIC-375 on the upper left, Micro-Strip 0.010 on the upper right, diamond cutter (Thorlabs S90R on the bottom left, holder (Thorlabs BFT1) bottom right

In the gluing and nickel piece attachment phase, a nickel piece is affixed to the fiber. This is done by attaching the fiber to a cap, applying glue to the polished end, placing a nickel piece using tweezers, and allowing the glue to dry. Moving on to the cartridge assembly, the bottom part of the cartridge is prepared by placing the vibrating fiber into a groove, gluing it, and repeating the process for the pick-up fiber in the opposite groove. The crucial distance between the fiber tips is maintained by visual estimation. After drying, excess fiber is cut using the diamond cutter.

This process ensures the precise preparation and assembly of optical fibers for use in the coagulation device, ultimately contributing to the reliability of the blood analysis system.

Following this, initial in-house cartridge biochemical assembly process involves a systematic sequence of steps for reagent preparation, loading, and drying, followed by the preparation of a hydrophilic solution (DOS in ethanol) with its subsequent loading and drying processes. For PT reagent preparation, Recombiplastin 2G is dissolved in 20 ml of deionized water, and a choice of stabilizing agent is prepared according to the protocol. A solution is created by mixing 90 µl of the reagent solution with 10 µl of the

stabilizing agent. Subsequently, 2 µl of this solution is loaded directly into the measurement chamber beneath the fiber using a 2.5 µl pipette, with careful avoidance of overflow and breaking of the fiber.

Simultaneously, the preparation of the hydrophilic solution involves creating a 0.5% DOS solution by dissolving 0.5 g of DOS in 100 ml of ethanol, which is refrigerated for future use. For loading, ~5 µl of this solution is carefully pipetted from the inlet until it reaches the end of the measurement chamber, avoiding overflow to the fluid stop zone. The loaded cartridge is then left to dry in the air for ~10 minutes. These steps ensure the precise assembly of the cartridge for subsequent diagnostic testing.

2.1.5 Cartridge Design & Optimization and Verification

Initially, the design of the cartridge after the MEMS phase had several different versions. The one before the microfluidic PMMA design with a cover foil combination was the cartridge shown below (Figure 8). This cartridge had bigger channel and measurement chamber compared to new design and had a lid made from the same material. According to the concept, the two surfaces needed to interlock and once aligned, be sealed by applying pressure on the snap fasteners.

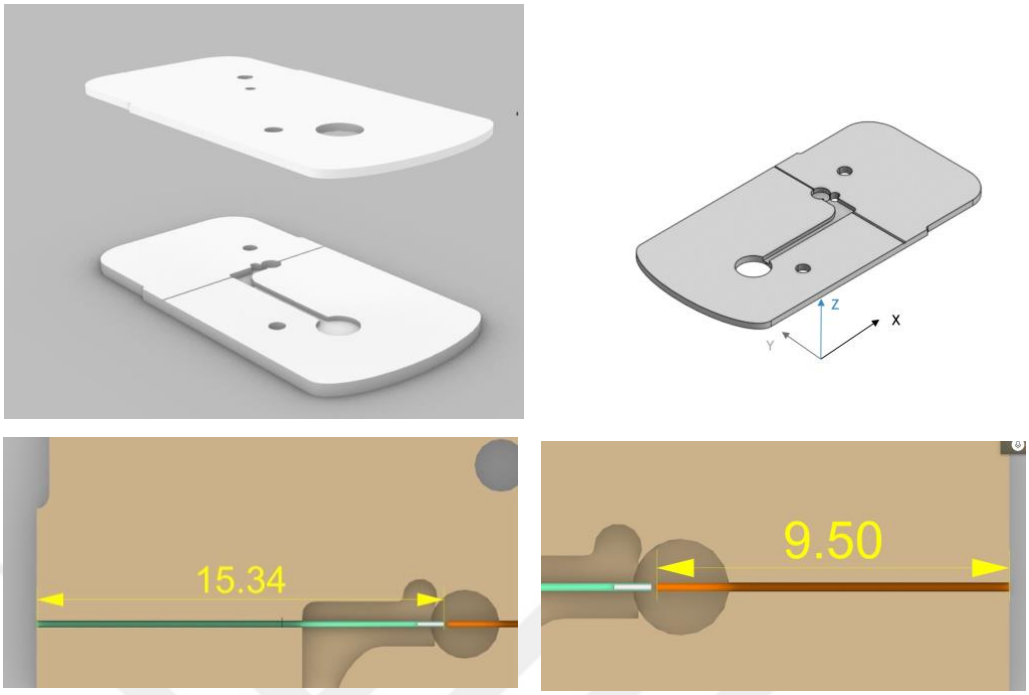

Figure 8: Cartridge design V1 with sealing mechanism from different angles. Fiber lengths are shown below.

Similarly, there was an adhesive-taped surface in between, enhancing the adhesion between the two surfaces. However, during the flow of blood through the microchannel, there were instances where the blood climbed onto the taped surface, spreading across the entire cartridge surface. As this parameter was not optimally controllable, it became a rationale we considered when applying changes in the cartridge design. The product characteristics for the cartridge encompassed several key specifications. The cartridge was required to incorporate a microfluidic chip, integrating both fibers that were optimized for light transmission at a specific wavelength of 628 nm. Furthermore, the cartridge components need to meet storage and shipping conditions. The tray also maintained a maximum distance of 200 µm to the heater, the electromagnetic coil, and provided essential electrical and optical interfaces to the device. The main reason to this change was to provide manufacturability. Later stages of the product development enabled change of the cartridge design according to feedback given after the cartridge was tested for coagulation as a part of the R&D process.

To enhance manufacturability, the original design, featuring two different fiber lengths, was streamlined to utilize equal-length fibers, eliminating unnecessary complexities in fabrication. This alteration complemented the redesign necessitated by the introduction of passive capillary flow in the final product. Simultaneously, the initial cartridge design, depicted in Figure 8, featured larger channel and chamber volumes. The blood or plasma samples were initially introduced using a micropipette.

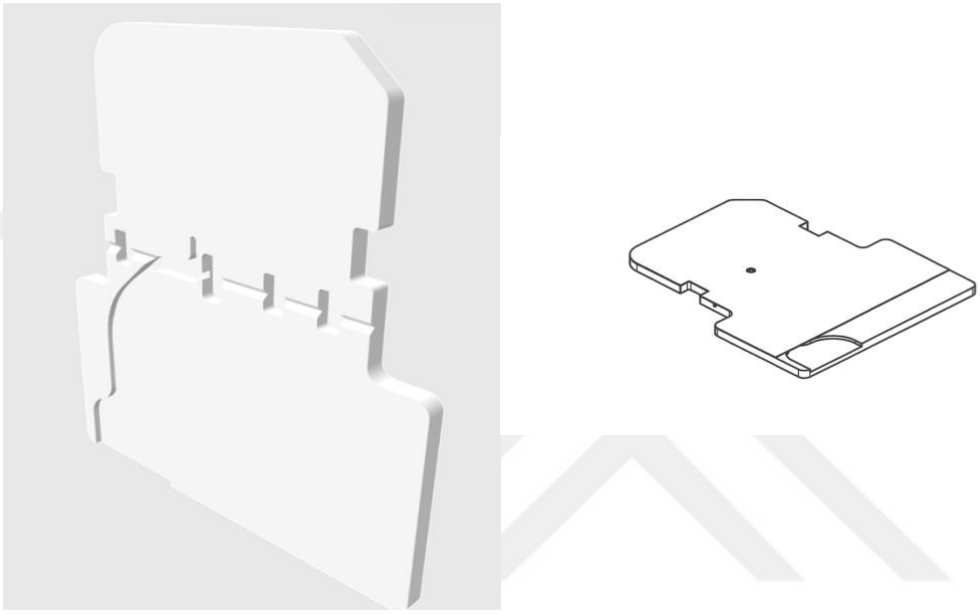

Figure 9: New shape of the designed cartridge that has passive capillary flow capabilities.

Due to the need for facile and safe capillary flow during commercialization there were some enhancements introduced that aimed at ensuring seamless initiation of measurements, aligning with practical requirements for user-friendly and efficient operation beyond the laboratory setting. Consequently, adjustments were made to reduce channel and chamber dimensions, critically affecting the overall size of the cartridge (Figure 9). This move allowed the successful implementation of a drop of blood obtained through a finger prick, facilitating one-step measurements, and emphasizing the device's ease of use and user-friendly nature.

Moreover, this change in cartridge design necessitated an external sealing mechanism due to the shift from a two-piece design. So, a pressure-sensitive 100-micron-thick foil was employed, meeting design requirements involved creating a functional device capable of operating with a minimal blood droplet, focusing primarily on reagent integration. In parallel, microfluidic volume was systematically reduced, aligning with

this thesis's three main components: optical fiber, biochemical design, and microfluidics. Additionally, the optimization of the two fibers' length to a standardized 1 cm further contributed to reduced costs and simplified design parameters. In contrast, the cost-effectiveness evaluation favored PMMA material over COC. Collectively, these strategic decisions synergistically contributed to an improved, cost-efficient, and streamlined design for the biosensor system.

2.1.6 Cartridge Material

The choice of material for a cartridge in various applications, including microfluidic devices, is crucial for many reasons. Particularly, products being exposed to human use that contact with bare skin has extra regulations. Several factors including biocompatibility, chemical compatibility, mechanical strength, and durability, as well as manufacturability, temperature stability along with regulatory compliance is of focus while deciding for the cartridge material. It should also be noted that the hydrophobic or hydrophilic properties of the cartridge material is an important aspect to consider.

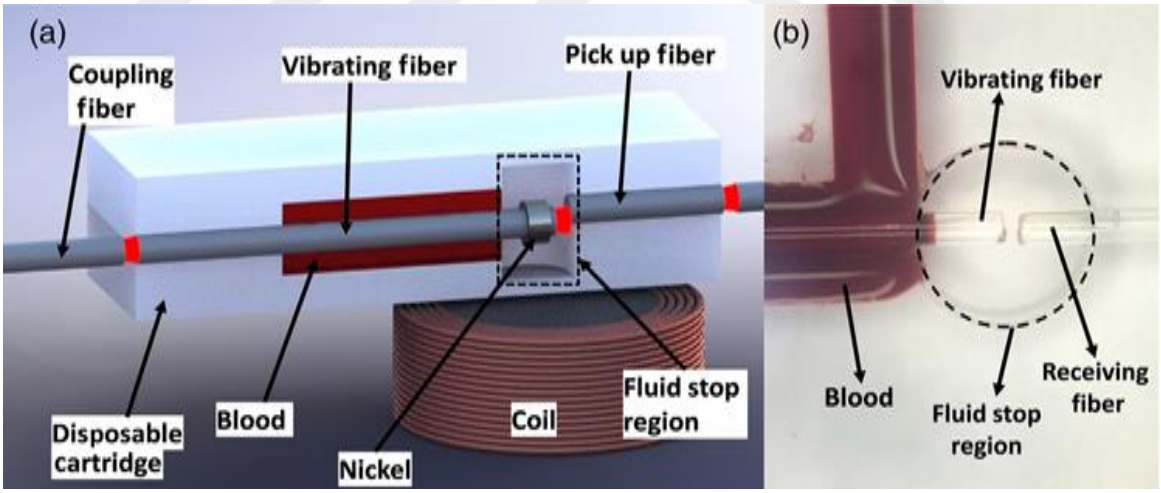

Figure 10: Inner design of the cartridge is shown above.

Cyclic-Olefin-Copolymer (COC)

The use of cyclic olefin copolymer (COC) as a material for microfluidic cartridges has gained significant attention in recent years due to its unique properties and advantages like rapid prototyping, high melting temperature suitable for autoclaving for cell culture applications, and its compatibility with mass fabrication techniques such as thermoforming or injection molding [58]. Besides, COC presents finer structural details

as micro and nano-structured features, making it more appropriate for injection molding microfluidic devices. It is widely used in microfluidics due to its UV transparency, biocompatibility, and high chemical resistance, making it suitable for various biological and chemical applications [59], [60]. On the contrary, COC's main drawbacks as a material for microfluidics are its surface chemical inertness and its hydrophobic properties. To address these challenges, researchers have explored surface modification techniques such as plasma-enhanced chemical vapor deposition and mild and selective C–H activation to enhance the surface properties of COC for microfluidic applications [61], [62]. In this pursuit, we've adopted a microfluidic substance called Dioctyl sulfosuccinate (DOS) to tailor the surface, facilitating passive capillary flow [63].

The manufacturing process of the cartridges involves several sequential steps. Firstly, bare cartridges are crafted using COC material and an aluminum injection mold. Subsequently, the optical fibers undergo preparation by removing their coating through acetone application and sonication. These fibers are then precisely cut using a Sumitomo Cutter, resulting in two equal-length fibers measuring 10 mm. Nickel rings, crucial components, are produced through laser cutting and affixed to the end of one fiber. During assembly, the fiber with the nickel ring is positioned on the left side, while the pick-up fiber is carefully placed on the right side, ensuring that both fiber ends are located at the fluid stop region, with the nickel ring oriented towards the bottom. To secure these components, UV polymerizable glue is meticulously applied to three allocated areas. Following the functionalization of the cartridge with reagent and a hydrophilic solution, a transparent foil is delicately pressed onto the cartridge, completing the assembly process.

However, due to issues related to microfluidic flow, signal, and reagent immobilization, we have decided not to proceed further with the COC cartridge. In this design, it was not as straightforward or cost-effective to implement geometry changes compared to CNC milling of PMMA. The chamber size was found to be insufficient for reagent immobilization, and there were frequent errors in detecting the coagulation signal.

CNC-Milled PMMA

Polymeric materials, notably PMMA, are valued in various industries, especially medicine, for their strength, low weight, and tissue compatibility. However, challenges arise in machining due to poor surfaces and low production rates. Optimal parameters, including spindle speed, feed rate, and depth of cut, are crucial. PMMA's machining

complexities are evident in studies emphasizing feed rate and spindle speed for minimal surface roughness and vibration control during micro-milling. CNC milling, crucial for material removal, is influenced by cutting speed and depth of cut [64]. CNC machining offers precision and flexibility, allowing for intricate designs and detailed carving of PMMA components. This method is particularly advantageous for low-volume production and prototyping, providing quick turnaround times and adaptability to design changes [65].

In this investigation, CNC-machined PMMA is employed as the subject of comparison with COC cartridge effects. The experimental design is meticulously structured to discern the distinctions arising from the PMMA cartridge fabrication methodology. Experiments conducted with blood and three plasma samples as testing substrates showed that the performance variations PMMA cartridge has advantages of easy control, low cost and better microfluidic properties compared to COC cartridges.

2.1.7 Cartridge Geometry/Microfluidic Design

Chamber Size

Initially both our COC and PMMA cartridges had 1 mm of chamber size with 650 microns of pool depth, wherein we had problems with reagent immobilization process. As will be explained in section “Approaches for Reagent Positioning” below, Recombiplastin 2G reagent is typically designed to be reactivated through the introduction of blood or plasma samples in the measurement chamber. However, the existence of the resonating fiber on the measurement chamber holds most of the volume of chamber and blocks most of the area belongs to the reagent. This issue caused problems in free movement of the fiber preventing a healthy measurement environment. Hence, to provide an alternative, we decided to test two additional cartridge design with bigger chamber sizes of 1.5 mm and 2 mm with pool depth of 900 microns. New designs of these cartridges are completed in our lab, and their production is performed by CNC-machining as per usual. The principal objective of this experiment was to elucidate the impact of chamber size on fiber movement, the post-reagent drying cleaning process under vacuum conditions, and the overall performance of the system.

Cartridge	Aperture	Plasma	PT	Reagent	Reagent
11.10-3	1.5 mm	HA	37	Normal	1h desiccator
12.10-4	1.5 mm	HA	127	Normal	Lyophilized
12.10-5	1.5 mm	LA	62	Normal	Lyophilized
12.10-6	1.5 mm	LA	255	Normal	Lyophilized
11.10-4	2 mm	LA	34	Normal	Lyophilized
12.10-1	2 mm	LA	190	Normal	Lyophilized
12.10-2	2 mm	LA	35	Normal	1h desiccator
13.10-2	2 mm	LA	40	Normal	3h desiccator
13.10-3	2 mm	LA	37	Normal	3h desiccator
13.10-6	1.5 mm	LA	6	Normal	3h desiccator
13.10-8	1.5 mm	LA	**28**	Normal	3h desiccator
21.07-2	1 mm	LA	5	Normal	3h desiccator
251-08	COC	LA	81	Normal	3h desiccator
244-02	COC	LA	5	Mannitol	Overnight
254-06	COC	LA	18	Mannitol	Overnight
17.10-1	2 mm	LA	-	Mannitol	Overnight
17.10-2	2 mm	LA	76	Mannitol	Overnight
17.10-3	2 mm	LA	4	Mannitol	Overnight
17.10-4	1.5 mm	LA	60	Mannitol	Overnight
17.10-5	1.5 mm	LA	-	Mannitol	Overnight
17.10-6	1.5 mm	LA	25	Mannitol	Overnight
04.08-1	1 mm	LA	10	Mannitol	Overnight
04.08-3	1 mm	LA	4	Mannitol	Overnight
21.07-1	1 mm	LA	53	Mannitol	Overnight
19.10-1	1.5 mm	LA	69	Mannitol	3h desiccator
19.10-3	1.5 mm	LA	-	Mannitol	3h desiccator
21.07-9	1 mm	LA	-	Mannitol	3h desiccator
21.07-10	1 mm	LA	305	Mannitol	3h desiccator
19.10-5	2 mm	LA	30	Mannitol	3h desiccator
19.10-6	2 mm	LA	6	Mannitol	3h desiccator

From the outcomes presented in the tabulated results, one cartridge demonstrated the optimal condition wherein the PT value for high abnormal plasma fell within the desired range. This specific case had desiccator-dried reagent in 2µL volume. Although the remaining cartridges exhibited experimentally acceptable outcomes without big measurement errors, prolonged PT values were observed. This phenomenon could potentially indicate inadequate reagent quantities in conjunction with a limited bead surface area or the deactivation of reagents under uncontrollable conditions such as temperature and humidity.

Subsequent experiments involved a comprehensive comparison of all available cartridges, encompassing COC and 1 mm PMMA. Unfortunately, no practical and viable solution emerged from these trials. Two instances of abrupt drops in results were noted, along with consistently elongated PT values. The inclusion of mannitol in the reagent formulation was explored as an alternative; however, handling cartridges containing mannitol was challenging.

Furthermore, some cartridges exhibited difficulty in handling with DOS, impeding the intended movement and leading to leakage into the liquid stop zone.

Conversely, COC cartridges posed substantial handling challenges as interactions between DOS and reagents resulted in the formation of a paste, disrupting fiber oscillation. Extensive cleaning procedures, including fiber and neck cleaning, were necessary, prolonging the overall process. Drying COC reagents and DOS in a desiccator post-hydrophilization was imperative. While PMMA cartridges generally did not require cleaning, residues of CNC machine on the cartridge occasionally impeded fiber movement, requiring fine-tuning for optimal cartridge signal performance.

In conclusion, we observed that challenges created by 1 mm cartridge was mostly eliminated by new design of the 1.5- and 2-mm cartridges. However, although reagent sticking problem was eliminated, we saw that 2 mm cartridge required higher volume of blood compared to previous cases, the calculated volume (Rhinoceros 3D) of the chamber with the inlet being completely full is 33.93 µL. Although we don't use that much of volume to initiate coagulation measurement, such high volume may be challenging. The volume without required to fill the channel and measurement chamber is measured to be 13.92 µL. This situation puts hardship to the commercialization of the cartridge since increased blood volume can be hard to obtained from just one prick of the finger also contradicting the nature of the design. Although we could obtain ~15-20 µL of blood

volume this may not be the case for most of the people. This situation possesses additional challenges to the situation. Besides, filling of the chamber was not as rapid as the smaller chamber volumes. Since higher chamber volume requires higher sample volume, the stable speed provided by the capillary flow is not as efficient as the former case. As the 2 mm cartridge had almost the double volume compared to initial design, having these challenges are plausible. The 1.5 mm cartridge design emerged as a promising solution, effectively addressing the challenges encountered with the 1 mm and 2 mm cartridges. Calculations revealed that the required volume to fill the cartridge was 32.22 μL with the inlet full, while the combined volume of the channel and chamber was 10.97 μL. This design offers a more manageable amount of blood, making it relatively easier to obtain from a finger prick. Furthermore, the observed flow behaviors with the 1.5 mm cartridge were found to be more applicable, enhancing overall efficiency.

2.1.8 Optical Fiber and Nickel Assembly

In our setup, the cartridge is a must, serving as an integral component that facilitates rapid and accurate diagnostic testing in our open setup. Designed as a low-cost disposable unit, this cartridge houses essential reagents (either PT or aPTT in our cases), optical fibers, a measurement chamber, liquid stop zone, a microfluidic channel, and a cover foil in a user-friendly format [66]. The former cartridge featured an oscillating fiber with a length of 15.34 microns and a receiving fiber of 9.5 microns, whereas the new design fixed the fiber length to 1 cm. Unjacketed fiber from Thor Labs UEA 200 fiber is used in the design. To remove the coating a razor blade is used. Removing the jacket facilitates easier trimming of the fiber on the sides of the cartridge using a diamond cutter, simplifying the removal of excess fiber from outer extremities.

Additionally, a nickel piece is affixed to the inner extremity of the oscillating fiber, positioned above the coil inside the device. This configuration provides magnetic actuation, contributing to the overall functionality of the biosensor system.

2.1.9 Biochemical Functionalization

Reagent Formulation

The inclusion of the Recombiplastin 2G in PT measurement is imperative for fast and reliable results, as it plays a crucial role as an enzyme in the coagulation cascade. The

reagent contains substances that activate the clotting factors in plasma, enabling the measurement of the time it takes for blood to clot. The reagent is in powder form, and this is often referred to as a "lyophilized" or "freeze-dried" reagent. The preparation of the reagent requires resuspension with 20µL of distilled/pure water. Once the reagent is prepared with distilled water, it is stable for 20 days and can be used as desired for the measurement of PT either with blood or plasma. On the other hand, the reagent should be implemented onto the cartridge in a way that it would be stable for months in appropriate storage conditions, should be easily resuspended once the finger pricked blood is introduced during the use of the patient, should not be hindering the fiber movement and should stay away from interfering with the initial signal so the measurement is not compromised while being enzymatically active and not interfering with the microfluidic flow within the measurement chamber. To perform such challenging task, we have developed several approaches considering the optical signal, enzymatic activity, microfluidic flow, and storage conditions. This chapter defines those approaches and discusses the results in terms of the measurement capability tested with our open setup.

Approaches for Reagent Optimization to the Cartridge

Reagent Formulation

In PoC testing devices, it is imperative that the targeted reagents are somehow integrated within the device, preferably in the cartridge so it can be disposed after the use. Typically, these reagents are desiccated and placed within a reagent pad positioned at the base of a channel [67]. Integration of reagent into the PoC device includes various approaches. For instance, liquid reagents can be directly stored in microchannels, microcapillaries, or tubing, and released as needed. Another approach involves adsorption, where reagents like antibodies are immobilized onto surfaces through physical or chemical interactions. Lyophilization/freeze-drying is employed to remove water, storing reagents in dry/solid form, which can be rehydrated when required. Nanocarriers such as gold nanoparticles, up conversion nanoparticles, and mesoporous silica nanoparticles are utilized for storing and delivering reagents. Hydrogel storage incorporates reagents within gel networks, releasing them through stimulus or dissolution. Dissolution-based release applies to solid reagents, released through dissolution. Stimulus-based release employs physical stimuli like temperature or light, or chemical stimuli like pH/redox, to trigger release. Printed or patterned reagents involve deposition or printing on surfaces using techniques like spray deposition or inkjet printing [48].

Sugar is commonly used in food products as a preservative to reduce water activity which inhibits the growth of microorganisms thereby increasing the shelf life of foods [68]. Sugars like sucrose, trehalose, or glucose are widely used to preserve microorganisms from changes in osmotic pressure, contributing to their conservation and maintenance after drying [69]. Additionally, mannitol is utilized as an additive in various applications as well including pharmaceutical and personal care product formulations [70]. As another additive we also investigated the use of glycerol, also known as glycerin in addition to mannitol. It is a versatile compound used in various applications, with its preservative and stabilizer character in different contexts. For instance, in the preservation of fresh sweet sorghum juice for subsequent bioethanol production, a combination of chemicals, including glycerol, is used as co-preservatives to prolong its storage and maintain its quality [71]. Also, glycerol was investigated for its potential in cryopreservation due to its ability to protect cells and tissues during freezing and thawing processes.

As another additive, PEG was also considered. PEG is a versatile cryoprotectant, preserving cell viability and functionality, enhancing recovery rates and maintaining pluripotency. It stabilizes complex formulations like polymeric microbubbles during lyophilization and has been deemed safe for various applications [72], [73], [74], [75].

Recombinant DNA technology has changed the pharmaceutical development landscape, making it possible to produce proteins with huge therapeutic possibilities. However, using these proteins for pharmaceutical purposes can be very difficult because of the difficulties involved in isolating and purifying them, as well as in formulating and delivering them. This is particularly evident due to the unique chemical and physical properties inherent to proteins, resulting in complex stability issues. Chemical instability may manifest as proteolysis, deamidation, oxidation, racemization, and β-elimination, while physical instability encompasses challenges like aggregation, precipitation, denaturation, and surface adsorption. This context sets the stage for the investigation into protein stability during freeze-drying and storage [76].

Investigating protein stability during freeze-drying and stsorage, the research delved into the interplay between additives and Humicola lanuginosa lipase (HLL). Various additives, such as sugars (including trehalose and sucrose), mannitol, dextran, and Tween 20, were systematically assessed at specified concentrations to comprehend their impact on HLL. The findings demonstrated that specific additives induced protein precipitation

or non-native aggregate formation, while others, like trehalose and sucrose, facilitated the preservation of the native protein structure and stability throughout the freeze-drying and storage processes. Employing advanced techniques like size exclusion high-performance liquid chromatography, moisture analysis, X-ray diffraction, and infrared spectroscopy, the study provided a thorough analysis of the diverse effects of these additives on the protein's structure and solubility in aqueous solutions, particularly emphasizing the distinctive behavior observed in proteins with relatively hydrophobic surfaces compared to more conventionally soluble proteins [77]. Shifting focus to another aspect of protein stability, a study centered on Clostridium difficile and its toxins A and B, the primary virulence factors linked to pseudomembranous colitis. The study primarily investigated freeze-dried proteins, specifically toxins A and B, with molecular weights of 308 kDa for Toxin A and 270 kDa for Toxin B, chosen for their widespread use in diagnostic tests for C. difficile infection. In pursuing the overarching goal of developing freeze-dried formulations that ensure the preservation of the toxins' physical and biological stability during both dried and liquid storage, the study systematically assessed additives, including crystalline bulking agents, amorphous bulking agents/stabilizers, sugars, cryoprotectants, and surfactants. This focused examination of additives aimed to optimize the freeze-drying process and enhance the storage properties of the toxins, thereby contributing valuable insights into the role of additives in maintaining protein stability under different biological contexts and processing stages [78].

Here we describe the protocols and approaches used to optimize the Recombiplastin 2G onto microfluidic chip having different positions as in the measurement chamber, inlet and microfluidic channel and formulations as in mannitol, glycerol and in combination for the reagent.

Reagent Bead Preparation Protocol for COC Cartridges

The objective of this protocol is to generate reagent beads of 5 µL as a crucial part in the experiments of COC cartridges. This set of experiment results also apply to the experimental results described in under Section Approaches for Reagent Drying-Lyophilization since lyophilized beads are described here. The procedure begins by shaking the mannitol mixture at 37°C until achieving homogeneity. A metallic cube holder is then frozen at -80°C for later use. Two distinct reagent mixtures, a 2% mannitol-reagent blend with Recombiplastin 2G and a PEG-added mannitol-reagent mixture are prepared. Liquid nitrogen is employed to create bead-shaped reagents, with Eppendorf

tubes serving as containers for this purpose. Following the introduction of 5 µL of the reagent mixture into the nitrogen-filled containers, beads are formed. Labeled containers are used to differentiate various reagents, and a 10 µL micropipette, along with compatible tips, is employed with attention to their effectiveness. Optionally, bead-shaped reagents are immediately transferred to a frozen metallic rack for convenience. After transferring the Eppendorf tubes to the -80°C freezer, they are kept there for an hour before being moved to a -20°C freezer for an additional hour. The final step involves the transfer of the tubes to a lyophilization machine located in the mini fridge, completing the comprehensive process.

All formulations are subjected to three replicates (n=3), and each is tested with three distinct plasma samples. This approach acknowledges that different plasma types can exhibit diverse behaviors depending on its type. The comprehensive design allows for a robust evaluation of the reagent formulations under varied conditions, contributing to a thorough understanding of their performance.

In the preparation of the assay, Recombiplastin 2G (Hemosil, 0020003051) is initially dissolved in 20 ml of Deionized (DI) water, and the mixture is gently stirred. The resulting solution is stored in the refrigerator at 5°C and has a recommended usage period of 20 days. Concurrently, a 20% Mannitol solution is meticulously prepared by micropipetting 20 g of D(-) Mannitol (Merck, K93436382646) into 100 ml of DI water. The solution is then subjected to vortexing and heating until a clear solution is obtained. Following this, 90 µl of the previously prepared reagent solution is meticulously combined with 10 µl of the 20% Mannitol solution.

Mannitol Formula

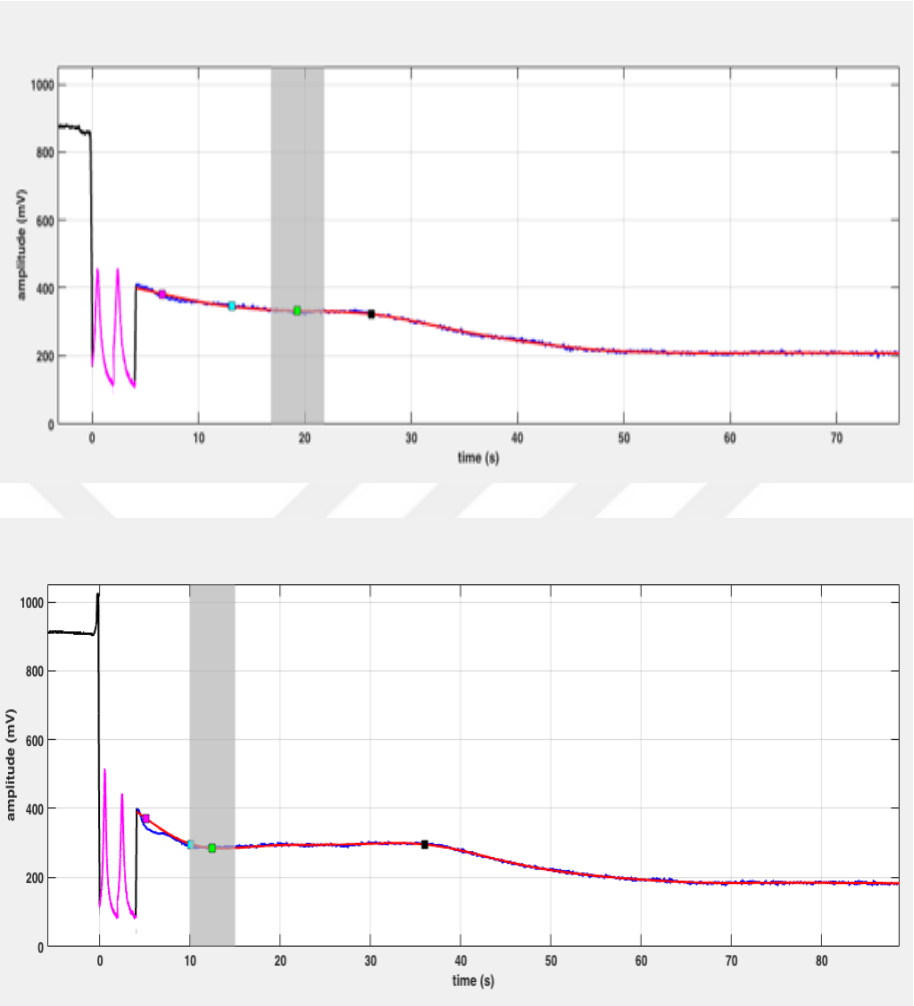

Figure 11: The beads, prepared utilizing the Mannitol formula were tested on open setup with low abnormal plasma.

Low abnormal plasma samples were introduced through the DOS applied channel. The TPV measurement indicated a sudden drop after injection, suggesting that the Mannitol formula, when applied in this context, may lead to an unexpected and abrupt decrease in the signal, highlighting the need for further investigation into the formulation's impact on coagulation dynamics (Figure 11).

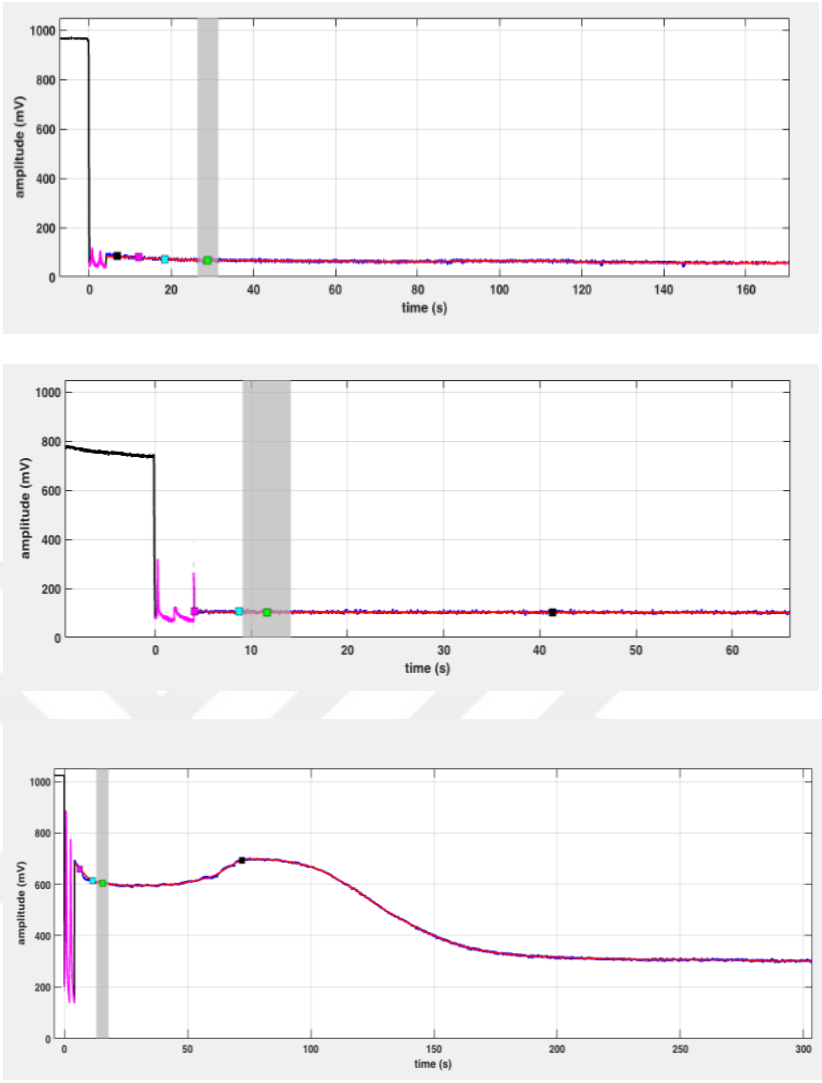

Figure 12: High abnormal plasma tests on beads prepared with mannitol formula

Similarly, beads prepared using the Mannitol formula were administered through the DOS applied and foil-covered COC cartridge, this time using high abnormal plasma. In all instances, the TPV measurement consistently indicated a sudden drop after injection. This observation emphasizes that the reagent with mannitol formula, under these conditions, may contribute to an unexpected and abrupt decrease in the signal during coagulation measurements with normal plasma (Figure 12).

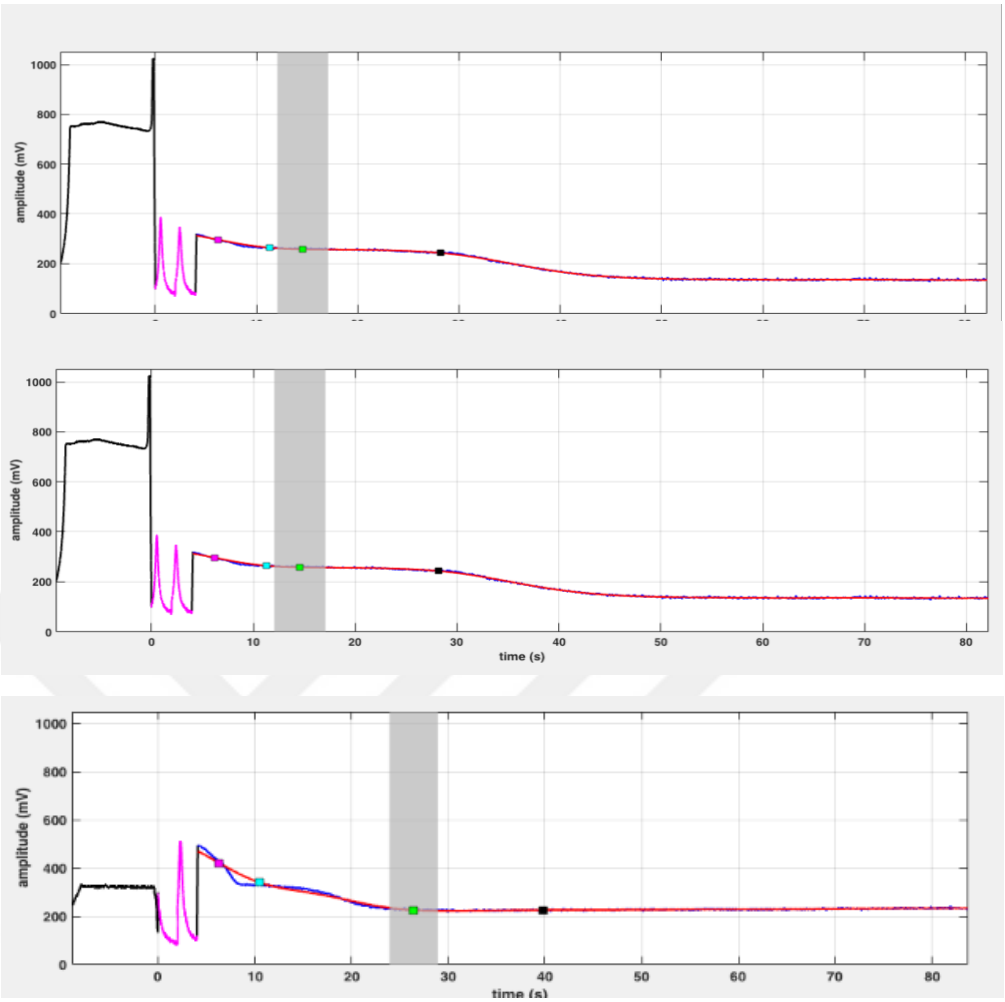

Figure 13: Normal plasma tests on beads prepared with mannitol formula.

The beads prepared using the Mannitol formula were introduced through the DOS applied and foil-covered COC cartridge, this time utilizing normal plasma (Figure 13). Once again, the TPV measurement consistently indicated a sudden drop after injection. This observation suggests that the Mannitol formula, under these specific conditions, may contribute to an unexpected and abrupt decrease in the signal during coagulation measurements with low abnormal plasma as we expect to see initial flat signal as a part of the quality control measurement.

Glycerol Mixing

The objective of this series of experiments is to investigate the impact of drying on the reagent by incorporating glycerol. The reagent mixture was prepared using the same procedural approach—one containing 0.25% glycerol. Both cartridges were then tested in an identical manner and subjected to the same drying conditions. A 2 µl reagent was

applied to each cartridge for every combination, and the drying process took place in a desiccator at 24°C with 28% humidity overnight. To discern the hydrophilic DOS effect on glycerol, parallel assays were meticulously planned, encompassing both scenarios with and without DOS.

Figure 16 shows experimental results from a solution that was prepared by combining a 0.25% glycerol formulation with Hemosil Recombiplastin 2G reagent. This mixture was applied to PMMA cartridge. The low abnormal plasma was used it was administered without DOS or a cover. The plasma volume utilized for the experiment was 13.5 µL.

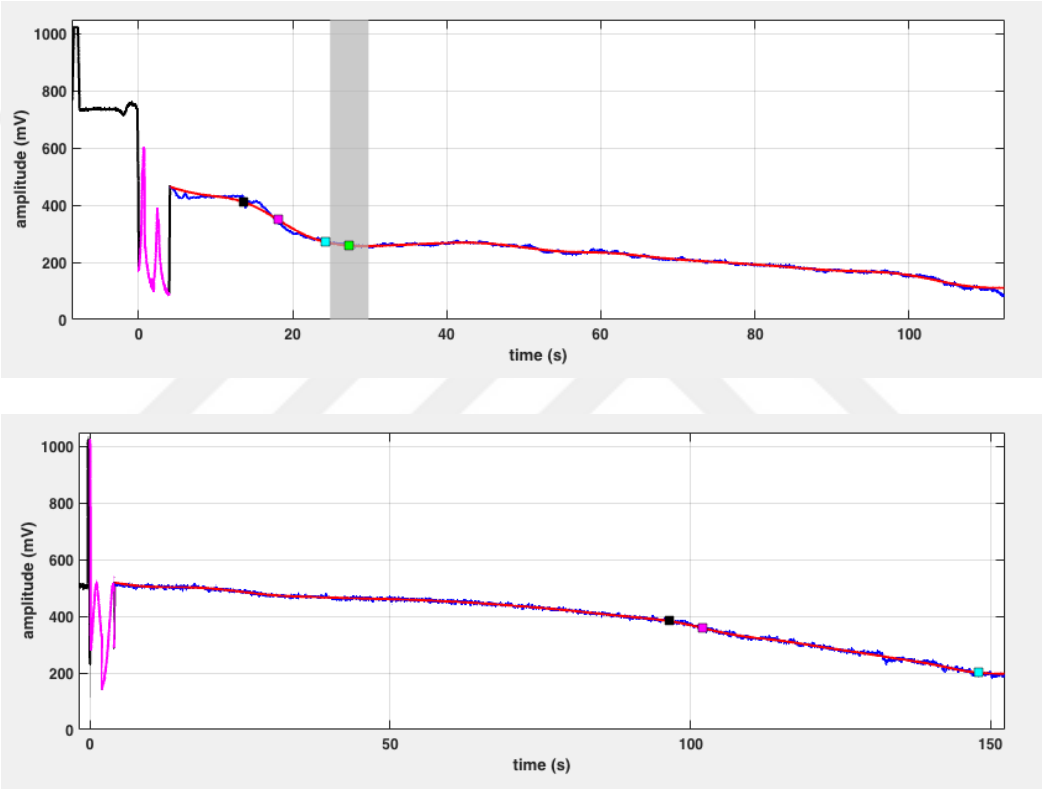

Figure 14: Low abnormal plasma tests conducted on PMMA cartridge, without DOS and cover.

Figure 15 demonstrates that the same experiment conducted with COC cartridge yielded PT value of 28 for low abnormal plasma which is 3 seconds prolonged compared to the acceptable range. It should be noted that this experiment was conducted without DOS and application of foil cover. Figure 16 shows that the same tests conducted with COC cartridge and application of DOS on top of the reagent formulation. However, it cannot be inferred that the reagent and cartridge combination is compatible with the expectations in terms of PT values and consistency.

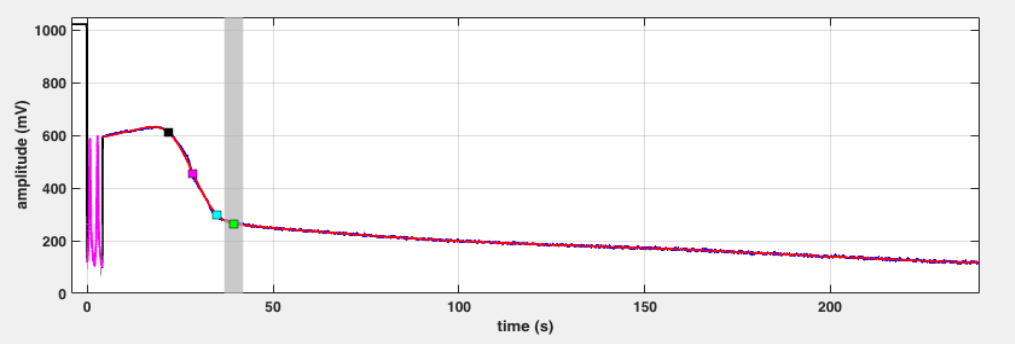

Figure 15: COC cartridge test with low abnormal plasma, without DOS and cover.

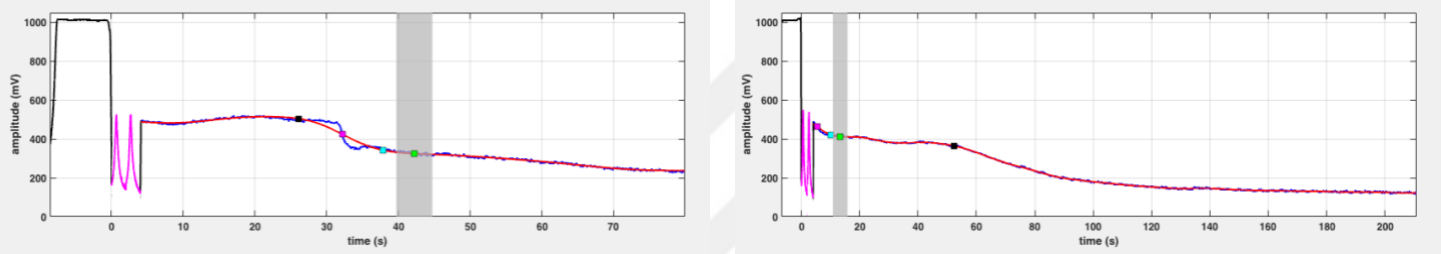

Figure 16: COC cartridge test with low abnormal plasma, with DOS and cover.

Glycerol – Mannitol Mixing

The objective of this series of experiments is to investigate the impact of glycerol addition on reagent drying. To achieve this goal, two distinct reagent mixtures were formulated: one containing 0.2% glycerol (MG) and the other without glycerol. Both mixtures were prepared using the same procedural steps and applied to cartridges under identical drying conditions. A uniform volume of 2 µl of reagent was applied to each cartridge for every combination, followed by overnight drying in a desiccator maintained at 24°C with 28% humidity. To discern the hydrophilic DOS effect on glycerol, parallel assays were designed, encompassing both conditions with and without DOS. Used materials are Recombiplastin 2G (HemosIL, cat no 3051, lot no N0504124), D (-)

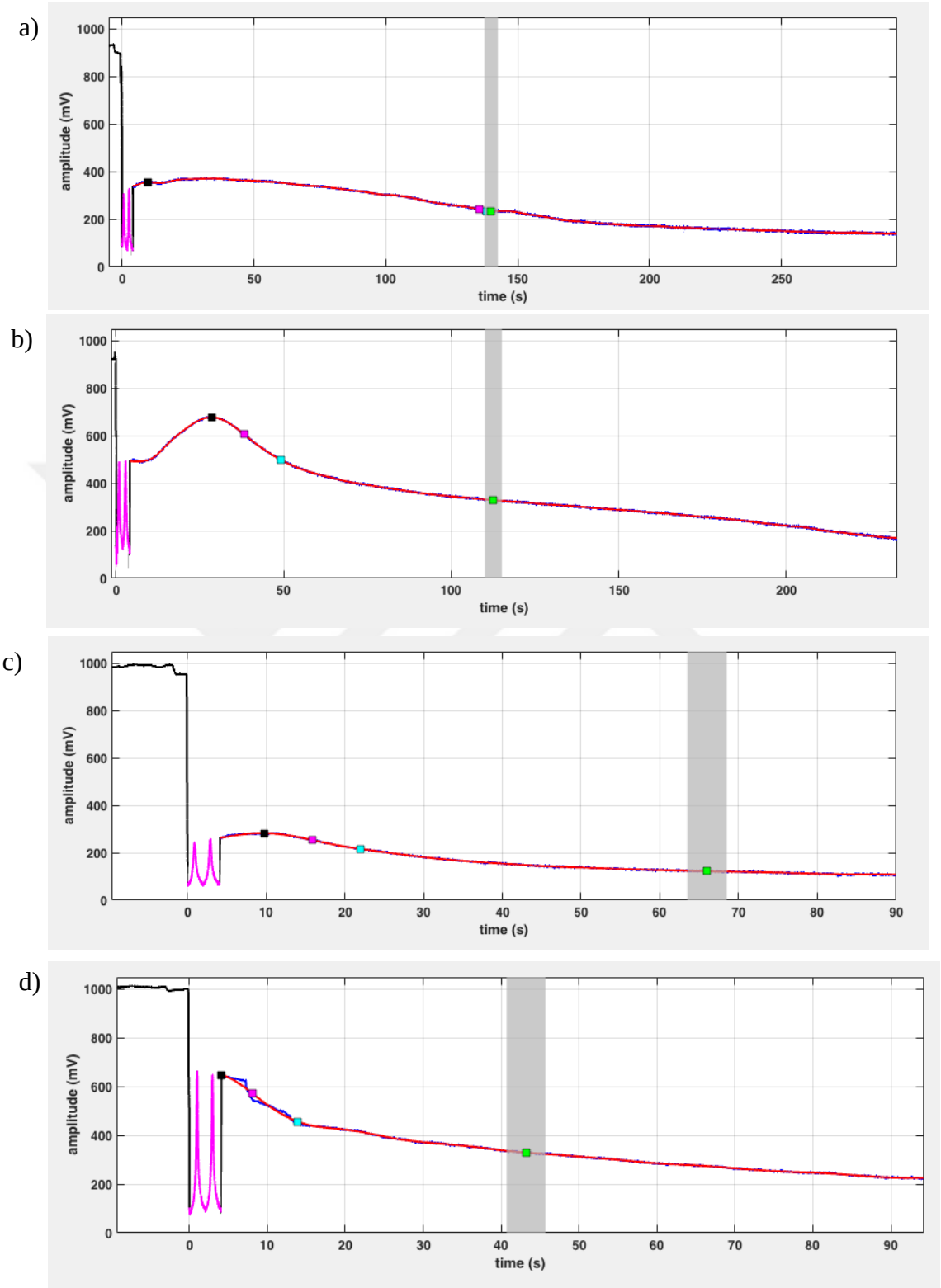

Figure 17: Recombiplastin 2G mannitol-glycerol formula (MG) – COC cartridges (a) and (b) are high abnormal plasma, (c) and (d) are low abnormal plasma.

mannitol (Merck, cat no K93436382 646, lot no 1059820500, prep date - 21.10.21),

Glycerol (Biofroxx, cat no 128LT002, lot no 5B617A74, prep date - 15.11.21), DOS (Sigma, cat no 323586, cas no 577-11-7), Low abnormal control assayed (HemosIL, cat no 3210, lot no N0604802, N0889961), $CaCl_2$ (lab made-20 uM), high pure DI water.

Figure 17 illustrates the analysis of high abnormal plasma using a COC cartridge with the MG formulation. DOS was applied with a foil cover; however, the TPV indicated a prolonged PT with a value of 135 seconds, suggesting a delayed coagulation response. In the second experiment conducted without a cover and DOS, the goal was to observe the exclusive effect of glycerol on the formula without being influenced by the presence of DOS and microfluidics. The results revealed an elevated signal amplitude after the addition of high plasma to the chamber, indicating an inconsistent set of results. Similarly, low abnormal plasma tests were conducted without DOS and a cover, yielding a 50% success rate. In Figure 17(c), the TPV value of 15 closely aligns with the low abnormal range specified by the manufacturer (17-25), while Figure 17(d) indicates a measurement

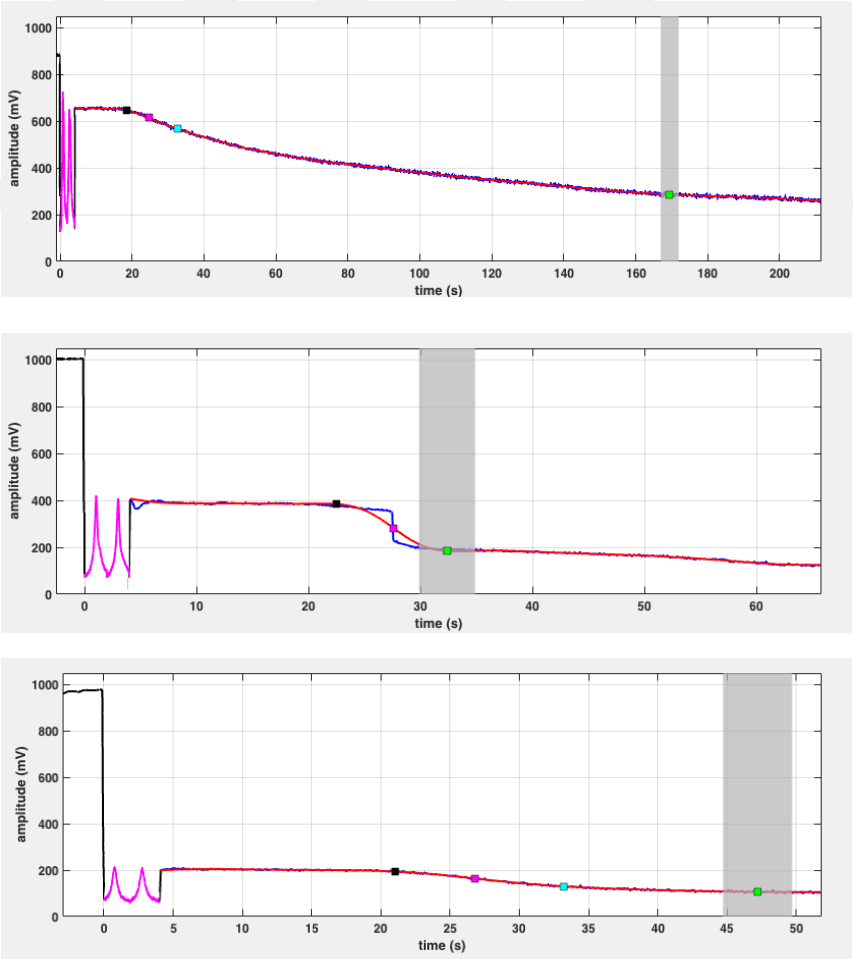

Figure 18: High abnormal plasma tested with PMMA cartridge. TPV values of 26, 27, and 24 seconds are yielded.

error. The cumulative findings suggest that the MG formula may not be fully compatible with the system.

Subsequent experiments were carried out using a PMMA cartridge to investigate the influence of the cartridge material. Figure 18 demonstrates that experiments conducted with PMMA yielded relatively better results compared to COC, with TPV values of 26, 27, and 24 seconds. These values are shorter than the high abnormal range specified by the manufacturer (26-45). It is essential to note that these experiments were conducted without DOS and a cover. Such inconsistent results led us to not consider MG formula for further experiments.

Approaches for Reagent Drying

Desiccator

A desiccator can be an essential tool in laboratory settings, particularly during the initial stages of a proof-of-concept study, where precise and controlled conditions are crucial such as in our case. Its primary purpose is the removal of water content from

Figure 19: Desiccator device found in our laboratory used for primary drying process of reagent.

reagents, ensuring that the experimental environment remains stable with the addition of mannitol.

Desiccator is an equipment utilized for getting rid of moisture from the atmosphere surrounding a sample. During this process, drying takes place thus any moistness or water vapor is removed from the air around a substance. It is made of materials such as glass or plastic that are sometimes sealed with a cap that fits tightly on it and are filled with silica gel or any other form of drying agent (Figure 19). Thereafter, within the desiccator, the drying agent absorbs the moisture present in the environment creating a dry environment.

In the last stages of lyophilization, desiccators play an important role. After lyophilization, material should be stored in a desiccator to keep its stability intact and prevent reabsorption of moisture. This ensures long-term preservation of lyophilized products. For example in one study discussing folding equilibrium of huntingtin exon 1 monomer, vacuum desiccators were used for storing lyophilized powder until further use [79] whereas in another study focusing on development of immunomodulatory ECM-like microspheres for bone regeneration, freeze-dried microspheres were kept inside a desiccator for future utilization [80]. This shows why it's vital to always have functional dessicators to ensure that your lyophilized materials stay intact all through this entire process. Furthermore, during preparation of gum odina-gelatine based antimicrobial loaded biodegradable spongy scaffolds dried scaffold was placed into vacuum dessicator for subsequent usage which indicates common practice on ways to preserve lyphilized material [81]. Additionally, in the field of pharmaceuticals, the lyophilized favipiravir-loaded PLGA nanoparticles were kept in a desiccator for further evaluation studies, emphasizing the significance of desiccator storage in maintaining the stability of lyophilized formulations [82]. Moreover, the desiccator is also utilized in other applications such as in the storage of herbal nanoparticles containing ointment of leaves extract of Rhynchosia rothii, where the lyophilized powder was stored in a desiccator containing saturated KBr solution for 24 hours before being kept at -20ºC [83] indicating how carefully they handle storage after lyophilization to keep the product stable. Consequently, a desiccator is an important component of any lyophilization process that ensures preservation and stability of freeze-dried material for future use.

While desiccator devices commonly do not involve the context of reagent drying, the use of the desiccator in our case mostly stems from the necessity for a fast and controllable integration of reagents in the initial experiments conducted in our lab.

Lyophilization

Lyophilization, also known as freeze-drying, is a process commonly used to enhance the stability and shelf life of reagents, particularly in situations where maintaining a liquid form may be challenging due to factors such as stability, reactivity, or ease of storage and transport [84]. In the context of PoC devices, lyophilization plays a crucial role in reagent immobilization. For instance, in the development of a point-of-need bioluminescence-based immunoassay, the lyophilization of all assay components, including labeled antibodies, was pursued to achieve stability at ambient temperatures for extended periods of time [85]. Similarly, in the development of a visually readable loop-mediated isothermal reverse transcriptase nucleic acid amplification test for the detection of Ebola Zaire RNA, lyophilized reaction mixtures retained activity for prolonged periods under dry conditions at room temperature [86]. Furthermore, in the standardization of real-time PCR and RT-qPCR diagnostics in virology, a lyophilized matrix containing ready-to-use primers and probe solution was prepared to achieve stability and ease of use [87]. Moreover, the impact of lyophilized cell-free protein expression systems has been growing, indicating the significance of lyophilization in immobilizing reagents for protein expression [88]. Also, a relationship has been shown between the amount of deuterium uptake and the length of time that monoclonal antibody formulations remain stable under lyophilized conditions which emphasizes on cases when biological reagents are preserved through lyophilization [89].

On the other hand, moisture presence in the reagent may cause instability as well as inefficiency. To solve this problem, numerous drying methods can be used. Foremost, desiccation with silica gel or molecular sieves effectively absorbs excessive water from reagent and preserves its integrity. In addition to that, lyophilization is also known as freeze drying where it involves freezing the reagent followed by removing ice crystals so that one can leave behind a substance that is dry and stable. Alternatively, some hygroscopic additives such as glycerol or polyethylene glycol can be incorporated to prevent moisture absorption in certain cases. Therefore, careful selection of drying method and reagent composition is critical for accurate PT measurements under laboratory conditions [90]. Hence, lyophilization is a versatile technique that plays a critical role in immobilizing reagents for PoC devices, ensuring their stability and shelf life, and enabling their ease of use in various applications. Careful consideration of the

reagent composition and the chosen drying method is essential to ensure accurate PT measurements in laboratory settings.

In another lyophilization study performed for CDG-3 substrate in an MES buffer, the impact of the lyophilization process on its stability and functionality was investigated, with a specific focus on the role of sugar excipients. CDG-3, a substrate utilized in enzymatic assays, was subjected to lyophilization to assess its performance under different conditions, including exposure to various temperatures. The results indicated that lyophilization, particularly with lactose or mannitol as excipients, effectively preserved the stability of CDG-3, providing crucial insights into potential applications for point-of-care devices and enzymatic assays involving this substrate [91]. In another lyophilization study conducted for CNBr-activated agarose beads (CAABs), the focus was on the effect of additives, specifically lactose and PEG, on preserving the spherical shape of CAABs after rehydration. The study aimed to address the challenge of maintaining the structural integrity of CAABs, crucial for their performance in bio-separation applications. Notably, the incorporation of 10% PEG8000 and 10% (PoC/v) lactose in a Na_2HPO_4–citric acid buffer (20mM, pH 4.0) emerged as an effective strategy to prevent the loss of spherical shape during the lyophilization process. This preservation method, involving specific additives and lyophilization, showcased the potential to retain the original properties of CAABs, making them suitable for applications like preparing affinity chromatographic media for protein purification [92]. In another lyophilization study, FTIR spectroscopy was used to investigate the protective mechanism of Ca-alginate and mannitol for *Bifidobacterium animalis* subsp. *lactis* Bb12 during freeze-drying and 10 weeks of storage at room temperature under different water activity levels (0.07, 0.1, and 0.2). Ca-alginate and Ca-alginate-mannitol micro encapsulants were prepared, and the water activity of the freeze-dried beads was adjusted. Mannitol in the Ca-alginate system interacted during freeze-drying and storage, while Ca-alginate-mannitol effectively preserved cell envelopes and proteins. The study suggests Ca-alginate-mannitol's superior efficacy in preservation after freeze-drying and 10 weeks of storage compared to Ca-alginate alone [93]. In another lyophilization study for improving the oral bioavailability of therapeutic proteins encapsulated in nanoparticles, cryoprotectants (mannitol, sorbitol, sucrose, trehalose) and their concentrations (1-10% PoC/v) were investigated. Mannitol at 7% PoC/v produced small-sized nanoparticles (313.2 nm) with positive charge and uniform distribution, preserving bioactivity against

mechanical stress during lyophilization. This study underscores the crucial role of an appropriate cryoprotectant in maintaining particle properties, structural integrity, and bioactivity, cautioning against incompatible choices that may lead to cake collapse and heterogeneous particle sizes [94].

The following study focused on enhancing the sensitivity of lateral flow devices for PoC applications, particularly in low-resource settings. Lateral flow devices are commonly used in PoC scenarios, but they often lack the required sensitivity for diagnosing diseases accurately. The research aimed to address this limitation by incorporating signal amplification, a technique commonly used in laboratory assays but challenging to implement in PoC settings. The proposed approach involved the dry storage of ELISA reagents—specifically, horseradish peroxidase conjugated antibody and diaminobenzidine substrate. The dry preservation method, involving $FeSO_4$–EDTA, trehalose, and BSA, demonstrated remarkable stability, with the HRP-antibody retaining around 80% enzymatic activity after over 5 months at an elevated temperature of 45°C. Additionally, the DAB substrate exhibited over 90% activity retention during a three-month period under the same conditions. The study successfully integrated these dry-preserved reagents into a lateral flow assay for detecting a malarial biomarker. This is a crucial advancement as lateral flow devices are widely used in PoC applications due to their simplicity and rapid results. By incorporating signal amplification in a format compatible with PoC requirements and ensuring long-term stability of the necessary reagents, the research paves the way for more sensitive and reliable diagnostic tools in resource-limited settings. The potential of these dry-preserved reagents was further demonstrated by their successful integration into an automated two-dimensional paper network (2DPN) ELISA card, highlighting their adaptability for various diagnostic platforms in point-of-care settings [95].

As discussed above, there are multiple scenarios where lyophilization can be employed in terms of biosensors and PoC devices. In our case, we used lyophilization for the bead formation made up of Recomplastin 2G and various sugar additive materials. This experiment investigates issues with reagent stickiness and heterogeneous dispersion in cartridges, hindering intended functionality. Four key parameters are varied: drying method, reagent ingredient, reagent applying area, and hydrophilic surface activator. Lyophilization is explored as an alternative to vacuum drying, with freezing at -200°C and subsequent drying at -3000 millibars. Reagent ingredient experiments omit D-

mannitol sugar to prevent stickiness. Different regions within cartridge channels (inlet, channel, measurement chamber) are tested for reagent application. Hydrophilic surface activator transition involves shifting from DOS to acetone-based P100 solution to assess their impact on reagent working capacity. This comprehensive method aims to address observed issues and improve reagent functionality within cartridges.

1st Set

Cartridge Number	Reagent Combination	Passed/Failed
C1-C5	Reagent applied in measurement chamber > freeze at -80 > lyophilization > measurement	Failed
C2-C3-C4	Reagent applied in measurement chamber > freeze top on liquid nitrogen > lyophilization > measurement	Passed

2nd Set

Cartridge Number	Reagent Combination	Passed/Failed
C1-C2	Reagent in channel and chamber > liquid nitrogen > lyophilization > measurement	Failed
C3-C4	2ul reagent inlet > liquid nitrogen > lyophilization > DOS (channel+chamber) > air dry > measurement	Failed
C5-C6	Reagent in channel and half of chamber > liquid nitrogen > lyophilization > DOS (reagent-free part) > air dry > measurement	Failed
C7-C8	Reagent in channel and half of chamber > H_2O (reagent-free part) > liquid nitrogen > lyophilization > measurement	Failed
C9-C10	2ul reagent in inlet > H_2O (reagent-free part) > liquid nitrogen > lyophilization > measurement	Failed

C11-C12	2ul reagent in chamber > liquid nitrogen > lyophilization > DOS (reagent-free part) > air dry > measurement	Passed
C13-C14	DOS whole channel and chamber > air dry > 3ul reagent in chamber > liquid nitrogen > lyophilization > measurement	Failed
C15-C16	2ul reagent in chamber > H_2O H_2O (reagent-free part) > liquid nitrogen > lyophilization > measurement	Failed
C17-C18	2ul reagent in chamber > liquid nitrogen > lyophilization > DOS whole channel and chamber > air dry > measurement	Failed
Manuel 1	Reagent + mannitol	Passed
Manuel 2	Reagent - mannitol	Passed

3rd Set

Cartridge Number	Reagent Combination	Passed/Failed
S1-S2-S3	S100 > air dry > reagent > lyophilization > measurement	Failed
S4-S5-S6	Reagent (chamber) > lyophilization > S100 > air dry > measurement	Failed
P1-P2-P3	P100 > air dry > Reagent > lyophilization > measurement	Passed
P4-P5-P6	Reagent (chamber) > lyophilization > P100 > air dry > measurement	Failed

4th Set

Cartridge Number	Reagent Combination	Passed/Failed

PH1-PH2-PH3	P100 (chamber) > air dry > reagent > lyophilization > DOS (inlet+channel) > measurement	Passed
PH4-PH5-PH6	P100 (channel) > air dry > reagent > lyophilization > DOS (channel) > measurement	Failed

5th Set

Cartridge Number	Reagent Combination	Passed/Failed
PH1 <...>PH10 (low abn plasma)	P100 (chamber) > air dry > reagent > lyophilization > DOS (inlet+channel) > measurement	Passed
PHK1-PHK2-PHK3 (blood)	P100 (chamber) > air dry > reagent > lyophilization > DOS (inlet+channel) > measurement	Failed

6th Set

Cartridge Number	Reagent Combination	Passed/Failed
PH1 <...> PH10 (normal plasma)	P100 (chamber) > air dry > reagent > lyophilization > DOS (inlet+channel) > measurement	Passed
PH11 <...> PH20 (high abn plasma)	P100 (chamber) > air dry > reagent > lyophilization > DOS (inlet+channel) > measurement	Passed
PHK1 <...> PHK5 (blood)	P100 (chamber) > air dry > reagent > lyophilization > DOS (inlet+channel) > measurement	Failed

The series of experiments conducted to address issues with reagent functionality within cartridges revealed valuable insights into the effects of the freeze-drying method on the working capacity of the reagent. The choice of lyophilization as an alternative to

vacuum drying in a desiccator stemmed from the information obtained in meetings with cartridge manufacturers, who predominantly use the lyophilization method. The lyophilization process, involving freezing the reagent at extremely low temperatures and subsequently drying it under high negative pressure and low humidity, demonstrated promise in preserving the structural integrity of the reagent. This method, commonly employed in the pharmaceutical industry, holds potential for resolving issues such as stickiness and heterogeneous dispersion observed in the conventional drying process. Moreover, it serves as a preliminary test for potential implementation in mass production, offering insights into its efficacy in addressing the identified problems. In investigating the impact of the freeze-drying method, the experiments also shed light on the influence of reagent ingredients. Notably, the omission of D-mannitol sugar, a previously used additive to prevent reagent loss, proved effective in preventing stickiness after lyophilization.

The freezing of reagents by using liquid nitrogen before lyophilization further addressed concerns regarding potential fiber breakage or changes in cartridge morphology at extremely low temperatures. This finding contributes to refining the understanding of optimal reagent formulations in freeze-drying processes. Exploration of different reagent applying areas within the cartridge channels, including the inlet, channel, and measurement chamber, aimed at addressing issues arising from reagent-induced structures hindering fiber movement. This investigation provided insights into the spatial distribution of reagents and their impact on preventing undesired interactions with the fiber surfaces, which is crucial for optimizing cartridge performance. The transition from the traditional DOS hydrophilic activator to acetone based P100 chemical was prompted by observed decreases in reagent working capacity associated with the ethyl alcohol content in DOS. The experiment sought to determine if the acetone-based alternative exhibited a less hydrophilic effect, potentially mitigating issues related to reagent diffusion and changes in surface chemistry. This shift in activator choice adds an important dimension to optimizing the hydrophilic properties of the cartridge channels, thereby contributing to improved sample progression. In conclusion, the comprehensive experimental approach addressed multiple facets of reagent-related challenges within cartridges. The findings underscore the potential benefits of the freeze-drying method, specifically lyophilization, in preserving reagent structure and preventing stickiness. The experiments also offered insights into optimal reagent formulations, spatial distribution

within the cartridge channels, and the choice of hydrophilic surface activators. These findings collectively contribute to advancing the understanding of factors influencing reagent performance and provide a foundation for refining cartridge design and production processes. Future studies may further explore the scalability and reproducibility of the lyophilization method in mass production settings, ensuring its viability as a practical solution to enhance cartridge functionality.

Bead Formation

Previously the challenges associated with developing recombinant protein pharmaceuticals were discussed emphasizing the complexity of protein production, purification, and their limited stability. To handle these difficulties, freeze-drying is usually employed in the pharmaceutical industry to form stable protein formulations. However, the lyophilization process leads to freezing and drying stresses that can result in protein denaturation. Even with the use of stabilizers, proteins in solid form may still face limitations in long-term storage stability. Lyophilization, commonly employed for the preparation of solid protein pharmaceuticals, introduces numerous freezing and drying stresses, encompassing solute concentration, ice crystal formation, pH alterations, and more. These stresses have the potential to denature proteins to varying extents. Consequently, the incorporation of stabilizers becomes essential in protein formulations, serving to safeguard protein stability throughout the freezing and drying phases [96]. In a nanoparticle design study, alginate–C18 conjugate nanoparticles, featuring reduced size and ζ potential, were developed as a non-toxic oral insulin delivery system. Coated calcium alginate beads served as carriers for these nanoparticles, exhibiting controlled drug release and enhanced mucus penetration. The combined dosage form, consisting of both nanoparticles and beads, demonstrated improved blood glucose lowering and elevated blood insulin levels compared to individual components, highlighting its potential for effective oral insulin delivery [97]. Accordingly, as an enzyme with its active ingredient of tissue factor, our design protocol required the stabilization of the reagent for testing PT in a PoC device. For the end-product stabilization approach, we have tried multiple methods, including freeze-drying, vacuum drying, desiccator and oven drying. The rest of the section discusses these approaches and the obtained results with our system.

Protocol / Materials

The purpose of this section is to explain results of the experiment regarding the -60°C lyophilization device and reagent formulation. We prepared mannitol added and plain reagent as in 3µL according to the reagent preparation protocol provided above. Plain reagent was used directly from the vial and nothing else was used as additive. Mannitol-reagent formula was prepared according to the protocol given above as well. The beads were prepared one day before the lyophilization process. They were kept at -80°C freezer overnight and next day they were dried 4-5 hours inside the lyophilization device Christ Alpha1-2 LD Plus / Serial No 26372.

Results

The tests were performed in terms of the efficiency of the reagent beads in two different set of cartridges as PMMA and COC. These tests were conducted by mixing the reagent beads inside a centrifuge tube with the desired plasma. This approach allows the observation of the effects of the reagent, eliminating any influences stemming from microfluidics and interactions between the reagent and fibers within the cartridge.

The results showed that COC cartridges yielded sudden drop after injection of the test sample where PMMA cartridge yielded a nice coagulation curve in an expected form. However, PT values were prolonged, this is speculated to be due to reagent formulation. PMMA cartridge gave 60-44-66 as PT values for low abnormal plasma (range of 17-25). Two of the COC cartridges were tested and one of them showed sudden drop of signal within 4 seconds and other one had saturated signal where we could not see the real signal properly. Although the signal was not ideal, the TPV yielded 55 seconds of coagulation similar to the PMMA cartridge's TPV values.

Figure 20: Beads after they are collected from the device.

Approaches for Reagent Positioning

Measurement Chamber

The immobilization of the reagent preceding the tests was undertaken by our partnering firm, adhering to the provided instructions from our laboratory. The specific reagent drying methodology employed during this process was within the purview of our partner, and detailed procedural protocols for this step were not explicitly provided by our institution. Following the completion of the immobilization process, the reagent was dispatched to our facility for further evaluation. In the subsequent testing phase, several challenges were encountered with cartridges containing foil designed for immediate use. To address this, three cartridges were purposefully selected from a batch of 50, namely the first, middle, and last cartridges. A meticulous inspection was conducted under a microscope to ascertain the proper positioning of the nickel piece at the bottom of the fiber. However, upon subjecting these cartridges to a reader for a frequency sweep in air, an unexpected flat signal was observed, indicative of restricted fiber oscillation. Consequently, due to this anomaly, further progression in the testing process was halted at this stage.

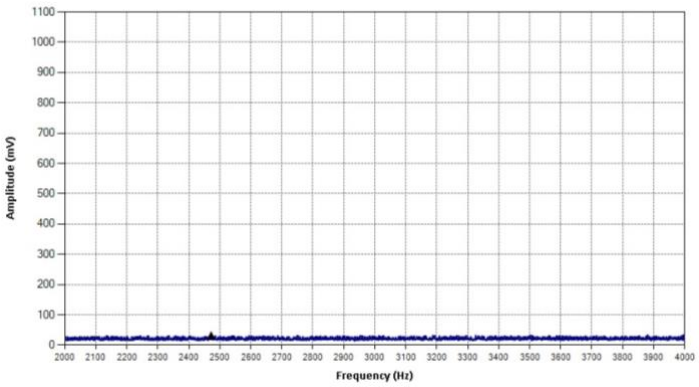

Figure 21: Flat signal in the absence of an expected resonating fiber.

In light of the challenges encountered with cartridges containing foil, we opted to extend our investigation by examining cartridges without foil. Three cartridges, selected from a batch of 50 (the first, middle, and last cartridges), underwent a meticulous inspection under a microscope to ascertain the proper positioning of the nickel piece at the bottom of the fiber. Of significance, upon close examination, images revealed a presence of dried excess material (depicted in white, Figure 22) in the right groove of the measurement chamber for all three cartridges. This material hindered the free oscillation of the fiber, rendering it impossible to achieve a frequency sweep in air. While the fiber

retained lateral mobility, vertical oscillation was impeded due to the presence of the dried material, presenting a substantial obstacle to the testing process.

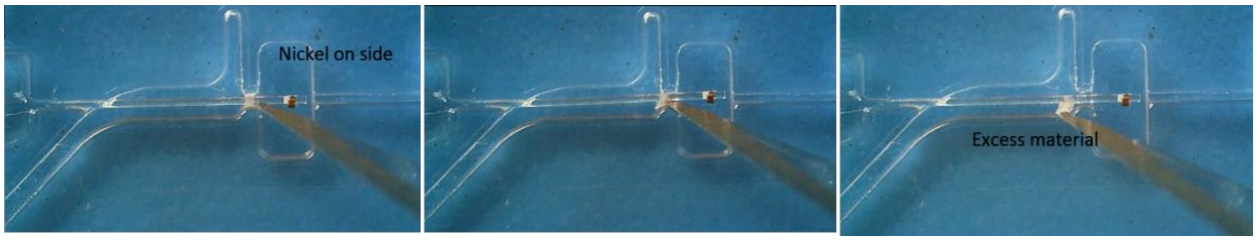

Figure 22: Above shown the reagent residue on the COC cartridge neck.

Following the removal of the residue, as depicted in Figure 22, foil was subsequently applied to the cartridges. Notably, frequency measurements in air were successfully obtained for two out of the three cartridges, leading to interference as the nickel piece came into contact with the foil.

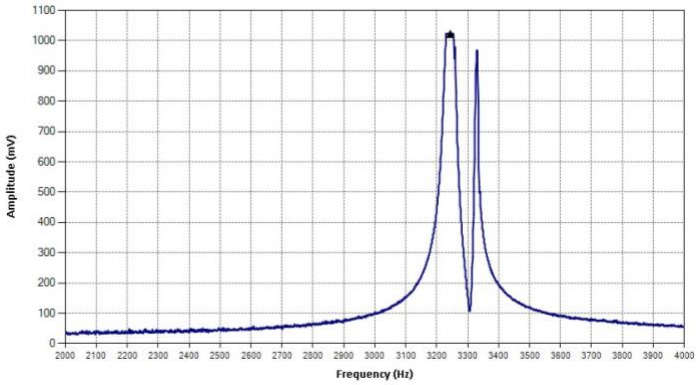

Figure 23: Frequency sweep after the removal of the residue from neck of the cartridge.

Subsequently, we proceeded to load whole blood directly from the fingertip, resulting in the observation of well-defined coagulation curves. From these curves, we derived time-to-peak velocity points for PT without correction factor, yielding values of approximately 9.6 and 8.1 seconds. This successful outcome underscored the optimal functionality of both capillary flow and the PT reagent in facilitating accurate and reliable coagulation assessments.

In conclusion, the persistence of excess dried reagent, possibly accompanied by DOS, remains a prominent challenge, impeding the unhindered movement of the fiber. Once the excess material is removed, the system functions optimally, with no reported issues concerning capillary flow or reagent performance. The positioning of the nickel piece emerged as another critical factor, as its side placement results in interference with

the foil, hindering free movement. There is a clear need for optimization and enhanced visualization in the placement process. Additionally, cartridges with foil are deemed unusable in their current state, necessitating the removal, cleaning, and reapplication of foil, albeit with inherent risks such as fiber breakage and challenges in complete foil removal. Consequently, production activities should be temporarily halted until this issue is effectively addressed. Regarding the stability of dried reagent, initial tests indicate functionality in one-week-old cartridges.

Inlet

To investigate the impact of the reagent spot on PT values, a series of experiments were devised. Reportedly, two distinct spots—namely, the inlet and chamber—were selected. These reagents were present in both normal and diluted concentrations, with final concentrations of 2% and 1%. All experiments were executed in an open setup configuration with high abnormal plasma obtained from a -80° freezer. Results from two distinct experimental conditions indicated that the measurement chamber outperformed

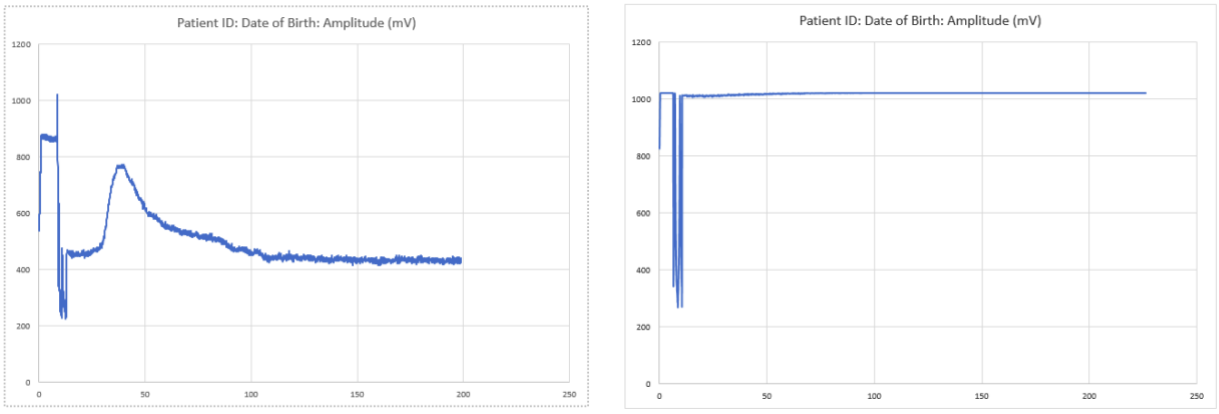

Figure 24: Experimental result from a cartridge whose reagent was placed in the inlet, a) normal concentration of reagent was applied in 1 uL, b) diluted reagent test applied in 1 uL.

the inlet as a preferable choice. In one instance, a flat signal was observed, while in the other, an unexpected signal increment occurred after the initiation of coagulation addressing an unexpected mechanical issue within the cartridge.

Hydrophilization of Microfluidic System

P100

The P100 Hydrophilic coating represents a pioneering and patented innovation known for its exceptional hydrophilic attributes, specifically crafted for versatile applications, with a primary emphasis on single-use diagnostic consumables utilizing

capillary microfluidics. This coating presents several distinctive features, including an impressive water contact angle of around 10°, ensuring the creation of a profoundly hydrophilic surface. Boasting a functional lifespan surpassing 10 years, P100 contributes to a two-year shelf life for coated medical devices. The application process is rapid, uncomplicated, and flexible, necessitating only 5 seconds for coating and an additional 10 seconds for drying. It is crucial to note that the coating demonstrates outstanding adhesion to diverse materials, ensuring consistency across surfaces such as polycarbonate, polystyrene, acrylic/PMMA, glass, and metals. P100's adaptability extends to its compatibility with various coating methods, encompassing spray, dip, spin, brush, roller, or ink-jet coating, rendering it suitable for diverse equipment and devices. Despite its biocompatibility and utilization of safe solvent chemistry, it is imperative to highlight that P100 is expressly recommended for single-use due to its significant interaction with liquid water. Moreover, the processing guidelines for P100 underscore the critical importance of surface cleanliness and provide insights into optimal coating thickness (10 nanometers) and removal methods, accentuating the straightforward application and maintenance of the coating. The demonstrated extended functional life of the coating, as evidenced through accelerated studies, ensures its durability, even when subjected to standard room temperature storage conditions. Guidelines for storage, disposal, and safety stress the necessity for proper handling and storage practices, highlighting the product's resilience to variations in temperature, humidity, and vibration. So, P100 has been identified as a creative solution that is great both at being hydrophilic and easy to use on different medical devices with a wide range of functionalities [98].

DOS

Sodium salt of dioctyl ester of sulfosuccinate (DOS) is a surfactant that is commonly used for surface property modification in microfluidics channels. This is because these types of devices known as lab-on-a-chip or PoC systems, are required to be hydrophilic so as to improve their efficiency and reliability. Efficient flow of fluid, minimizing air bubbling, and increased interaction between sample and channel surfaces can thus enhance diagnostic accuracy and sensitivity. By employing surfactants like DOS hydrophilicity can get promoted thereby enabling efficient sample manipulation inside the gadget by altering the surface characteristics of micro channels [99]. Hence, we have been using this substance in order to create a microfluidic-friendly environment.

In the hydrophilic solution preparation and loading processes, a 0.5% DOS solution is first created by dissolving 0.5 grams of DOS in 100 ml of ethanol. This solution is then stored in the refrigerator for future use.

Subsequently, 5 µl of the prepared DOS solution is carefully loaded via a pipette from the inlet until it reaches the end of the measurement chamber, with special attention to avoiding overflow into the fluid stop zone. Following the loading step, the system is left to dry in the air for a duration of 10 minutes, ensuring the proper setting and adherence of the hydrophilic solution within the measurement chamber.

Concentration of DOS

The objective of this experiment is to investigate the impact of hydrophilicity on the abrupt signal decline following two sweeping signals. DOS, in both its original concentration and a 1/20 ethanol diluted concentration, is employed. Plasma and blood are utilized in both diluted and standard concentrations. The experimental setup is conducted in an open configuration. Cartridges made of COC are supplied by our partner firm, while PMMA cartridges are manually prepared in the laboratory. There are no specific requirements stipulated for room temperature or humidity. The liquid volume for each test is precisely 13.5 µL. Lyophilization is executed in accordance with the established protocol, with and without mannitol, and the lyophilization duration spans 24 hours. After the extraction of samples from the device, they are stored in aluminum foil without silica beads. A new vial of Recombiplastin 2G, exclusive to this experiment, is opened and did not dissolved. Post-liquid nitrogen exposure, the samples are not subjected to a one-hour wait at -80°C. Instead, the -80°C environment is utilized solely

as a transitional holding point until the completion of freezing, after which the samples are promptly transferred to the Alpha 1-2LD Plus lyophilization device.

The initial measurement involved the application of DOS at a 1/20 concentration, left to dry for a minimum of 15 minutes. Subsequently, the cover was applied, and low

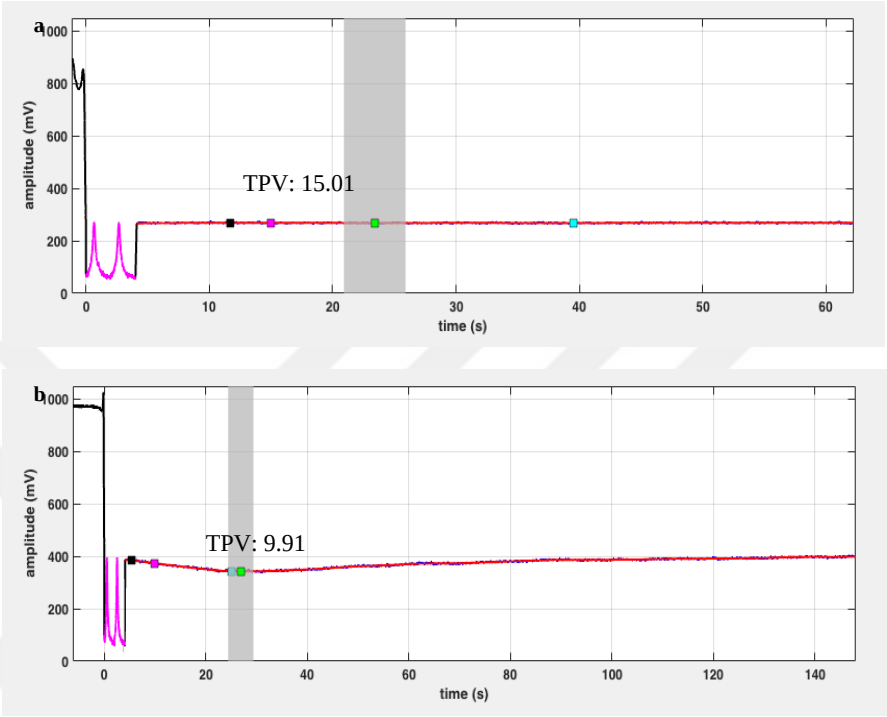

Figure 25: Figures a) and b) represent the two replicas of the same experiment conducted with COC cartridges.

abnormal plasma was introduced into the inlet in the standard volume of 13.5 µL. Notably, the observation did not reveal a sharp and sudden decrease in the signal. This prompts consideration regarding the potential influence of liquid introduction speed and its concentration on signal behavior. It's worth highlighting that this specific measurement did not incorporate a reagent, and as a result, the expectation was the absence of a coagulation curve, as the result indicated.

Under identical conditions to the previous two measurements, the current test was conducted using blood instead of low abnormal plasma (Figure 26). Notably, the coagulation time fell within the expected range of 200-250 seconds, aligning with predictions for healthy blood in the absence of a reagent. This observation reinforces the

sensitivity of the measurement to variations in sample type and further underscores the impact of specific conditions on coagulation behavior.

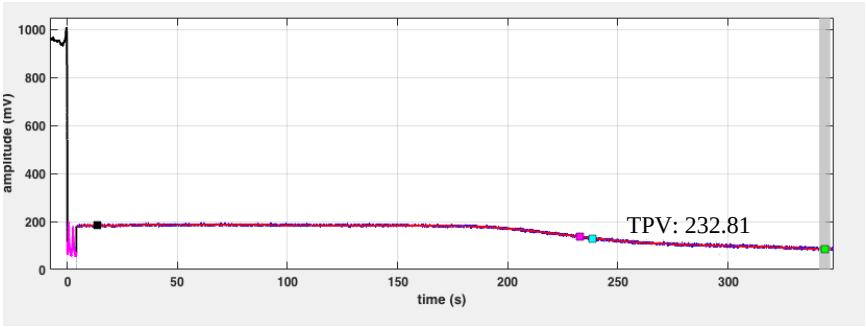

Figure 26: Under identical conditions to the previous two measurements, the current test was conducted using blood instead of low abnormal plasma.

This control measurement given below at Figure 27 aimed to assess whether normal concentrations of DOS would still induce a sudden decrease in the signal when using low abnormal plasma. The graphical representation indicates that TPA, TPV, and TPD values align consistently with anticipated results, generating values akin to those observed before the designated range of 17-25 seconds and yielding a PT of 14 seconds. These findings suggest that the control conditions produced the expected outcomes, providing a baseline for evaluating the impact of DOS concentrations on signal behavior.

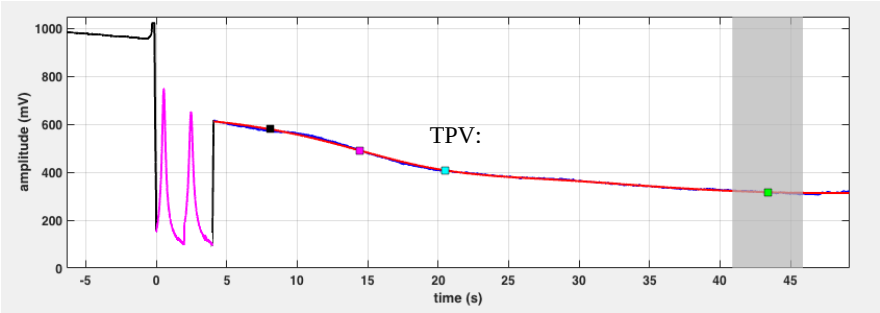

Figure 27: The control measurement.

In the case of the 1/20 DOS-applied cartridge with the addition of reagent and low abnormal plasma, the observation reveals a distinctive coagulation curve (Figure 28). Unlike previous instances where a sudden decrease was typical, the current scenario does not exhibit such behavior. Notably, the PT value for low abnormal plasma is recorded as 14.0 seconds, indicating a deviation of 3 seconds earlier than the initial value within the specified range. This shift in PT values suggests a nuanced influence of DOS concentration and the presence of reagent on the coagulation dynamics, possibly

highlighting the complexity of the interplay between components in the measurement process.

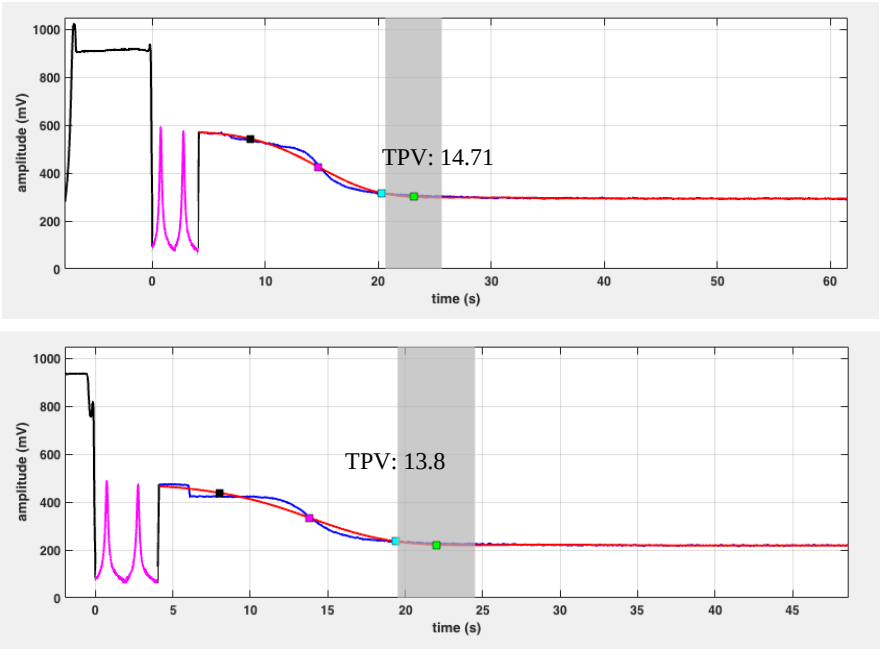

Figure 28: 1/20 DOS-applied cartridge with the addition of reagent and low abnormal plasma.

In this experiment conducted with blood and reagent at a 1:1 ratio, a distinct sudden decrease is observed, reminiscent of previous instances (Figure 29). The combination of blood and reagent, introduced to the system in a 13.5 µL volume, produces a coagulation curve. It's noteworthy that while the presence of reagent may expedite the coagulation process, the resulting curve appears misleading. The PT value recorded in this case, typically indicating a healthy range of 10-12 seconds, deviates from expectations. This

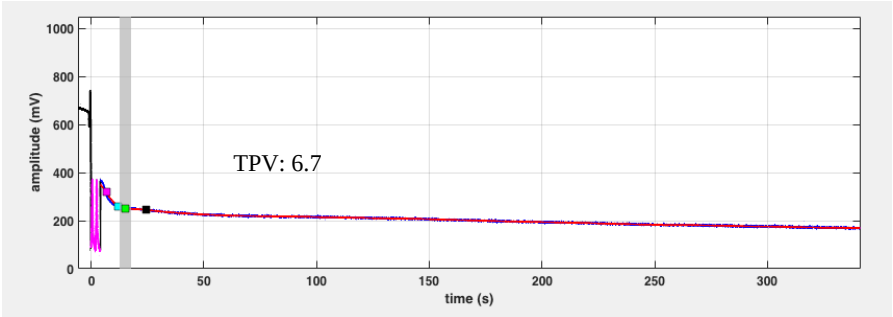

Figure 29: Experiment conducted with diluted reagent.

discrepancy underscores the intricate nature of interpreting coagulation dynamics, particularly when influenced by the interaction between blood components and reagents.

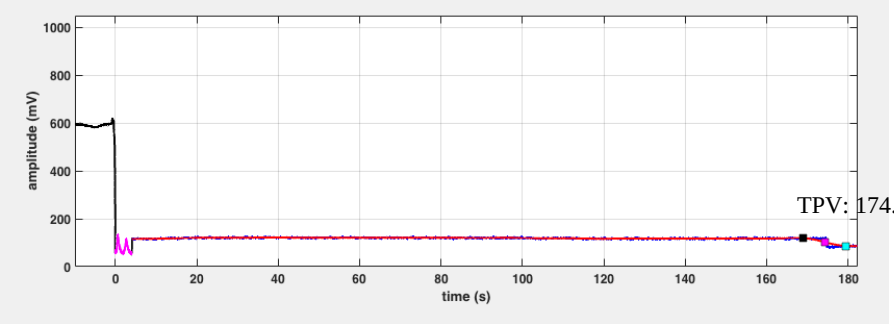

Figure 30: PBS applied cartridge

In Figure 30, a comparison between the reagent and an equivalent liquid, PBS, was conducted to explore the assumed impact of liquid density, viscosity, and speed. The results indicate that diluted versions of blood, when combined with the reagent, do not exhibit the previously observed sudden decrease problem. This observation suggests that the characteristics of the liquid, such as density, viscosity, and speed, play a role in mitigating the issue, providing valuable insights into the factors influencing coagulation behavior in the system.

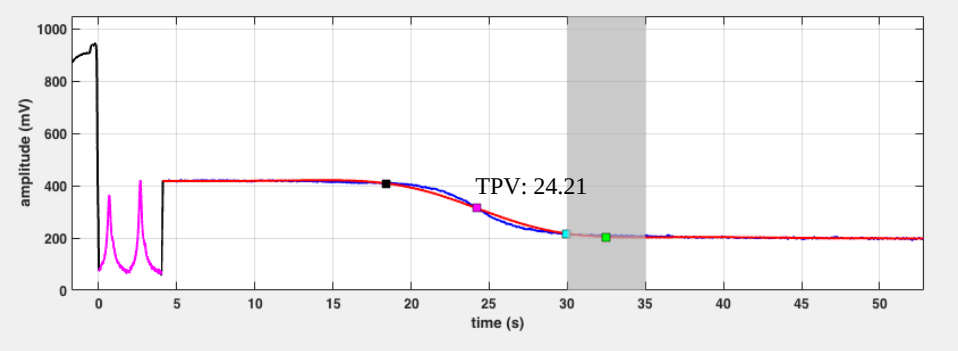

Figure 31: The tests using high abnormal plasma and the 1/20 DOS formula

In Figure 31, the tests using high abnormal plasma and the 1/20 DOS formula have been conducted, and notably, no sudden signal decrease is observed. This outcome suggests that the specific formulation of 1/20 DOS is effective in preventing the abrupt decline in the signal during tests with high abnormal plasma. These results contribute to a better understanding of the formulation's impact on coagulation dynamics, offering

promising insights for its potential application in maintaining stability under various conditions.

In summary, our investigations revealed that the concentration of DOS plays a pivotal role in influencing signal behavior, irrespective of whether coagulation occurs or not. Lower concentrations of DOS exhibited remarkable effectiveness in maintaining a stable signal, particularly evident when introducing liquid through the inlet via a pipette. The comparison between DI water and reagent, both prepared with DI water, further emphasized the significance of DOS concentration on signal stability.

While the densities of plasma and blood remain unknown as they change in person, high abnormal plasma yielded optimal results when combined with the 1/20 DOS formula. Notably, lyophilization procedures, including variations with and without mannitol, were executed according to the prescribed protocol, with a lyophilization time of 24 hours. After extracting samples from the device, they were stored in aluminum foil without silica beads, completing all tests within a few hours. The positioning of the reagent at different spots, including the vent, neck, and under the fiber, did not result in a significant change, with the form of the reagent emerging as the most impactful factor observed thus far.

In testing PMMA cartridges with the 1/20 DOS formula, two separate experiments were conducted, both indicating that the plasma did not traverse through the channel. This suggests that the 1/20 DOS formula may not be compatible with PMMA cartridges. In conclusion, the DOS concentration has proven to be a critical determinant of signal stability, showcasing its potential as a stabilizing agent.

Application of Cover Foil

As described in previous sections, the initial design of the cartridge featured a two-piece design with a sealing mechanism attaching the two pieces together. The initial in-house produced cartridges, exemplifying this design with a sealing mechanism, are represented in Figure 33. This design incorporated a self-adhesive band tape to improve sealing and prevent blood leakage from the sides of the measurement chamber and channel. However, due to increased sample volume demands, challenges in mass production, and elevated production costs, modifications were implemented in this cartridge design. The preference shifted to a microfluidic chamber with a cover foil mechanism, as depicted in Figure 33, replacing the cartridge with a sealing mechanism.

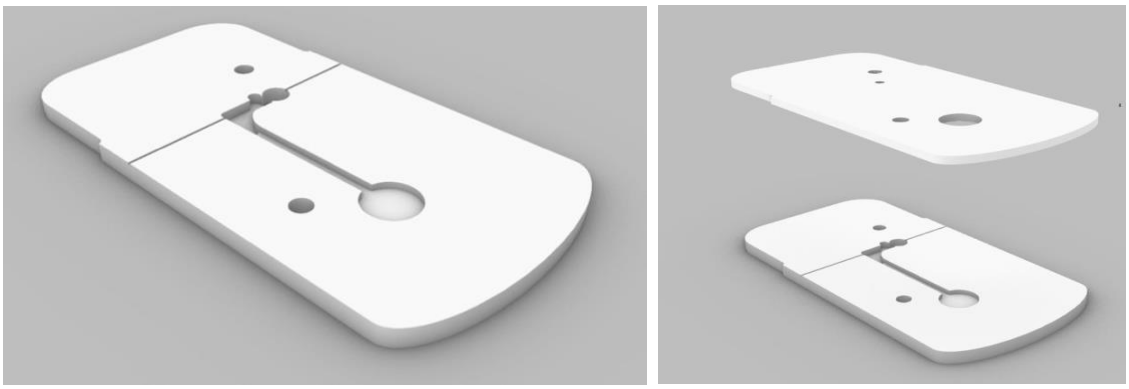

Figure 32: Initial cartridge prototype with sealing mechanism.

To reduce complexity and cost and enhance the user-friendliness of the cartridge while allowing for the initial method of covering optimized for passive capillary flow, a pressure-sensitive one-sided transparent tape of 100 microns was chosen from 3M (9793-R). Another reason for using such a thin cover is to facilitate better heat transfer from the heater inside the tray of the PoC device, ensuring that the measurement is not compromised. While the inner surface remains hydrophobic, we also explored alternatives for the inner surface as a substitute for DOS hydrophilic substance. However, the design requirement of blood filling the chamber in 8-10 seconds was not met due to overfilling of the blood throughout the cartridge. This idea was quickly disregarded after such results.

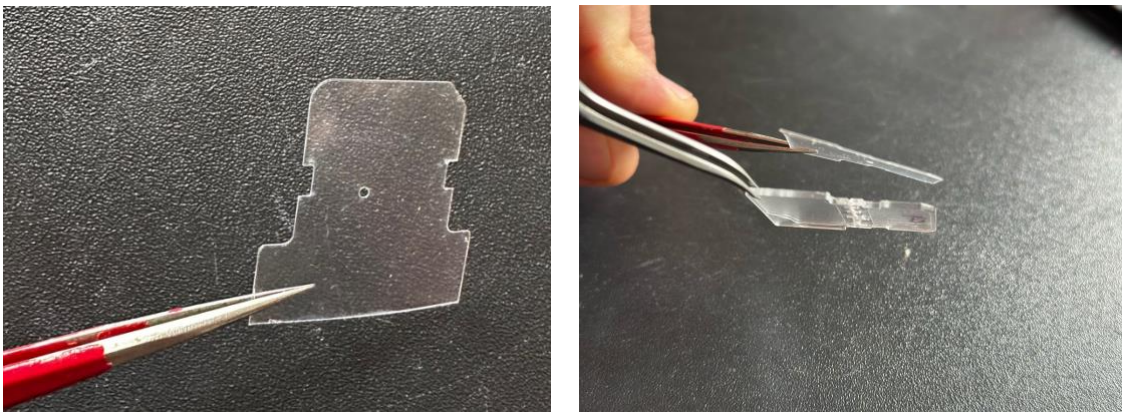

Figure 33: Latest version of the cartridge shown with pressure sensitive cover foil.

The following chapter of this thesis explains the aPTT-based coagulation measurement with the methods developed so far. Although most of the R&D process was focused on product development in terms of commercialization, side experiments were conducted to establish an aPTT measurement protocol with the proposed PoC device. For that, the open set up in our lab was used. From the same supplier aPTT reagent was provided and plasma and blood samples were as test subjects. The design of the experiments were based on measuring commercial plasmas then followed by measuring healthy blood samples and patient blood samples.

Chapter 3:
APTT MONITORING AND PROOF OF CONCEPT STUDY

In addition to PT/INR coagulation monitoring used for patients undergoing VKAs therapy, we also started to expand the research and application field towards the monitoring of aPTT parameter used by patients undergoing heparin treatments. While the mechanical concept of the cartridge remains the same, only the type of reagent integrated into the cartridge changes. As the reagent integration method and particularly the drying technique was not completely solved, we decided to use the liquid form of the reagent directly mixed with the test sample outside the cartridge and this sample is applied to the measurement chamber.

We initiated the proof of concept and performance study by testing three different control plasmas (normal plasma, low abnormal plasma and high abnormal plasma) of known aPTT values. We then identified three healthy subjects from which we collected citrated-blood and citrated-plasma to perform in-vitro heparin dose response spiking experiments. In vitro heparin sensitivity curves were generated by adding increasing amounts of heparin to aliquots of normal donor citrated plasma but also citrated blood. As two types of heparins (Unfractionned heparin (UFH) and Low molecular weight Heparin (LMWH)) is used in hospitals, both were tested in both dose response experiments with blood and plasma. The main goal was to observe an increase of aPTT values when increasing the dose of heparin (indicative of performance validation) while also evaluating precision and repeatability of the measurements.

3.1 aPTT Tests with Control Plasmas

Protocol

In the laboratory setup at, calibrated equipment is employed to conduct aPTT tests using commercially available test plasmas from Hemosil.

1. Lyophilized commercially available test plasmas from Hemosil were resuspended in a distilled water.
2. The plasma samples were aliquoted if not used immediately for future uses.

Test Description

1. Take liquid aPTT-SS reagent from the fridge and set aside a few milliliters to be used inside an Eppendorf tube.

2. Take 20 mM $CaCl_2$ and set aside as well [100], [101].
3. Take assembled cartridge and apply DOS directly to the chamber.
4. Place the cartridge to the open setup. Heat it up.
5. Take equal volumes of desired type of control plasma and aPTT reagent.
6. Next, take this mixture and mix it with 15 µl of $CaCl_2$ and mix it with plasma/reagent sample and immediately introduce it to the cartridge for aPTT test.

Table 2: Control plasma test results (n=6).

Plasma	**aPPT (TPA)**	**aPPT (TPV)**	**aPTT (TPD)**
High Abnormal	61	67	74
	72	79	86
	64	70	77
	61	68	74
	63	69	75
	66	73	80
	62	68	75
Low Abnormal	44	50	56
	41	47	53
	49	55	61
	39	46	52
	47	53	60
	43	49	56
Normal Plasma	32	39	176
	28	34	40
	26	32	38
	30	36	43
	27	33	39
	29	35	41

In the conducted tests, a comprehensive overview involved n=6 repetitions with control plasmas, ensuring a robust evaluation of the coagulation parameters. The results, as depicted in Figure 34, demonstrate a noteworthy alignment with the acceptance range established by the manufacturer for the control plasma, indicating the accuracy and reliability of the measurements.

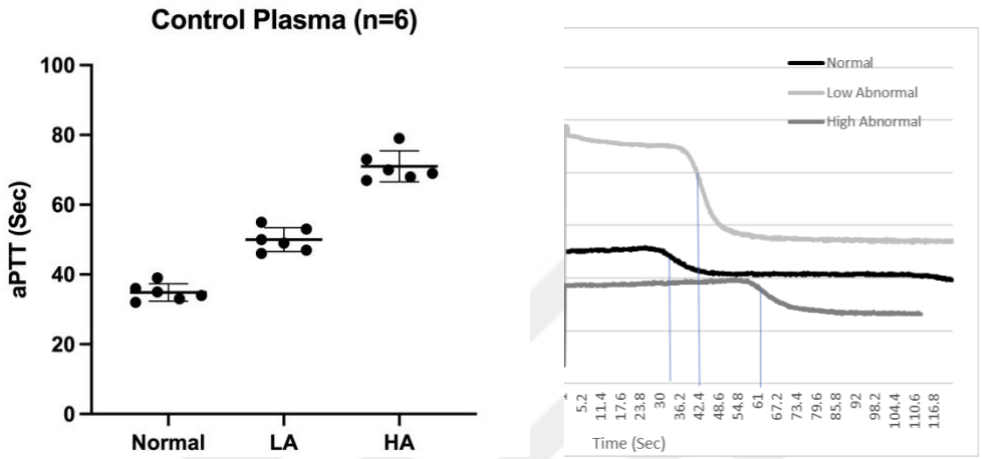

Figure 34: aPTT values of Normal, Low Abnormal, and High Abnormal plasmas (n=6) on the right and signal of the control plasmas in the same ampere (mV) vs time graph on the left.

The defined normal range, spanning from 23 to 33, serves as a baseline for typical coagulation times. Additionally, the ranges for low abnormal (32-49) and high abnormal (45-62) provide an understanding of coagulation dynamics in varying conditions. This allows for a more detailed interpretation of the test outcomes within different clinical contexts. Furthermore, the calculated standard deviation across the tests highlights the high repeatability of the measurements. A low standard deviation indicates a consistent and reliable performance of the coagulometer in multiple repetitions. Notably, as the abnormality in the samples increases, the coagulation time exhibits a corresponding increase. This underscores the sensitivity of the coagulometer in detecting variations in coagulation dynamics, making it a valuable tool for diagnostic purposes. Overall, these findings underscore the precision, reliability, and responsiveness of the coagulometer in detecting subtle changes within coagulation parameters.

3.2 aPTT Tests with Spiked Plasma from Healthy Donor Plasma

The Clinical and Laboratory Standards Institute (CLSI) furnishes a comprehensive document addressing the general establishment of Normal Reference Intervals (NRIs) for clinical tests, including aPTT, while providing valuable foundational insights into the subject. The guidance delves into theoretical aspects of sampling techniques, data treatment, determining normal individual numbers for NRI, outlier removal, and NRI verification methods. It suggests a sample size of 39 for a 5th-95th percentile interval but generally recommends 120 for most analytes, while another document proposes that 20 normal individuals are sufficient for PT and aPTT NRI [102].

Sample Collection

aPTT tests are performed with blood samples collected from healthy donors. For the sample collection citrated blood tubes are used. There are multiple blood collection tubes that have a variety of anticoagulant effects, including trisodium citrate- being the most common one, followed by EDTA-based tubes, oxalate, and heparin. Generally, a 9:1 blood-to-anticoagulant ratio is applied with those blood collection tubes [103].

The variability of coagulation assays in the lab is attributed to several factors including wrongly performed sample collection where the tube is filled inadequately or if it is overfilled. Besides, the anticoagulant type affects the performance, where trisodium citrate is preferred in coagulation assays instead of EDTA [103].

Centrifugation Protocol [104]:

1. Collect whole blood into a citrate-treated (light blue tops) tube.
2. Cells are removed from plasma by centrifugation for 30 minutes at 3000 x g using a refrigerated centrifuge at 4°C.
3. The resulting supernatant is designated plasma (Figure 35).
4. Use “no brake” or minimum to prevent hemolysis and poor separation
5. The samples should be maintained at 2–8°C while handling. If the plasma is not analyzed immediately, the plasma should be apportioned into 0.5 ml aliquots, stored, transported at -80°C for a day, then transferred to –20°C.
6. It is important to avoid freeze-thaw cycles. Samples which are hemolyzed, icteric, or lipemic can invalidate certain tests.

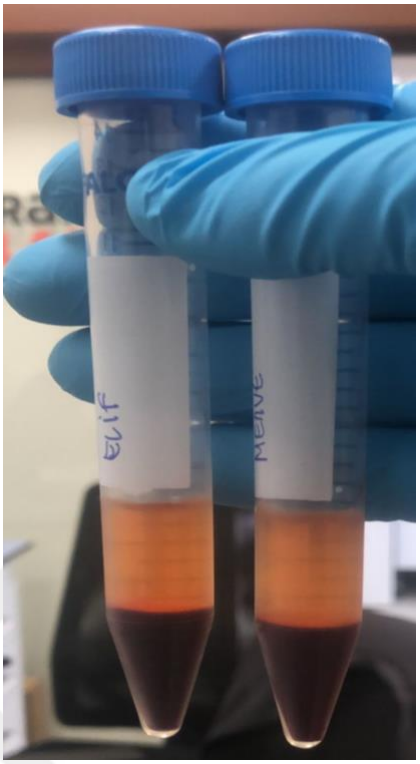

Figure 35: Separated plasma from whole blood

3.2.2 UFH Spiking

Spiking Protocol

Table 3: UFH dilution protocol is shown for UFH Heparin, Nevparin 25.0000IU/5ml (Gensenta).

Main Stock= 5000 UI	C1	V1	C2	V2	PBS Volume	C3 (PBS)	V3 (PBS)	C4 (Blood)	V4 (Blood +PBS)	Blood Volume
Stock 1	5000	10	1000	50	40	1000	5	250	20	15
Stock 2	1000	10	200	50	40	200	5	50	20	15
Stock 3	200	10	40	50	40	40	5	10	20	15
Stock 4	40	10	8	50	40	8	5	2	20	15
Stock 5	8	10	4	20	10	4	5	1	20	15
Stock 6	4	10	2	20	10	2	5	0,5	20	15
Stock 7	2	10	1	20	10	1	5	0,25	20	15
Stock 8	1	10	0,5	20	10	0,5	5	0,125	20	15

Test Description (Protocol)

1. Take liquid aPTT-SS reagent from the fridge and set aside a few milliliters to be used inside an Eppendorf tube.
2. Take 20 mM $CaCl_2$ and set aside as well [100], [101].
3. Take assembled cartridge and apply DOS directly to the chamber.
4. Place the cartridge to the open setup. Heat it up.
5. Take equal volumes of plasma/blood and aPTT reagent
6. Mix 15 µl of plasma with 5 µl of a desired drug concentration in PBS and immediately apply vortex at the lowest intensity for 30 seconds. Then leave the mixture on a hot plate for 30 seconds. Repeat this for 5 minutes.
7. Next, take 15 µl from this mixture and mix it with 15 µl of aPTT-SyntASIL reagent. Apply vortex to this mixture a total of 3 times for 5 minutes, with 30 seconds of vortexing each time.
8. Take 15 µl $CaCl_2$ and mix it with plasma/reagent sample and immediately introduce it to the cartridge for aPTT test.

Acceptance Criteria

The measurement is invalid if;

1. The coagulation curve is saturated, and signal is above the 1023 mV amplitude value. This will look like there is no coagulation initially and keep steady until it is not, and we will be looking at only one part of the curve with a smaller perception. This is a misleading result. There might be a problem with the signal and cartridge that we do not see.
2. Ensure that the test sample volume is adequate; a half-filled chamber may be prone to external disturbances.
3. The signal should be meaningful, we don’t expect to see abnormal increase or decrease at the beginning of the coagulation. Abnormal increase of the signal means relieved mass load off of the fiber.

Results

The achievement of an accurate dose-response curve was hindered by suboptimal mixing conditions during the experiment. Despite efforts to conduct vortexing at a relatively low intensity, it is acknowledged that the level of mixing during the initial incubation period may not have been sufficient. This limitation introduces potential variability in the concentrations of Nevparin, impacting the reliability of the observed

dose-response relationship. Subsequent to the identified challenge in mixing during the initial experiment, it is noteworthy to mention that this issue was successfully addressed in subsequent iterations of the study. The new vortexing approach incorporated 30 seconds of heating inside a heater block to prevent excessive temperature loss during prolonged vortexing. Additionally, 30 seconds of vortexing at the lowest level was implemented to prevent any hemolysis or disruption of the plasma components.

Table 4: aPTT values obtained from healthy donor's plasma samples. Results are shown with TPA, TPV, and TPD values where the TPV values regarded as aPTT. Each concentration tested three times (n=3) for three different people.

UI	Subject 1			Subject 2			Subject 3		
0	23	25	26	19	18	18	27	26	27
0,125	54	53	57	50	49	50	32	35	33
0.25	93	104	112	76	87	81	58	81	78
0.50	169	145	177	101	93	133	151	170	136
1	211	227	229	250	233	200	302	289	312

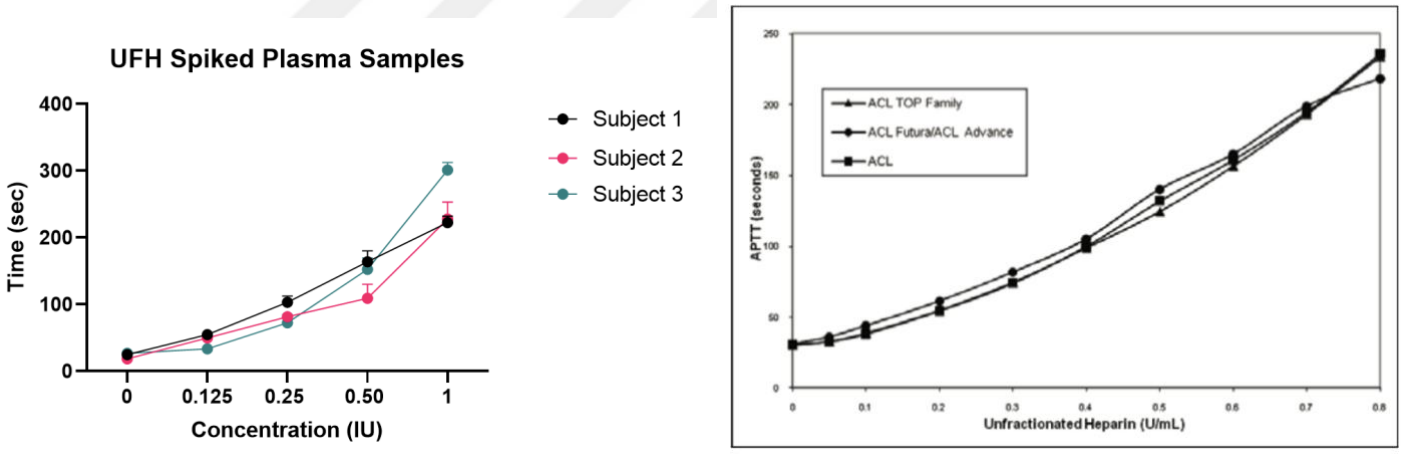

Figure 36: Dose-response values for each subject are displayed on the left, depicting varying doses ranging from 0 to 1 IU/mL, reference dose-response curve for UFH spiked plasma samples is shown on the right [105].

In general, we observe a notable increase in aPTT values, consistent with the trends depicted in Figure 36 shown on the right. The displayed figure illustrates curves generated using a single lot of SynthASil reagent and one Normal Plasma Pool spiked with graduated quantities of Unfractionated Heparin (UFH). The therapeutic range specified for these curves is 0.2 - 0.4 U/mL. It is essential to acknowledge the presence of numerous

variables, including varying sources of heparin, which can impact clotting times [105]. This variability may arise due to differences in reagents and materials used across various laboratory settings. While the provided therapeutic range serves as a valuable reference point, the inherent variability in heparin sources necessitates individualized assessments to ensure accuracy and reliability in clinical settings.

Upon comparison with our results, it becomes evident that similar doses of UFH fall within comparable ranges. As the doses increase, both our laboratory results and the depicted figure yield similar dose-response curves for the increasing amounts of UFH. Our results, obtained through triplicate testing for each dose, consistently fall within a similar range.

This comparability is a positive indication of the performance and reliability of our laboratory results. It reinforces the confidence in the accuracy and consistency of our coagulation measurements, validating our methodology against established standards. For instance, at a dose of 0.125 IU, our results for three different subjects are as follows: Subject 1 - 54, 53, 57 seconds; Subject 2 - 50, 49, 50 seconds; and Subject 3 - 32, 35, 33 seconds. The reference guideline for the same dose hovers around 50 seconds. As the dose increases, for example, for the highest dose of 1 IU, we observed a range deviating from 200 to 312. Comparing these results with the reference, we can observe that a dose of 0.8 IU falls around 250 seconds.

3.2.3 LMWH Spiking

LMWH is a drug that has been in use and since it has anticoagulant qualities, it is frequently used in clinical settings. Medical indications are usually considered when starting LMWH therapy. Clinically, deep vein thrombosis (DVT), pulmonary embolism (PE) treatment as well as acute coronary syndrome (ACS) that comprises of atrial fibrillation (AF) can be dealt with using LMWH [65]–[67]. A comprehensive evaluation of the patient's medical history, risk factors, and the particular clinical indication is used to determine whether to initiate LMWH therapy.

Low-molecular-weight heparins (LMWHs) are used in the prevention and treatment of thrombotic diseases and along with unfractionated heparin (UFH) because of their predictable pharmacokinetics and ease of use. LMWHs have unique biochemical and pharmacological profiles. The variety of LMWHs and their advantages over UFH are

significant factors to consider in clinical practice, especially in terms of pharmacy costs [68].

In 2001, Turpie et al. indicated that enoxaparin, a LMWH has demonstrated a decreased risk of acute coronary events and the necessity for revascularization in patients with ACS compared to treatment with UFH [67]. They are increasingly replacing UFH for therapeutic anticoagulation due to several advantages, including a more predictable pharmacokinetic profile and ease of use. As outlined in the 2008 guidelines of the American College of Chest Physicians (ACCP), LMWHs, UFH, or fondaparinux (Arixtra, Glaxo-SmithKline) are recommended for VTE prophylaxis in surgical and acutely sick patients [68]. Despite their similar antithrombotic effects, LMWHs are diverse compounds, being manufactured through different processes and possessing distinct biochemical and pharmacological properties and this diversity among LMWHs has significant implications for clinical practice, particularly due to ongoing efforts to reduce costs by opting for the least expensive product, assuming pharmacological and clinical equivalence among different LMWHs. However, such equivalence has not been established. In spite of FDA, WHO, ACCP, AHA, and ACC announcement that LMWHs are not clinically interchangeable, the therapeutic interchange continues to be deemed a worthwhile practice. Furthermore, concerns are also growing with the introduction of biosimilar LMWH formulations: these may not necessarily have the same biochemical or pharmacological properties as their branded counterparts [68]. In comparison to heparin, LMWHs have a longer half-life meaning that dosing is more predictable and they are usually administered less often, frequently once daily [65].

Therefore, given the widespread clinical use of LMWH, monitoring, particularly in emergency cases, needs to be performed regularly. Up to date there have been multiple cases where the aPTT values have been measured with custom made PoC devices similar to one we propose here.

While several bench-top instruments are available for aPTT measurements, there is a need for quick and accurate bleeding risk assessment. PoC devices address this need by enabling rapid and reliable testing. In this context, LMWH spiking experiments were conducted to assess whether the our device can accurately measure the administered drug levels in plasma and blood samples obtained from three healthy volunteers. To perform such experiments, preliminary tests are conducted with our open setup found in our lab. Cartridges are meticulously prepared following the outlined cartridge preparation

protocol. To mitigate the influence of plasma/blood flow effects, a straightforward solution involves blocking the channel using a simple patafix. This creates a stable pool for the test object, ensuring it remains undisturbed and free from potential interferences that could compromise the integrity of the experimental results. Oksapar 4000 Anti-Xa IU/0.4 ml IV is used to spike the blood samples.

Spiking Protocol

See the protocol for dilution of LMWH Enoxaparin, Oksapar shown in Table 5 below. The spiking was completed similar to UFH spiking and experimental protocol holds the same principles as described above.

Table 5: Dilution protocol is shown for Oksapar 4000 Anti-Xa IU/0.4 ml IV subcutaneous drug (Koçak Farma).

Main Stock=5000 UI	C1	V1	C2	V2	PBS Volume	C3 (PBS)	V3 (PBS)	C4 (Blood)	V4 (Blood +PBS)	Blood Volume
Stock 1	4000	100	800	500	400	800	5	200	20	15
Stock 2	800	100	160	500	400	160	5	40	20	15
Stock 3	160	100	80	200	100	80	5	20	20	15
Stock 4	80	100	40	200	100	40	5	10	20	15
Stock 5	40	100	20	200	100	20	5	5	20	15
Stock 6	20	100	10	200	100	10	5	2,5	20	15
Stock 7	10	100	4	250	150	4	5	1	20	15
Stock 8	4	100	2	200	100	2	5	0,5	20	15
Stock 9	2	100	1	200	100	1	5	0,25	20	15
Stock 10	1	100	0,5	200	100	0,5	5	0,125	20	15
Stock 11	0,5	100	0,25	200	100	0,25	5	0,0625	20	15
Stock 12	0,25	100	0,125	200	100	0,125	5	0,03125	20	15

Results

Table 6: Time values obtained using open setup with different LMWH Enoxaparin given for TPA, TPV and TPD for plasma samples.

	Subject 3			Subject 1			Subject 2		
	TPA	TPV	TPD	TPA	TPV	TPD	TPA	TPV	TPD
1 UI	186	208	214	146	154	175	81	90	99

1 UI	143	153	161	6	154	159	121	129	138
1 UI	159	166	173	131	138	156	96	103	110
0,5 UI	75	82	90	63	70	77	76	82	88
0,5 UI	84	93	100	85	93	101	75	82	89
0,5 UI	71	79	100	101	108	132	85	91	102
0,25 UI	52	59	67	46	54	61	48	42	36
0,25 UI	59	66	72	58	65	73	36	41	47
0,25 UI	42	47	70	44	51	61	32	38	43
0,125 UI	48	53	58	34	40	46	25	33	40
0,125 UI	36	42	48	30	36	43	27	33	39
0,125 UI	46	52	60	39	46	54	27	33	40

The dose-response curve obtained in our study presents a compelling illustration of the relationship between LMWH dosage and aPTT values. The curve exhibits a characteristic upward trend, indicating a dose-dependent impact of LMWH on coagulation dynamics.

One notable feature is the consistency of the response across varying doses. For example, at a dose of 0.125 IU, we observe a moderate increase in aPTT values for all subjects, aligning closely with the reference [72]. This suggests a reliable and predictable response to lower doses of LMWH, indicative of the drug's expected anticoagulant effect within the therapeutic range. However, slight differences are observed between two sets of experiments conducted with Enoxaparin LMWH. The reference values for donors indicate comparably lower time points, approximately around 100 seconds, at 1 IU, while our results showcase a range of 90-208 seconds including variability across different subjects.

These variations in aPTT values may stem from individual differences among donors, variations in laboratory conditions, or specific characteristics of the Enoxaparin LMWH used in our experiments. While our results demonstrate a consistent and dose-dependent trend, the observed differences underscore the importance of considering factors such as donor variability and specific LMWH formulations in interpreting anticoagulant responses.

3.3 aPTT Tests with Spiked Blood

This section describes the tests conducted with blood spiked with two different heparins as an anticoagulant. aPTT tests conducted with spiked blood protocol follow the same guideline described above except the fact that the blood samples were not treated

with centrifugation instead kept on the roller at 4°C for the span of the tests being conducted [69].

3.3.1 UFH Spiking

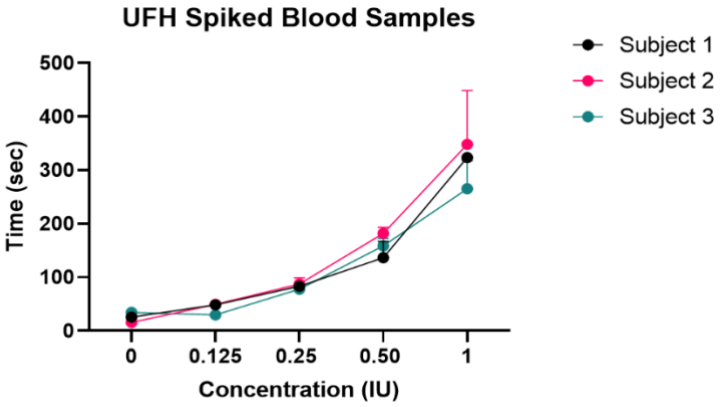

Figure 37: Comparison of the aPTT values for three different spiked blood samples.

Results

Table 7: Results of the UFH spiking experiments performed on three different healthy subjects.

	Subject 1	Subject 3	Subject 2
Control	29	33	17,41
Control	26	28	15,5
Control	25	25	15,9
0,125	50	30	52,5
0,125	51,3	29	48
0,125	45	30	48
0,25	84	75	97,9
0,25	88	88	74,1
0,25	78	58	94
0,5	166	143	175,1
0,5	105	162	176
0,5	138	170	195
1	330	313	399
1	317	274	413
1	324	209	232

Below, Figure 38 presents a comparison of blood and plasma samples for UFH-spiked samples. Evidently, each subject exhibited a similar reaction, with Subject 3 displaying the most compatible results, showcasing almost overlapping graphs. This consistency across subjects underscores the reliability and comparability of results, particularly in the context of finger-prick blood measurements. The uniformity in the response among subjects reinforces the potential applicability and effectiveness of the measurement method for point-of-care scenarios involving fingerprick blood samples.

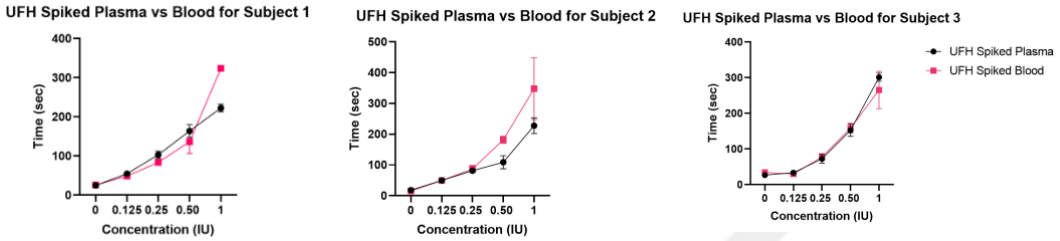

Figure 38: UFH spiked plasma vs blood results are shown for each subject.

3.3.2 LMWH Spiking

Results

Table 8: Results of the LMWH spiking experiments performed on three different healthy subjects.

	Subject 3	Subject 1	Subject 2
Control	35,1	29	17,41
Control	34,2	26	15,5
Control	34,4	25	15,9
0,125	52,09	56,71	36,71
0,125	48,21	45,9	29,59
0,125	39,8	49,1	33,11
0,25	54,29	57,37	37,3
0,25	53,01	51,31	44,11
0,25	43,6	62	39,21
0,5	73,41	66,58	73,41
0,5	78	86,21	66,905
0,5	83,21	82,29	63
1	153,9	93,58	188
1	144,1	120,701	197
1	146,6	120,605	85,8

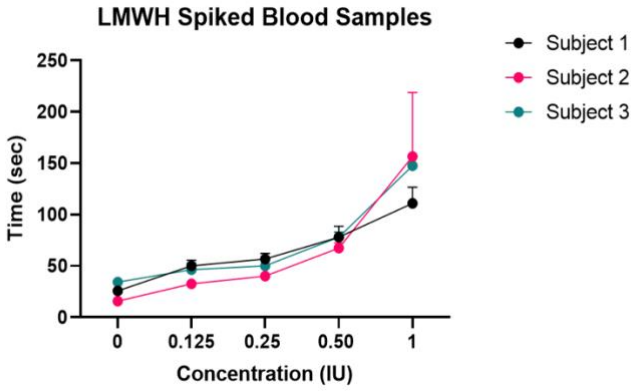

Figure 39: Spiked blood samples of three subjects.

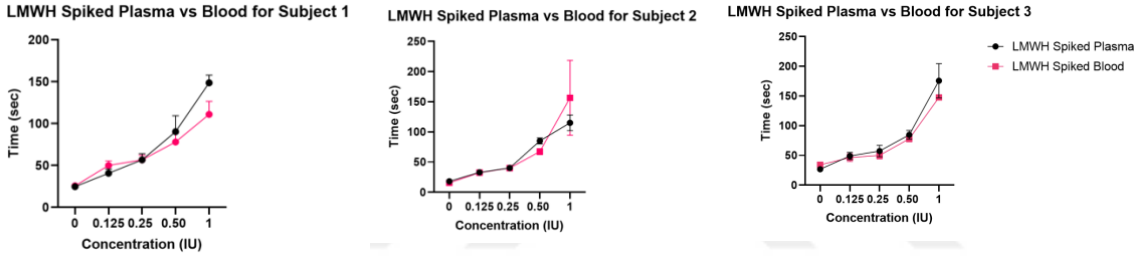

Figure 40: LMWH spiked plasma vs blood results are shown for each subject.

The comparison of plasma and whole blood in terms of aPTT values in a dose-response curve, with similar time points for both LMWH and UFH, provides valuable insights into their anticoagulant effects.

In this study, we observed comparable time points for both LMWH and UFH in plasma and whole blood samples, revealing the consistency of their anticoagulant effects across these two sample types. The similarity in aPTT values between plasma and whole blood suggests that the intrinsic coagulation pathway responds similarly to both LMWH and UFH in these sample matrices. This finding underscores the reliability of aPTT measurements and supports their utility in monitoring the anticoagulant activities of LMWH and UFH in different blood components. The comparable curves for plasma and whole blood enhance the translatability of these findings to clinical practice, reinforcing the reliability of aPTT as a valuable indicator in assessing the anticoagulant effects of LMWH and UFH across different blood compositions. Notably, Subject 3 exhibited the

most favorable correlation in the graph, indicating a consistent and comparable response in both plasma and whole blood across varying doses of anticoagulants.

Conversely, Subject 2 displayed differences in aPTT values as the dose increased, suggesting potential variations in the anticoagulant response between plasma and whole blood. Meanwhile, Subject 1 demonstrated similar results for both plasma and blood, emphasizing a consistent response to LMWH and UFH across the tested doses. These observations underscore the importance of individual variability in anticoagulant response, even among healthy donors.

3.4 Pilot study

To compare aPTT results obtained with our technology and the HemosIL SynthASIL reagent, blood samples from ICU patients were concurrently tested using both our device and the gold standard hospital measurements. This pilot study was conducted in compliance with the ethical guidelines provided by the Ethical Committee of Koc University (Approval Number: 2017.125.IRB2.039).

In the design of these experimental processes Said Incir, M.D., Fatma Yurdakul, M.D., Hatice Kant Caltı from Koc University Hospital played a pivotal role in addition to our group. Koc University Hospital intensive care unit nurses provided necessary blood samples over a two-week period.

3.4.1 Blood Collection and Method

Blood samples were collected in two different blood collection tubes, one is for the standard aPTT tests that needed to be tested via hospital equipment, whereas the other one is spared for our equipment and testing. Blood samples were collected between 4 – 5 a.m. within the first round of blood collection in accordance with the hospital setting and those blood samples were tested within 4 hours after collection. The blood samples were transferred from Koc University Hospital to Koc University and relevant aPTT tests were conducted in our lab, SNA 256.

Koc University Hospital is using Sysmex CN6000 device for routine coagulation parameters measurement with Dade Innovin reagent for PT [106] and Dade Actin for aPTT [107], whereas our measurements are conducted with HemosIL reagents [108]. We use Recombiplastin 2G as PT reagent, and SynthASIL as aPTT reagent from HemosIL,

Werfen. In the context of clinical assessment of aPTT, a series of experiments was carried out utilizing authentic patient blood samples obtained from the Intensive Care Unit (ICU) at Koc University Hospital. Adhering to our established methodology, citrated blood specimens were procured daily during early morning rounds following the blood collection protocols outlined by the Clinical and Laboratory Standards Institute (CLSI) [109]. Blood samples were collected in duplicate with one set allocated for comparison against the hospital's gold standard measurements, conducted using the Sysmex CN6000 device and Dade Actin aPTT reagent (Siemens, Marburg, Germany). For our assessments, we employed the SynthASIL aPTT reagent (HemosIL, Werfen). Subsequent to the blood collection, these samples were transferred to our laboratory at Koc University for analysis, employing an open setup methodology as previously described. Each test was repeated twice (n=2) using two cartridges for each blood sample, thus ensuring the robustness and reliability of our experimental approach.

3.4.2 Results

Table 9: aPTT values obtained from both devices are given below (n=42). Our measurements are repeated twice (n=2), while KUH data is obtained according to the hospital standard protocol.

Patient	**aPTT 1**	**aPTT 2**	**Mean**	**aPTT KUH**
1	**27,9**	**25,4**	26,7	17,3
2	**92,6**	**85,8**	89,2	42,1
3	**58,3**	**61,1**	59,7	41,2
4	**46,9**	**41,6**	44,3	27,2
5	**41,5**	**36,7**	39,1	26,8
6	**58,5**	**54,6**	56,6	33,8
7	**53,6**	**52**	52,8	35,1
8	**43,3**	**33,3**	38,3	21,5
9	**41,5**	**38,1**	39,8	28,3
10	**45,1**	**51**	48,1	29,4
11	**24,9**	**24,1**	24,5	21,2
12	**20,6**	**21,1**	20,9	15,2

13	**33**	**32,3**	32,7	27,7
14	**48,3**	**49,2**	48,8	31,2
15	**31,1**	**32,5**	31,8	20,3
16	**25,7**	**25,3**	25,5	21,8
17	**71**	**83,2**	77,1	34,4
18	**36**	**34,4**	35,2	27,7
19	**24,6**	**24,7**	24,7	21,2
20	**33,7**	**29,9**	31,8	23
21	**37,9**	**36,6**	37,3	22,1
22	**89,5**	**87,7**	88,6	39,7
23	**31,8**	**31,1**	31,5	25,9
24	**41,6**	**41,0**	41,3	37,8
25	**40**	**43**	41,5	26,4
26	**36,7**	**34,6**	35,7	26,9
27	**37,3**	**34,4**	35,9	19,7
28	**29,1**	**28**	28,6	18,6
29	**31,5**	**41,3**	36,4	25,3
30	**44,7**	**45,5**	45,1	28,5
31	**25,4**	**30,6**	28,0	19,8
32	**33,9**	**31,3**	32,6	20,3
33	**46,9**	**53**	50,0	22,2
34	**47,7**	**51**	49,4	30,7
35	**44,9**	**52,2**	48,6	29,8
36	**36,1**	**35,5**	35,8	21,7
37	**36,0**	**31,6**	33,8	22,1
38	**53,1**	**46,7**	49,9	37,1
39	**41**	**45,8**	43,4	27,9
40	**34,9**	**35,6**	35,3	21,8
41	**38,1**	**35,4**	36,8	21,6

42	**43,7**	**43,3**	43,5	37,1

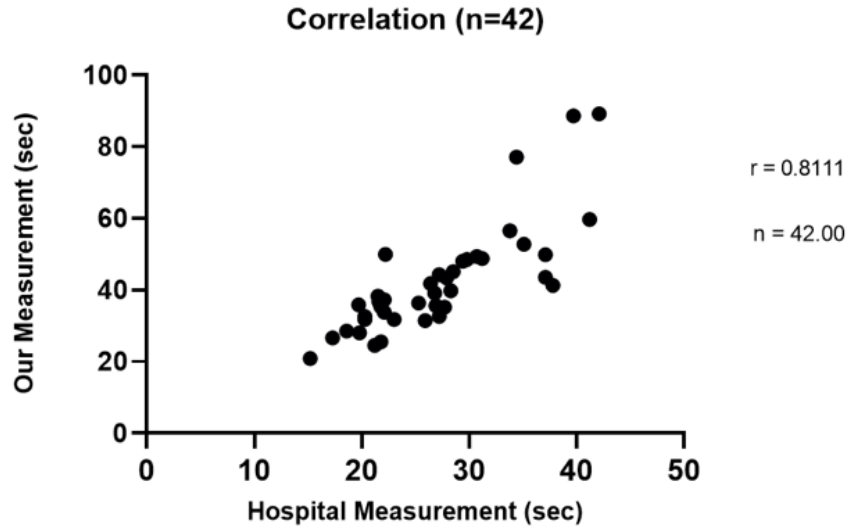

Figure 41: Summary statistics and significance test results for Pearson correlation analysis between hospital measurements and our method.

Here it is shown that the The Pearson correlation coefficient (r) is 0.8111 with a 95% confidence interval ranging from 0.6731 to 0.8945. The coefficient of determination (R2= 0.6579). The two-tailed P value is <0.0001, indicating statistical significance (****) at alpha = 0.05. The analysis is based on 42 pairs of data points.

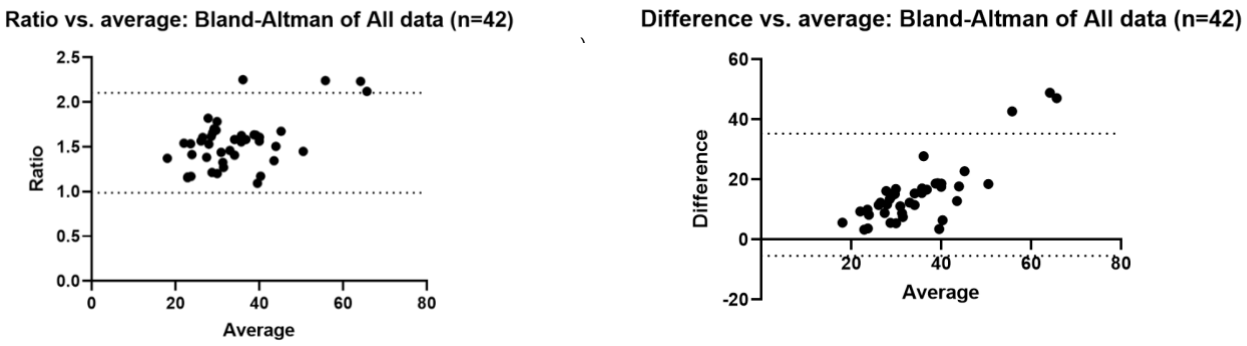

Figure 42: Summary of Bias and Limits of Agreement.

The findings indicate notable disparities between our proposed method and the standard hospital approach when assessed through the Bland-Altman analysis. For the difference versus average Bland-Altman comparison, we observed a bias of 14.93 with a standard deviation of bias at 10.40, and 95% Limits of Agreement ranging from -5.440 to 35.31. Similarly, examining the ratio versus average Bland-Altman analysis revealed a bias of 1.545 with a standard deviation of bias at 0.2847, and 95% Limits of Agreement ranging from 0.9866 to 2.102 (Figure 42).

Clinic administers use Clex-an and ENOX as LMWH heparin in intensive care unit. The patient intake of anticoagulant data is shared below.

Table 10: The list of drugs that the clinical patients were taking during the clinical study

Patient	Drug	Dose
1	CLEx-an 40mg/0,4 mL Subcutaneous/IV (4000 Unit/Injector)	1 x 0,4 mL
2	ENOX 40 mg/0,4 mL Subcutaneous/IV (4000 Unit/Injector)	1 x 0,4 mL
3	ENOX 60 mg/0,6 mL Subcutaneous/IV (6000 Unit/Injector)	2 x 0,6 mL
4	ENOX 60 mg/0,6 mL Subcutaneous/IV (6000 Unit/Injector)	2 x 0,6 mL
5	CLEx-an 40mg/0,4 mL Subcutaneous/IV (4000 Unit/Injector)	2 x 0,4 mL
6	ENOX 40 mg/0,4 mL Subcutaneous/IV (4000 Unit/Injector)	1 x 0,4 mL
7	ENOX 60 mg/0,6 mL Subcutaneous/IV (6000 Unit/Injector)	2 x 0,6 mL
	ENOX 40 mg/0,4 mL Subcutaneous/IV (4000 Unit/Injector)	2 x 0,6 mL
8	ENOX 60 mg/0,6 mL Subcutaneous/IV (6000 Unit/Injector)	2 x 0,6 mL
9	CLEx-an 40mg/0,4 mL Subcutaneous/IV (4000 Unit/Injector)	2 x 0,4 mL
10	ENOX 60 mg/0,6 mL Subcutaneous/IV (6000 Unit/Injector)	1 x 0,6 mL
	CLEx-an 40mg/0,4 mL Subcutaneous/IV (4000 Unit/Injector)	1 x 0,4 mL
11	ENOX 40 mg/0,4 mL Subcutaneous/IV (4000 Unit/Injector)	2 x 0,4 mL
	ENOX 60 mg/0,6 mL Subcutaneous/IV (6000 Unit/Injector)	1 x 0,6 mL
	CLEx-an 40mg/0,4 mL Subcutaneous/IV (4000 Unit/Injector)	2 x 0,4 mL
12	CLEx-an 40mg/0,4 mL Subcutaneous/IV (4000 Unit/Injector)	2 x 0,4 mL
	ENOX 40 mg/0,4 mL Subcutaneous/IV (4000 Unit/Injector)	2 x 0,4 mL
13	ENOX 60 mg/0,6 mL Subcutaneous/IV (6000 Unit/Injector)	1 x 0,6 mL
	CLEx-an 40mg/0,4 mL Subcutaneous/IV (4000 Unit/Injector)	2 x 0,4 mL
	ENOX 40 mg/0,4 mL Subcutaneous/IV (4000 Unit/Injector)	2 x 0,4 mL
14	ENOX 60 mg/0,6 mL Subcutaneous/IV (6000 Unit/Injector)	2 x 0,6 mL
	ENOX 60 mg/0,6 mL Subcutaneous/IV (6000 Unit/Injector)	2 x 0,6 mL
15	ENOX 40 mg/0,4 mL Subcutaneous/IV (4000 Unit/Injector)	1 x 0,4 mL
16	ENOX 40 mg/0,4 mL Subcutaneous/IV (4000 Unit/Injector)	1 x 0,4 mL
17	ENOX 40 mg/0,4 mL Subcutaneous/IV (4000 Unit/Injector)	1 x 0,4 mL
18	ENOX 60 mg/0,6 mL Subcutaneous/IV (6000 Unit/Injector)	1 x 0,6 mL
19	ENOX 40 mg/0,4 mL Subcutaneous/IV (4000 Unit/Injector)	1 x 0,4 mL
20	ENOX 40 mg/0,4 mL Subcutaneous/IV (4000 Unit/Injector)	2 x 0,4 mL

	CLEx-an 40mg/0,4 mL Subcutaneous/IV (4000 Unit/Injector)	2 x 0,4 mL
21	ENOX 60 mg/0,6 mL Subcutaneous/IV (6000 Unit/Injector)	1 x 0,4 mL
	ENOX 60 mg/0,6 mL Subcutaneous/IV (6000 Unit/Injector)	1 x 0,6 mL
22	ENOX 40 mg/0,4 mL Subcutaneous/IV (4000 Unit/Injector)	1 x 0,4 mL
23	ENOX 40 mg/0,4 mL Subcutaneous/IV (4000 Unit/Injector)	1 x 0,4 mL
	ENOX 40 mg/0,4 mL Subcutaneous/IV (4000 Unit/Injector)	1 x 0,4 mL
24	CLEx-an 40mg/0,4 mL Subcutaneous/IV (4000 Unit/Injector)	1 x 0,4 mL
25	ENOX 60 mg/0,6 mL Subcutaneous/IV (6000 Unit/Injector)	1 x 0,6 mL
	ENOX 60 mg/0,6 mL Subcutaneous/IV (6000 Unit/Injector)	1 x 0,6 mL
26	CLEx-an 40mg/0,4 mL Subcutaneous/IV (4000 Unit/Injector)	1 x 0,4 mL
	ENOX 60 mg/0,6 mL Subcutaneous/IV (6000 Unit/Injector)	1 x 0,6 mL
	ENOX 60 mg/0,6 mL Subcutaneous/IV (6000 Unit/Injector)	2 x 0,6 mL
	ENOX 60 mg/0,6 mL Subcutaneous/IV (6000 Unit/Injector)	1 x 0,6 mL
27	ENOX 60 mg/0,6 mL Subcutaneous/IV (6000 Unit/Injector)	2 x 0,4 mL
	ENOX 60 mg/0,6 mL Subcutaneous/IV (6000 Unit/Injector)	1 x 0,4 mL
	ENOX 60 mg/0,6 mL Subcutaneous/IV (6000 Unit/Injector)	1 x 0,4 mL
	ENOX 60 mg/0,6 mL Subcutaneous/IV (6000 Unit/Injector)	1 x 0,6 mL
28	CLEx-an 40mg/0,4 mL Subcutaneous/IV (4000 Unit/Injector)	2 x 0,4 mL
29	ENOX 40 mg/0,4 mL Subcutaneous/IV (4000 Unit/Injector)	1 x 0,4 mL
30	ENOX 40 mg/0,4 mL Subcutaneous/IV (4000 Unit/Injector)	1 x 0,3 mL
31	CLEx-an 40mg/0,4 mL Subcutaneous/IV (4000 Unit/Injector)	2 x 0,4 mL
32	ENOX 60 mg/0,6 mL Subcutaneous/IV (6000 Unit/Injector)	1 x 0,4 mL
	ENOX 60 mg/0,6 mL Subcutaneous/IV (6000 Unit/Injector)	1 x 0,4 mL
	ENOX 60 mg/0,6 mL Subcutaneous/IV (6000 Unit/Injector)	2 x 0,4 mL
	ENOX 60 mg/0,6 mL Subcutaneous/IV (6000 Unit/Injector)	1 x 0,6 mL
33	ENOX 40 mg/0,4 mL Subcutaneous/IV (4000 Unit/Injector)	1 x 0,4 mL
34	CLEx-an 40mg/0,4 mL Subcutaneous/IV (4000 Unit/Injector)	1 x 0,4 mL
	ENOX 60 mg/0,6 mL Subcutaneous/IV (6000 Unit/Injector)	1 x 0,6 mL
	ENOX 60 mg/0,6 mL Subcutaneous/IV (6000 Unit/Injector)	2 x 0,6 mL
	ENOX 60 mg/0,6 mL Subcutaneous/IV (6000 Unit/Injector)	1 x 0,6 mL
	ENOX 60 mg/0,6 mL Subcutaneous/IV (6000 Unit/Injector)	2 x 0,6 mL
35	CLEx-an 60mg/0,6 mL Subcutaneous/IV (6000 Unit/Injector)	2 x 0,6 mL
	ENOX 60 mg/0,6 mL Subcutaneous/IV (6000 Unit/Injector)	1 x 0,6 mL
36	ENOX 60 mg/0,6 mL Subcutaneous/IV (6000 Unit/Injector)	2 x 0,4 mL
	ENOX 60 mg/0,6 mL Subcutaneous/IV (6000 Unit/Injector)	1 x 0,4 mL
37	CLEx-an 40mg/0,4 mL Subcutaneous/IV (4000 Unit/Injector)	2 x 0,4 mL
38	ENOX 60 mg/0,6 mL Subcutaneous/IV (6000 Unit/Injector)	1 x 0,6 mL
	ENOX 60 mg/0,6 mL Subcutaneous/IV (6000 Unit/Injector)	2 x 0,6 mL
	ENOX 60 mg/0,6 mL Subcutaneous/IV (6000 Unit/Injector)	1 x 0,6 mL
	ENOX 60 mg/0,6 mL Subcutaneous/IV (6000 Unit/Injector)	2 x 0,6 mL
	CLEx-an 40mg/0,4 mL Subcutaneous/IV (4000 Unit/Injector)	1 x 0,4 mL
39		
40	ENOX 60 mg/0,6 mL Subcutaneous/IV (6000 Unit/Injector)	2 x 0,4 mL

	ENOX 60 mg/0,6 mL Subcutaneous/IV (6000 Unit/Injector)	1 x 0,4 mL
41		
42	CLEx-an 40mg/0,4 mL Subcutaneous/IV (4000 Unit/Injector)	1 x 0,4 mL
	ENOX 60 mg/0,6 mL Subcutaneous/IV (6000 Unit/Injector)	1 x 0,6 mL
	ENOX 60 mg/0,6 mL Subcutaneous/IV (6000 Unit/Injector)	2 x 0,6 mL
	ENOX 60 mg/0,6 mL Subcutaneous/IV (6000 Unit/Injector)	1 x 0,6 mL
	ENOX 60 mg/0,6 mL Subcutaneous/IV (6000 Unit/Injector)	2 x 0,6 mL

3.4.3 ISI Calibration Kit

As mentioned earlier, these comparative tests were conducted by using two different brands of aPTT reagents, which creates an issue of alignment between aPTT results that were conducted with two different devices. In order to understand the alignment between these two devices, we wanted to see the agreement when the same reagent is used with the same plasmas. In order to compare, we used the ISI Calibrate Kit (0020010600, HemosIL, Werfen), which has four different plasmas: A, B, C, and D.
We tested the same plasmas with both Sysmex CN6000 and our device by using Dade Innovin PT reagent as in hospital standard method and our reagent Recombiplastin 2G. Relative results are given below.

Table 11: Calibrator plasma tests results are given below for both hospital device and our method (tested with two different reagents)

Calibrators	**KUH**	**Our Method-Innovin**	**Our Method-R2G**
Kal A	11,6	9,3	8,5
	11,6	7,1	10,4
	11,6	7,5	11
	11,7	10	-
Kal B	18,4	18,3	23,2
	18,5	18,1	27,3
	18,4	18,4	20,7
Kal C	26,7	33,5	34,3
	27	34,7	32,9
	26,9	30,3	35,1
	27,2	30	-
Kal D	35,2	39,5	50,3
	35,7	39,4	49,3

	35,8	39,5	47,8

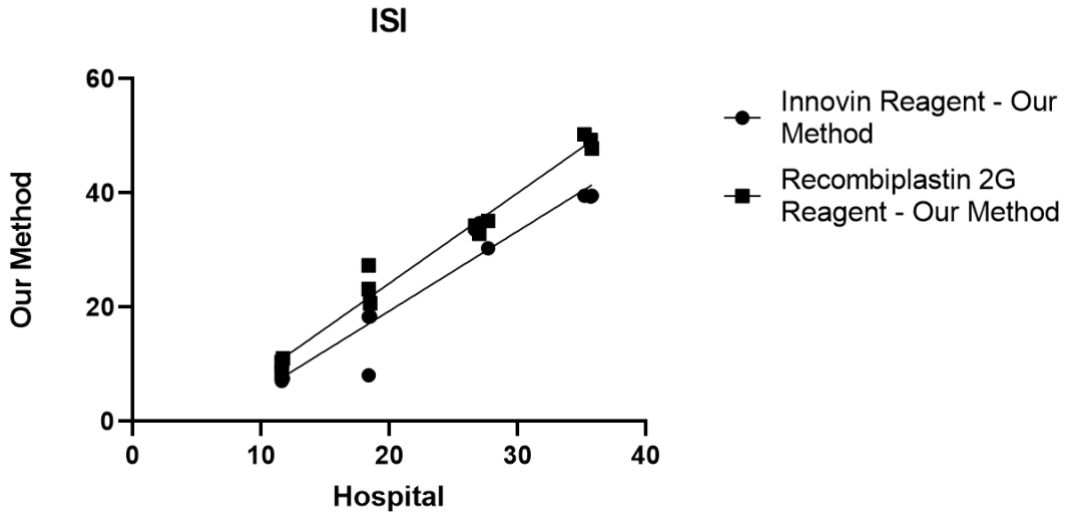

Figure 43: Correlation analysis between Hospital with Innovin Reagent and Hospital with Recombiplastin 2G Reagent using our method.

For Hospital vs. Innovin Reagent, Pearson's correlation coefficient (r) was found to be 0.9629, with a 95% confidence interval of 0.8694 to 0.9898, and an R squared value of 0.9271. The two-tailed p-value was <0.0001, indicating a significant correlation (p-value summary: ****). Similarly, for Hospital vs. Recombiplastin 2G Reagent, the correlation coefficient was 0.9889, with a 95% confidence interval of 0.9595 to 0.9970, and an R squared value of 0.9779. The two-tailed p-value was <0.0001, indicating a significant correlation (p-value summary: ****). Both correlations were statistically significant at the alpha level of 0.05. Each analysis was conducted on 12 XY pairs. For the repeatability of the tests conducted with our device, the Coefficient of Variation (CV) is considered. Two-Way ANOVA analysis indicates that there are significantly different measurements taken for each patient. The column factor that represents the two sets of measurements contributes only 0.003672% to the total variation and possesses a non-significant p-value (0.7891). Moreover, the difference between the predicted means of the two sets of measurements is 0.1833, with a standard error of 0.6809 and a 95% confidence interval spanning from -1.192 to 1.558.

Table 12: 2-Way ANOVA Results conducted for two sets of measurement data obtained with our device. Each patient is represented in a row, and the two 'y' columns denote two different repetitive measurements for each patient

Source of Variation	**% of total variation**	**P value**	**P value summary**	**Significant?**
Row Factor	97.92	<0.0001	****	Yes
Column Factor	0.003672	0.7891	ns	No

ANOVA table	**SS (Type III)**	**DF**	**MS**	**F (DFn, DFd)**	**P value**
Row Factor	18824	41	459.1	F (41, 41) = 47.16	<0.0001
Column Factor	0.7058	1	0.7058	F (1, 41) = 0.07251	0.7891
Residual	399.1	41	9.735		

Difference between column means	
Predicted (LS) mean of 1	41.90
Predicted (LS) mean of 2	41.72
Difference between predicted means	0.1833
SE of difference	0.6809
95% CI of difference	-1.192 to 1.558

Data summary	
Number of columns (Column Factor)	2
Number of rows (Row Factor)	42
Number of values	84

Discussion

Typically, Bland-Altman method is used to compare the accuracy and agreement between two measurement methods [112], [113], [114]. In our case, we investigated the correlation between our method and standard hospital method. It is important to note that, our measurements were taken with whole blood samples while hospital measurements followed standard protocol of plasma separation with Sysmex CN6000 device. In a similar study conducted with ICU patients, the Bland – Altman method revealed inadequate overall agreement. The widest 95% limits of agreement were -27.266 to 64.791 and the highest mean percentage bias (24%) were observed comparing PoC aPTT

using citrated blood to laboratory aPTT. On the other hand, when comparing PoC aPTT results of less than 90 seconds using whole blood to laboratory aPTT results, the limits of agreement narrowed to the range of -23.243 to 28.419, and the mean percentage bias decreased to 5%. The agreement between clinical decisions on heparin dosage based on the two methods was poor for plain and citrated blood. Which in the end making PoC aPTT results insufficiently accurate for patients on heparin infusion compared to laboratory aPTT assay [115]. In a similar study that included a total of 286 pairs of aPTT results from 63 patients a weak correlation between PoC-aPTT and LAB-aPTT ($r = 0.385$, $P < 0.001$) was observed. The overall difference (bias) between PoC-aPTT and LAB-aPTT was 7.78 seconds [95%CI (−32.49, 48.05)]. Similarly, the overall bias between PoC-aPTT and LAB-aPTT ratio (to normal value) was 0.54 [95%CI (−0.68, 1.76)]. In that study, a higher plasma fibrinogen level was associated with a higher likelihood of PoC-aPTT underestimating LAB-aPTT [OR 1.353 (1.057, 1.733), $P = 0.017$]. Conversely, a lower plasma fibrinogen level [OR 0.809 (0.679, 0.963), $P = 0.017$] and a lower UFH rate [OR 0.928 (0.868, 0.992), $P = 0.029$] were associated with a higher probability of PoC-aPTT overestimating LAB-aPTT [116].

Our findings indicate notable disparities between our proposed method and the standard hospital approach when assessed through the Bland-Altman analysis. For the difference versus average Bland-Altman comparison, we observed a bias of 14.93 with a standard deviation of bias at 10.40, and 95% Limits of Agreement ranging from -5.440 to 35.31. Similarly, examining the ratio versus average Bland-Altman analysis revealed a bias of 1.545 with a standard deviation of bias at 0.2847, and 95% Limits of Agreement ranging from 0.9866 to 2.102 (Figure 42). Here, it is important to note that, our device is not calibrated for its final measurement parameters, meaning that with further assays and measurements, it is possible and most likely that there will be a “correction factor” defined in order to make our measurement comparable and compatible with standard hospital measurement method.

While there are still some perquisites to complete all these steps, in next step we showed the compatibility between two devices by using calibration plasmas. These experiments were conducted in accordance with the hospital equipment as well, where we compared PT values by using both devices and two different brands of PT reagents. The correlation analyses conducted between the hospital method and two different reagents, Innovin Reagent and Recombiplastin 2G Reagent, utilized in our method

yielded compelling results. For the comparison between the hospital method and Innovin Reagent, Pearson's correlation coefficient (r) was defined to be 0.9629, with a 95% confidence interval ranging from 0.8694 to 0.9898. The coefficient of determination (R^2) was calculated as 0.9271. Indicating that when the same reagent is used with the same plasma types, there is a highly accurate correlation between devices. Similarly, for the comparison between the hospital device with Innovin reagent and our device with Recombiplastin 2G Reagent, the Pearson's correlation coefficient (r) was even higher at 0.9889, with a 95% confidence interval ranging from 0.9595 to 0.9970. The coefficient of determination (R^2) was notably high at 0.9779. However, there is a clear difference between two lines shown on the graph given in Figure 43, which indicates an offset between two measurements conducted with two different reagents, addressing the difference between the type of the reagent used.

Conclusion

In summary, our study showed notable disparities between our proposed method and the standard hospital method to assess aPTT value. We observed a bias of 14.93 with a standard deviation of bias at 10.40 in the difference versus average comparison and a bias of 1.545 with a standard deviation of bias at 0.2847 in the ratio versus average comparison. The 95% Limits of Agreement ranged from -5.440 to 35.31 and from 0.9866 to 2.102 respectively. These findings underscore the importance of further refining and calibrating our device to align its measurements more closely with the standard hospital method. Additionally, our experiments with calibration plasmas demonstrated promising compatibility between our device and the hospital equipment, mainly when using the same reagents. The differences observed between measurements conducted with different reagents emphasize the necessity for standardization and calibration to provide the clinical utility of our proposed method for measuring aPTT.

Chapter 4:
CONCLUSION

While clinics perform coagulation measurements using large volumes of blood and plasma, PoC devices offer measurements from low volumes without plasma separation, offering a device for the PoC measurement of PT/INR and aPTT comes with advantages. This provides rapid and accurate detection of vitals, ranging from routine measurements to crucial emergency cases. The device offered in the scope of this thesis calculates the PT by measuring a cantilever oscillation change inside a cartridge in which a sample of whole blood is applied. The measurement data of the device helps patients monitor blood coagulation levels and helps with consultations with physicians regarding the appropriate amount of medication. Its direct measurement principle based upon variation of viscoelasticity makes it more advantageous to other commercial and electrochemical-based PoC coagulometers as measurements are not affected by chemical interactions and other factors. The system, in the first step, measures the resonance frequency of the empty cartridge as a quality control. A second measurement of the resonance frequency is done directly after cartridge insertion with blood. Once blood is applied to the inlet, it flows into a measurement chamber that contains a dried PT reagent, where the frequency is used to drive the magnetic field via a coil that actuates the resonating fiber. The coagulation of the blood will change the amplitude and frequency of the vibrating fiber over time, and this change is used to calculate the PT and aPTT.

On the other hand, there are several challenges in designing and developing such a device. There has been a reduction in the system dimensions due to optimization of capillary flow requirements in our microfluidic system, aiming for a rapid flow of less than 10 seconds and a blood sample volume of 15 µl. Notably, the reaction chamber, where the reagent is dried, has undergone substantial narrowing in both width and depth compared to the first design of the sealed cartridge. This reduction has resulted in a decreased distance between the bottom of the chamber and the optical fiber. This reduction in space has created challenges in loading the reagent into the chamber. The dynamics of the drying process have complicated matters as well by causing the semi-vacuum-dried reagent to adhere to the fiber, hindering its free motion within the chamber. This challenge has been manually handled by removing the residue from the proximity of the resonating fiber after the application of microfluidic substance -DOS. The reason

for such application order lies within the nature of the DOS; since the application of it causes a moister and more dissolved situation for the dried reagent, cleaning the residues beforehand is not preferred. Because the sticky and rigid form of the reagent partly dissolves after the DOS application. However, this dissolution is not adequate to remove this reagent from the proximity of the fiber. So, removing this reagent after the DOS application enables the removal of less active reagents, providing more room for reagents to work. To address these challenges, it is important to acknowledge that the revised system, with a narrower and shallower reaction chamber, demands a careful reassessment of the loading and drying processes.

Besides, the challenges posed by the 1 mm cartridge were largely addressed in the redesigned 1.5- and 2-mm cartridges. Although the reagent sticking issue was resolved, the 2 mm cartridge necessitated a higher blood volume, posing difficulties for commercialization due to the challenge of obtaining sufficient blood from a single finger prick. Despite obtaining 15-25 μL of blood, this may not be universally applicable. Additionally, the larger chamber in the 2 mm cartridge resulted in slower filling compared to smaller volumes, impacting the efficiency of capillary flow. Given these challenges, the 1.5 mm cartridge design appears to be a more viable option for further R&D tests and eventual commercialization.

Additionally, covering the 'dried' reagent with a hydrophilic substance while aiming fast capillary flow introduces a possible concern about its impact on the reagent morphology and functionality too. This dual consideration—loading challenges and the influence of the hydrophilic substance on reagent characteristics—requires a thorough examination to provide the optimal performance and reliability for the microfluidic system. Adjustments in the loading technique, drying dynamics, and the choice of the hydrophilic substance may be critical to overcome these matters and maintain the functionality of the reagent in the altered microfluidic environment.

The initial in-house cartridge biochemical assembly process focused on PT reagent preparation and hydrophilization procedures. Challenges arose with reagent stickiness and heterogeneous dispersion, impacting the intended functionality of the cartridges. The methodology involved lyophilization as an alternative to vacuum drying, which initially showed promising results in terms of preventing stickiness. However, inconsistencies emerged, and the difficulties were attributed to changes in microfluidic system dimensions, particularly in the reaction chamber.

Several potential solutions have been identified to address the challenges arising from the modified microfluidic system. One option was to consider utilizing the lyophilization process instead of vacuum drying during reagent preparation, which offered improved loading dynamics and prevent the reagent from adhering to the optical fiber. Another approach involved adjusting the formulation of the reagent, potentially excluding mannitol, and simultaneously modifying the volume and dose. The positioning of the reagent within the microfluidic system was also reconsidered, either by altering its location within the channel or relocating it to a different section. Additionally, exploring the optimization of hydrophilic functionalization through wet chemistry techniques contributed to enhancing capillary flow while maintaining the integrity of the reagent. Lastly, placing the optical fiber after the surface functionalization and reagent drying process |was considered to mitigate issues associated with reagent adherence, allowing for improved movement within the reaction chamber.

The transition from the initial PT reagent preparation to recent lyophilization trials showcased advancements in the methodology. The freeze-drying process offered benefits such as uniform drying, improved reagent characteristics, and enhanced capillary flow. The use of DOS in ethanol for hydrophilization and the introduction of lyophilized beads demonstrated a more intricate approach to optimizing reagent functionality. Despite these improvements, challenges persist. Lyophilized beads exhibited delayed dissolution in blood, impacting coagulation times. Shelf-life optimization remains a concern, with cartridges losing functionality after 24 hours. The microfluidic system's reduced dimensions continue to pose challenges in loading the reagent and maintaining consistent results.

Each of these solutions represents a potential solution for identified challenges, and evaluation of these options is crucial to determine the most effective approach for the specific requirements of the microfluidic system.

The proof-of-concept study conducted with healthy donor plasma and blood samples produced well-defined dose-response curves for each subject. These experiments spanned over a couple of months, with blood samples donated at different time intervals by the same individuals identified as Subjects 1, 2, and 3. In the plasma tests, we aliquoted healthy donor plasma and stored it at -80°C throughout the experimental period. The blood samples, collected from the same individuals, were used within 24 hours, with the majority of experiments completed within 4 hours of collection. To replicate

physiological conditions, blood samples were stored at 4°C in a cold room on a roller device to simulate movement within veins. Uniform spiking was achieved by using an equal volume of PBS + drug concentration, ensuring an equivalent blood vs PBS ratio in all experiments. Outliers were retained in the collected data, acknowledging potential variations caused by human error and adherence to the experimental protocol. It is worth noting that minor differences were observed between the healthy subjects, emphasizing the importance of individual variability in response to anticoagulant treatments.

In the pilot study, we showed that a data analysis was conducted with 42 different measurements of patients in the ICU. In comparing Bland-Altman analyses, our study reveals notable disparities between our proposed method and the standard hospital approach. When examining the difference versus average Bland-Altman comparison, we observed a bias of 14.93 with a standard deviation of bias at 10.40 and 95% Limits of Agreement ranging from -5.440 to 35.31. Similarly, the ratio versus average Bland-Altman analysis displayed a bias of 1.545 with a standard deviation of bias at 0.2847 and 95% Limits of Agreement ranging from 0.9866 to 2.102. These results emphasize the differences in measurement outcomes between our device and the standard hospital method. While the bias and limits of agreement vary, indicating discrepancies in accuracy and agreement, it is the correlation factor turned out to be r=0.81 with a 95% confidence interval ranging from 0.6731 to 0.8945, indicating a high correlation between two measurement methods. It is important to note that our device is not yet fully calibrated for its final measurement parameters. This suggests that with further refinement and calibration, our device has the potential to align more closely with the standard hospital method, thereby enhancing its utility and reliability in clinical practice.

Acknowledging that most PT and aPTT tests were conducted using plasma, the consistency of time point data between blood and plasma samples in our results underscores the potential for the PoC coagulometer. This alignment in results indicates the viability of using whole blood samples in a PoC setting, highlighting the device's potential for accurate and remote monitoring of coagulation parameters, thereby contributing to the advancement of telemedicine applications. On the other hand, despite the advantages of PoC devices, the challenge of translating research into market-ready solutions for global health is recognized in scientific and business circles. The transition from lab prototypes to market products requires years, substantial technical efforts, and significant investments. Collaborative efforts among scientists in disciplines like

chemistry, biochemistry, optics, and engineering, alongside healthcare professionals, are crucial from the device's conception to prevent the development of impractical solutions for clinical settings.

BIBLIOGRAPHY

[1] L. Asarian, V. Gloy, and N. Geary, “Homeostasis,” *Encyclopedia of Human Behavior: Second Edition*, pp. 324–333, Jan. 2012, doi: 10.1016/B978-0-12-375000-6.00191-9.

[2] N. López-Santago, “Coagulation Tests,” *Acta Pediatrica de Mexico*, vol. 37, no. 4, pp. 241–245, 1990, doi: 10.18233/apm37no4pp241-245.

[3] W. Barmore, T. Bajwa, and B. Burns, “Biochemistry, Clotting Factors,” *StatPearls*, Feb. 2023, Accessed: Dec. 14, 2023. [Online]. Available: https://www.ncbi.nlm.nih.gov/books/NBK507850/

[4] V. Nguyen, “Microfluidic Paper Analytic Device for Assessment of Blood Coagulation Item Type text; Electronic Thesis,” 2017. [Online]. Available: http://hdl.handle.net/10150/624139

[5] D. Gailani and T. Renné, “Intrinsic Pathway of Coagulation and Arterial Thrombosis,” *Arterioscler Thromb Vasc Biol*, vol. 27, no. 12, pp. 2507–2513, Dec. 2007, doi: 10.1161/ATVBAHA.107.155952.

[6] S. Robertson and M. R. Miller, “Ambient air pollution and thrombosis,” *Particle and Fibre Toxicology 2018 15:1*, vol. 15, no. 1, pp. 1–16, Jan. 2018, doi: 10.1186/S12989-017-0237-X.

[7] N. López-Santago, “Coagulation Tests,” *Acta Pediatrica de Mexico*, vol. 37, no. 4, pp. 241–245, 1990, doi: 10.18233/apm37no4pp241-245.

[8] R. C. Gosselin *et al.*, “International Council for Standardization in Haematology (ICSH) Recommendations for Laboratory Measurement of Direct Oral Anticoagulants,” *Thromb Haemost*, vol. 118, no. 03, pp. 437–450, Mar. 2018, doi: 10.1055/S-0038-1627480.

[9] W. Yang, J. Ma, W. Hu, H. Dai, and H. Xu, “Associated factors and safety of the rapidly achieving first therapeutic target of warfarin in hospitalized patients: a retrospective cohort study,” *Int J Clin Pharm*, vol. 44, no. 4, pp. 939–946, Aug. 2022, doi: 10.1007/S11096-022-01404-9.

[10] L. C. Godoy *et al.*, “Association between time to therapeutic INR and length of stay following mechanical heart valve surgery,” *J Card Surg*, vol. 37, no. 1, pp. 62–69, Jan. 2022, doi: 10.1111/JOCS.16083.

[11] C. A. Balendran *et al.*, "Prothrombin time is predictive of low plasma prothrombin concentration and clinical outcome in patients with trauma hemorrhage: analyses of prospective observational cohort studies," *Scand J Trauma Resusc Emerg Med*, vol. 25, no. 1, Mar. 2017, doi: 10.1186/S13049-016-0332-2.

[12] B. C. Chinko and F. S. Amah-Tariah, "Haemostatic Effects of Ethanolic Extracts of Amaranthus hybridus on Wistar Rats," *International Blood Research &Amp; Reviews*, pp. 14–21, Apr. 2020, doi: 10.9734/IBRR/2020/V11I130121.

[13] Q. Lin, T. Li, S. J. Ding, Q. Yu, and X. Zhang, "Anemia-Associated Platelets and Plasma Prothrombin Time Increase in Patients with Adenomyosis," *J Clin Med*, vol. 11, no. 15, Aug. 2022, doi: 10.3390/JCM11154382.

[14] H. S. Wang, X. X. Ge, Q. P. Li, J. J. Nie, and L. Miao, "Clinical Significance of Prothrombin Time in Cholangiocarcinoma Patients with Surgeries," *Can J Gastroenterol Hepatol*, vol. 2019, 2019, doi: 10.1155/2019/3413969.

[15] M. Xia *et al.*, "Coagulation parameters are associated with the prognosis of immunoglobulin A nephropathy: a retrospective study", doi: 10.21203/RS.3.RS-34312/V2.

[16] E. J. Favaloro, G. Kershaw, S. Mohammed, and G. Lippi, "How to Optimize Activated Partial Thromboplastin Time (APTT) Testing: Solutions to Establishing and Verifying Normal Reference Intervals and Assessing APTT Reagents for Sensitivity to Heparin, Lupus Anticoagulant, and Clotting Factors," *Semin Thromb Hemost*, vol. 45, no. 01, pp. 22–35, 2019, doi: 10.1055/S-0038-1677018.

[17] D. M. Funk, Clinical and Laboratory Standards Institute., and DIN/NAMed., *Procedures for validation of INR and local calibration of PT/INR systems : approved guideline*. Clinical Laboratory Standards Institute, 2005.

[18] "Guidelines for thromboplastins and plasma used to control oral anticoagulant therapy with vitamin K antagonists, Replacement of Annex 3 of WHO Technical Report Series, No. 889." Accessed: Dec. 14, 2023. [Online]. Available: https://cdn.who.int/media/docs/default-source/biologicals/blood-products/document-migration/trs_979_annex_6.pdf?sfvrsn=5c960b91_3

[19] M. L. Taylor, E. E. Thomas, C. L. Snoswell, A. C. Smith, and L. J. Caffery, "Does remote patient monitoring reduce acute care use? A systematic review," *BMJ Open*, vol. 11, no. 3, p. e040232, Mar. 2021, doi: 10.1136/BMJOPEN-2020-040232.

[20] B. M. C. Silva, J. J. P. C. Rodrigues, I. de la Torre Díez, M. López-Coronado, and K. Saleem, "Mobile-health: A review of current state in 2015," *J Biomed Inform*, vol. 56, pp. 265–272, Aug. 2015, doi: 10.1016/J.JBI.2015.06.003.

[21] S. Iyengar, "Mobile health (mHealth)," *Fundamentals of Telemedicine and Telehealth*, pp. 277–294, Jan. 2020, doi: 10.1016/B978-0-12-814309-4.00012-4.

[22] S. Kalasin and W. Surareungchai, "Challenges of Emerging Wearable Sensors for Remote Monitoring toward Telemedicine Healthcare," *Anal Chem*, vol. 95, no. 3, pp. 1773–1784, 2023, doi: 10.1021/ACS.ANALCHEM.2C02642/ASSET/IMAGES/LARGE/AC2C02642_0005.JPEG.

[23] A. Bertini *et al.*, "Impact of Remote Monitoring Technologies for Assisting Patients With Gestational Diabetes Mellitus: A Systematic Review," *Front Bioeng Biotechnol*, vol. 10, p. 819697, Mar. 2022, doi: 10.3389/FBIOE.2022.819697/BIBTEX.

[24] C. Costa *et al.*, "A Wearable Monitoring Device for COVID-19 Biometric Symptoms Detection," *IRBM*, vol. 44, no. 6, p. 100810, Dec. 2023, doi: 10.1016/J.IRBM.2023.100810.

[25] A. F. Al-Anazi *et al.*, "Home versus Clinic Blood Pressure Monitoring: Evaluating Applicability in Hypertension Management via Telemedicine," *Diagnostics 2023, Vol. 13, Page 2686*, vol. 13, no. 16, p. 2686, Aug. 2023, doi: 10.3390/DIAGNOSTICS13162686.

[26] A. L. Bleda *et al.*, "Enabling Heart Self-Monitoring for All and for AAL—Portable Device within a Complete Telemedicine System," *Sensors 2019, Vol. 19, Page 3969*, vol. 19, no. 18, p. 3969, Sep. 2019, doi: 10.3390/S19183969.

[27] M. Di Rienzo, G. Rizzo, Z. M. Işilay, and P. Lombardi, "SeisMote: A Multi-Sensor Wireless Platform for Cardiovascular Monitoring in Laboratory, Daily Life, and Telemedicine," *Sensors 2020, Vol. 20, Page 680*, vol. 20, no. 3, p. 680, Jan. 2020, doi: 10.3390/S20030680.

[28] C. M. Jackson and M. P. Esnouf, "Has the Time Arrived to Replace the Quick Prothrombin Time Test for Monitoring Oral Anticoagulant Therapy?," *Clin Chem*, vol. 51, no. 3, pp. 483–485, Mar. 2005, doi: 10.1373/CLINCHEM.2004.045393.

[29] M. J. Pioz *et al.*, “A review of Optical Point-of-Care devices to Estimate the Technology Transfer of These Cutting-Edge Technologies,” *Biosensors (Basel)*, vol. 12, no. 12, p. 1091, Dec. 2022, doi: 10.3390/BIOS12121091/S1.

[30] C. M. Curtis, G. J. Kost, R. F. Louie, R. J. Sonu, E. B. Ammirati, and S. L. Sumner, “Point-of-care hematology and coagulation testing in primary, rural emergency, and disaster care scenarios,” *Point Care*, vol. 11, no. 2, pp. 140–145, Jun. 2012, doi: 10.1097/POC.0B013E31825A9D3A.

[31] “Point of Care Coagulation Testing Devices Market Growth, 2028.” Accessed: Dec. 15, 2023. [Online]. Available: https://www.fortunebusinessinsights.com/industry-reports/point-of-care-coagulation-testing-devices-market-101235

[32] R. Zhang *et al.*, “Systematic review and meta-analysis of the prevalence of venous thromboembolic events in novel coronavirus disease-2019 patients,” *J Vasc Surg Venous Lymphat Disord*, vol. 9, no. 2, pp. 289-298.e5, Mar. 2021, doi: 10.1016/J.JVSV.2020.11.023.

[33] “Therapeutic Anticoagulation with Heparin in Critically Ill Patients with Covid-19,” *New England Journal of Medicine*, vol. 385, no. 9, pp. 777–789, Aug. 2021, doi: 10.1056/NEJMOA2103417.

[34] A. C. Spyropoulos *et al.*, “Scientific and Standardization Committee communication: Clinical guidance on the diagnosis, prevention, and treatment of venous thromboembolism in hospitalized patients with COVID-19,” *J Thromb Haemost*, vol. 18, no. 8, pp. 1859–1865, Aug. 2020, doi: 10.1111/JTH.14929.

[35] L. K. Moores *et al.*, “Prevention, Diagnosis, and Treatment of VTE in Patients With Coronavirus Disease 2019: CHEST Guideline and Expert Panel Report,” *Chest*, vol. 158, no. 3, pp. 1143–1163, Sep. 2020, doi: 10.1016/J.CHEST.2020.05.559.

[36] G. D. Barnes *et al.*, “Thromboembolism and anticoagulant therapy during the COVID-19 pandemic: interim clinical guidance from the anticoagulation forum.,” *J Thromb Thrombolysis*, vol. 50, no. 1, pp. 72–81, Jul. 2020, doi: 10.1007/S11239-020-02138-Z.

[37] X. Li, L. Li, Y. Shi, S. Yu, and X. Ma, “Different signaling pathways involved in the anti-inflammatory effects of unfractionated heparin on lipopolysaccharide-

stimulated human endothelial cells," *J Inflamm (Lond)*, vol. 17, no. 1, Feb. 2020, doi: 10.1186/S12950-020-0238-7.

[38] S. Mousavi, M. Moradi, T. Khorshidahmad, and M. Motamedi, "Anti-Inflammatory Effects of Heparin and Its Derivatives: A Systematic Review," *Adv Pharmacol Sci*, vol. 2015, 2015, doi: 10.1155/2015/507151.

[39] M. R. Garvin *et al.*, "A mechanistic model and therapeutic interventions for COVID-19 involving a RAS-mediated bradykinin storm," *Elife*, vol. 9, pp. 1–16, Jul. 2020, doi: 10.7554/ELIFE.59177.

[40] M. M. G. Mulder, I. Fawzy, and M. D. Lancé, "ECMO and anticoagulation: A comprehensive review," *Netherlands Journal of Critical Care*, vol. 26, no. 1, pp. 6–13, 2018, Accessed: Dec. 15, 2023. [Online]. Available: https://scholars.aku.edu/en/publications/ecmo-and-anticoagulation-a-comprehensive-review

[41] A. Protti, G. E. Iapichino, M. Di Nardo, M. Panigada, and L. Gattinoni, "Anticoagulation Management and Antithrombin Supplementation Practice during Veno-venous Extracorporeal Membrane Oxygenation: A Worldwide Survey," *Anesthesiology*, vol. 132, no. 3, pp. 562–570, 2020, doi: 10.1097/ALN.0000000000003044.

[42] J. R. Choi, "Development of Point-of-Care Biosensors for COVID-19," *Front Chem*, vol. 8, p. 556443, May 2020, doi: 10.3389/FCHEM.2020.00517/BIBTEX.

[43] C. T. Lin and S. M. Wang, "Biosensor commercialization strategy - A theoretical approach," *Frontiers in Bioscience*, vol. 10, no. 1, pp. 99–106, Jan. 2005, doi: 10.2741/1512/PDF.

[44] E. H. Yoo and S. Y. Lee, "Glucose Biosensors: An Overview of Use in Clinical Practice," *Sensors 2010, Vol. 10, Pages 4558-4576*, vol. 10, no. 5, pp. 4558–4576, May 2010, doi: 10.3390/S100504558.

[45] A. Villalonga, A. M. Pérez-Calabuig, and R. Villalonga, "Electrochemical biosensors based on nucleic acid aptamers," *Anal Bioanal Chem*, vol. 412, no. 1, pp. 55–72, Jan. 2020, doi: 10.1007/S00216-019-02226-X/FIGURES/18.

[46] L. F. Harris, V. Castro-López, and A. J. Killard, "Coagulation monitoring devices: Past, present, and future at the point of care," *TrAC - Trends in Analytical Chemistry*, vol. 50. Elsevier B.V., pp. 85–95, 2013. doi: 10.1016/j.trac.2013.05.009.

[47] N. N. Faber, S. C. Bulmer, M. A. Gandhi, and A. K. Nagel, "Point-of-care testing in hypercoagulable conditions managed with warfarin: A review," *Point Care*, vol. 19, no. 4, pp. 101–105, Dec. 2020, doi: 10.1097/POC.0000000000000215.

[48] J. Deng and X. Jiang, "Advances in Reagents Storage and Release in Self-Contained Point-of-Care Devices," *Adv Mater Technol*, vol. 4, no. 6, Jun. 2019, doi: 10.1002/ADMT.201800625.

[49] Y. Yaras *et al.*, "Disposable cartridge biosensor platform for portable diagnostics," *https://doi.org/10.1117/12.2254729*, vol. 10055, no. 3, pp. 71–80, Mar. 2017, doi: 10.1117/12.2254729.

[50] "A sensing device using fiber based cantilevers embedded in a cartridge," Sep. 2015.

[51] J. E. Sader, "Frequency response of cantilever beams immersed in viscous fluids with applications to the atomic force microscope," *J Appl Phys*, vol. 84, no. 1, pp. 64–76, Jul. 1998, doi: 10.1063/1.368002.

[52] J. E. Sader, J. W. M. Chon, and P. Mulvaney, "Calibration of rectangular atomic force microscope cantilevers," *Review of Scientific Instruments*, vol. 70, no. 10, pp. 3967–3969, Oct. 1999, doi: 10.1063/1.1150021.

[53] Y. S. Yaraş, "A Portable Blood Coagulation Time Measurement Platform with Fiber-Optic Based Disposable Cartridge," 2016.

[54] J. W. M. Chon, P. Mulvaney, and J. E. Sader, "Experimental validation of theoretical models for the frequency response of atomic force microscope cantilever beams immersed in fluids," *J Appl Phys*, vol. 87, no. 8, pp. 3978–3988, Apr. 2000, doi: 10.1063/1.372455.

[55] C. Wang, H. H. Yu, M. Wu, and W. Fang, "Implementation of phase-locked loop control for MEMS scanning mirror using DSP," *Sens Actuators A Phys*, vol. 133, no. 1, pp. 243–249, Jan. 2007, doi: 10.1016/J.SNA.2006.03.026.

[56] M. Kucera, T. Manzaneque, J. L. Sánchez-Rojas, A. Bittner, and U. Schmid, "Q-factor enhancement for self-actuated self-sensing piezoelectric MEMS resonators applying a lock-in driven feedback loop," *Journal of Micromechanics and Microengineering*, vol. 23, no. 8, p. 085009, Jun. 2013, doi: 10.1088/0960-1317/23/8/085009.

[57] "Glycerol 3 M 3M 56-81-5." Accessed: Feb. 09, 2024. [Online]. Available: https://www.sigmaaldrich.com/TR/en/product/sial/12146?utm_source=google&u

tm_medium=cpc&utm_campaign=8691857233&utm_content=95771709055&gclid=CjwKCAiAt5euBhB9EiwAdkXWO5-fvdlOAORFDCnm57ke8YooTgm2InC3ZFII7DQ98ox96aIgSfo8UxoC77UQAvD_BwE

[58] G. Kulsharova, A. Kurmangaliyeva, E. Darbayeva, L. Rojas-Solórzano, and G. Toxeitova, "Development of a Hybrid Polymer-Based Microfluidic Platform for Culturing Hepatocytes towards Liver-on-a-Chip Applications," *Polymers (Basel)*, vol. 13, no. 19, Oct. 2021, doi: 10.3390/POLYM13193215.

[59] B. Guan, J. H. Pai, M. Cherrill, B. Michalatos, and C. Priest, "Injection moulding of micropillar arrays: a comparison of poly(methyl methacrylate) and cyclic olefin copolymer," *Microsystem Technologies*, 2022, doi: 10.1007/S00542-022-05350-4.

[60] N. Keller *et al.*, "Tacky cyclic olefin copolymer: A biocompatible bonding technique for the fabrication of microfluidic channels in COC," *Lab Chip*, vol. 16, no. 9, pp. 1561–1564, 2016, doi: 10.1039/C5LC01498K.

[61] R. R. Carvalho, S. P. Pujari, E. X. Vrouwe, and H. Zuilhof, "Mild and Selective C-H Activation of COC Microfluidic Channels Allowing Covalent Multifunctional Coatings," *ACS Appl Mater Interfaces*, vol. 9, no. 19, pp. 16644–16650, May 2017, doi: 10.1021/ACSAMI.7B02022.

[62] S. Bourg *et al.*, "Surface functionalization of cyclic olefin copolymer by plasma-enhanced chemical vapor deposition using atmospheric pressure plasma jet for microfluidic applications," *Plasma Processes and Polymers*, vol. 16, no. 6, Jun. 2019, doi: 10.1002/PPAP.201800195.

[63] "Dioctyl sulfosuccinate = 97 577-11-7." Accessed: Feb. 09, 2024. [Online]. Available: https://www.sigmaaldrich.com/TR/en/product/aldrich/323586

[64] J. M. Wambua, F. M. Mwema, B. Tanya, and T. C. Jen, "CNC Milling of Medical-Grade PMMA: Optimization of Material Removal Rate and Surface Roughness," *https://services.igi-global.com/resolvedoi/resolve.aspx?doi=10.4018/IJMMME.293226*, vol. 12, no. 1, pp. 1–15, Jan. 1AD, doi: 10.4018/IJMMME.293226.

[65] J. H. Shin and S. Choi, "Open-source and do-it-yourself microfluidics," *Sens Actuators B Chem*, vol. 347, p. 130624, Nov. 2021, doi: 10.1016/J.SNB.2021.130624.

[66] "MINIATURIZED INTEGRATED MICRO ELECTO-MECHANICAL SYSTEMS (MEMS) OPTICAL SENSOR ARRAY FOR VISCOSITY AND MASS DETECTION," 2013.

[67] V. Gubala, L. F. Harris, A. J. Ricco, M. X. Tan, and D. E. Williams, "Point of care diagnostics: Status and future," *Anal Chem*, vol. 84, no. 2, pp. 487–515, Jan. 2012, doi: 10.1021/AC2030199.

[68] M. J. Sadler, S. Gibson, K. Whelan, M. A. Ha, J. Lovegrove, and J. Higgs, "Dried fruit and public health–what does the evidence tell us?," *Int J Food Sci Nutr*, vol. 70, no. 6, pp. 675–687, Aug. 2019, doi: 10.1080/09637486.2019.1568398.

[69] N. Vassilev *et al.*, "Formulation of Microbial Inoculants by Encapsulation in Natural Polysaccharides: Focus on Beneficial Properties of Carrier Additives and Derivatives," *Front Plant Sci*, vol. 11, Mar. 2020, doi: 10.3389/FPLS.2020.00270.

[70] S. Migliozzi, P. Angeli, and L. Mazzei, "Effect of D-Mannitol on the Microstructure and Rheology of Non-Aqueous Carbopol Microgels," *Materials*, vol. 14, no. 7, Apr. 2021, doi: 10.3390/MA14071782.

[71] C. Zhang *et al.*, "A combination of evaporation and chemical preservation for long-term storage of fresh sweet sorghum juice and subsequent bioethanol production," *J Food Process Preserv*, vol. 42, no. 12, Dec. 2018, doi: 10.1111/JFPP.13825.

[72] V. Bampidis *et al.*, "Safety of Lactococcus lactis NCIMB 30160 as a feed additive for all animal species," *EFSA Journal*, vol. 17, no. 11, Nov. 2019, doi: 10.2903/J.EFSA.2019.5890.

[73] T. Ojha *et al.*, "Shelf-Life Evaluation and Lyophilization of PBCA-Based Polymeric Microbubbles," *Pharmaceutics*, vol. 11, no. 9, Sep. 2019, doi: 10.3390/PHARMACEUTICS11090433.

[74] P. Zhang, R. Zou, S. Wu, L. A. Meyer, J. Wang, and T. Kraus, "Gold Nanoprobes Exploring the Ice Structure in the Aqueous Dispersion of Poly(Ethylene Glycol)–Gold Hybrid Nanoparticles," *Langmuir*, vol. 38, no. 8, pp. 2460–2466, Mar. 2022, doi: 10.1021/ACS.LANGMUIR.1C02783.

[75] M. Patel, J. K. Park, and B. Jeong, "Rediscovery of poly(ethylene glycol)s as a cryoprotectant for mesenchymal stem cells," *Biomater Res*, vol. 27, no. 1, Dec. 2023, doi: 10.1186/S40824-023-00356-Z.

[76] M. C. Manning, K. Patel, and R. T. Borchardt, "Stability of Protein Pharmaceuticals," *Pharmaceutical Research: An Official Journal of the American*

Association of Pharmaceutical Scientists, vol. 6, no. 11, pp. 903–918, 1989, doi: 10.1023/A:1015929109894/METRICS.

[77] L. Kreilgaard, S. Frokjaer, J. M. Flink, T. W. Randolph, and J. F. Carpenter, "Effects of additives on the stability of Humicola lanuginosa lipase during freeze-drying and storage in the dried solid," *J Pharm Sci*, vol. 88, no. 3, pp. 281–290, 1999, doi: 10.1021/JS980399D.

[78] S. Passot, F. Fonseca, M. Alarcon-Lorca, D. Rolland, and M. Le Marin, "Physical characterisation of formulations for the development of two stable freeze-dried proteins during both dried and liquid storage," 2005, doi: 10.1016/j.ejpb.2005.02.013.

[79] J. M. Bravo-Arredondo *et al.*, "The folding equilibrium of huntingtin exon 1 monomer depends on its polyglutamine tract," *Journal of Biological Chemistry*, vol. 293, no. 51, pp. 19613–19623, Dec. 2018, doi: 10.1074/JBC.RA118.004808.

[80] Z. Hu, C. Ma, X. Rong, S. Zou, and X. Liu, "Immunomodulatory ECM-like Microspheres for Accelerated Bone Regeneration in Diabetes Mellitus," *ACS Applied Materials &Amp; Interfaces*, vol. 10, no. 3, pp. 2377–2390, Jan. 2018, doi: 10.1021/ACSAMI.7B18458.

[81] S. Das, A. De, B. Das, B. Mukherjee, and A. Samanta, "Development of gum odina-gelatin based antimicrobial loaded biodegradable spongy scaffold: A promising wound care tool," *J Appl Polym Sci*, vol. 138, no. 12, Mar. 2021, doi: 10.1002/APP.50057.

[82] R. Venkata Kavya and B. Jeevana Jyothi, "Central Composite Face-Centered Design-Based Optimisation, Development and Characterisation of Favipiravir-Loaded Plga Nanoparticles," *International Journal of Applied Pharmaceutics*, vol. 15, no. 1, pp. 234–249, Jan. 2023, doi: 10.22159/IJAP.2023V15I1.46289.

[83] S. D. Tayade, N. Silawat, and N. K. Jain, "Formulation Development and Evaluation of Herbal Nanoparticles containing Ointment of Leaves extract of Rhynchosia rothii," *J Pharm Negat Results*, pp. 724–738, Oct. 2022, doi: 10.47750/PNR.2022.13.S05.113.

[84] "PHARMACEUTICAL APPLICATIONS OF LYOPHILIZATION: RECENT UPDATES AND ADVANCEMENTS | INTERNATIONAL JOURNAL OF PHARMACEUTICAL SCIENCES AND RESEARCH." Accessed: Jan. 23, 2024.

[Online]. Available: https://ijpsr.com/bft-article/pharmaceutical-applications-of-lyophilization-recent-updates-and-advancements/?view=fulltext

[85] M. P. Hall *et al.*, "Toward a Point-of-Need Bioluminescence-Based Immunoassay Utilizing a Complete Shelf-Stable Reagent," *Anal Chem*, vol. 93, no. 12, pp. 5177–5184, Mar. 2021, doi: 10.1021/ACS.ANALCHEM.0C05074/ASSET/IMAGES/LARGE/AC0C05074_0008.JPEG.

[86] C. Carter, K. Akrami, D. Hall, D. Smith, and E. Aronoff-Spencer, "Lyophilized visually readable loop-mediated isothermal reverse transcriptase nucleic acid amplification test for detection Ebola Zaire RNA," *J Virol Methods*, vol. 244, pp. 32–38, Jun. 2017, doi: 10.1016/J.JVIROMET.2017.02.013.

[87] L. Thirion *et al.*, "Lyophilized Matrix Containing Ready-to-Use Primers and Probe Solution for Standardization of Real-Time PCR and RT-qPCR Diagnostics in Virology," *Viruses*, vol. 12, no. 2, 2020, doi: 10.3390/V12020159.

[88] J. P. Hunt, S. O. Yang, K. M. Wilding, and B. C. Bundy, "The growing impact of lyophilized cell-free protein expression systems," *Bioengineered*, vol. 8, no. 4, pp. 325–330, Jul. 2017, doi: 10.1080/21655979.2016.1241925.

[89] B. S. Moorthy *et al.*, "Solid-State Hydrogen–Deuterium Exchange Mass Spectrometry: Correlation of Deuterium Uptake and Long-Term Stability of Lyophilized Monoclonal Antibody Formulations," *Mol Pharm*, vol. 15, no. 1, pp. 1–11, Jan. 2018, doi: 10.1021/ACS.MOLPHARMACEUT.7B00504.

[90] E. A. Pumford *et al.*, "Developments in integrating nucleic acid isothermal amplification and detection systems for point-of-care diagnostics," *Biosens Bioelectron*, vol. 170, Dec. 2020, doi: 10.1016/J.BIOS.2020.112674.

[91] M. ; Benjamin *et al.*, "Stabilization of Tuberculosis Reporter Enzyme Fluorescence (REFtb) Diagnostic Reagents for Use at the Point of Care," *Diagnostics 2022, Vol. 12, Page 1745*, vol. 12, no. 7, p. 1745, Jul. 2022, doi: 10.3390/DIAGNOSTICS12071745.

[92] Q. Q. Meng, J. X. Wang, G. H. Ma, and Z. G. Su, "Lyophilization of CNBr-activated agarose beads with lactose and PEG," *Process Biochemistry*, vol. 44, no. 5, pp. 562–571, May 2009, doi: 10.1016/J.PROCBIO.2009.01.013.

[93] D. Dianawati, V. Mishra, and N. P. Shaha, "Role of calcium alginate and mannitol in protecting Bifidobacterium," *Appl Environ Microbiol*, vol. 78, no. 19, pp. 6914–

6921, Oct. 2012, doi: 10.1128/AEM.01724-12/ASSET/3E775E8A-3D2D-45C0-A521-7F8372160895/ASSETS/GRAPHIC/ZAM9991037130002.JPEG.

[94] C. Y. Wong, H. Al-Salami, and C. R. Dass, "Lyophilisation Improves Bioactivity and Stability of Insulin-Loaded Polymeric-Oligonucleotide Nanoparticles for Diabetes Treatment," *AAPS PharmSciTech*, vol. 21, no. 3, pp. 1–20, Apr. 2020, doi: 10.1208/S12249-020-01648-6/FIGURES/5.

[95] S. Ramachandran, E. Fu, B. Lutz, and P. Yager, "Long-term dry storage of an enzyme-based reagent system for ELISA in point-of-care devices †," 2014, doi: 10.1039/c3an02296j.

[96] W. Wang, "Lyophilization and development of solid protein pharmaceuticals," *Int J Pharm*, vol. 203, no. 1–2, pp. 1–60, Aug. 2000, doi: 10.1016/S0378-5173(00)00423-3.

[97] M. Alfatama, L. Y. Lim, and T. W. Wong, "Alginate-C18 Conjugate Nanoparticles Loaded in Tripolyphosphate-Cross-Linked Chitosan-Oleic Acid Conjugate-Coated Calcium Alginate Beads as Oral Insulin Carrier," *Mol Pharm*, vol. 15, no. 8, pp. 3369–3382, Aug. 2018, doi: 10.1021/ACS.MOLPHARMACEUT.8B00391/ASSET/IMAGES/LARGE/MP-2018-00391B_0008.JPEG.

[98] Jonsman Innovation ApS, "Processing guidelines Surface preparation- P100 Hydrophilic coating." [Online]. Available: www.joninn.com

[99] F. Dal Dosso, L. Tripodi, D. Spasic, T. Kokalj, and J. Lammertyn, "Innovative Hydrophobic Valve Allows Complex Liquid Manipulations in a Self-Powered Channel-Based Microfluidic Device," *ACS Sens*, vol. 4, no. 3, pp. 694–703, Mar. 2019, doi: 10.1021/ACSSENSORS.8B01555.

[100] M. M. Dudek, L. F. Harris, and A. J. Killard, "Evaluation of activated partial thromboplastin time (aPTT) reagents for application in biomedical diagnostic device development," *Int J Lab Hematol*, vol. 33, no. 3, pp. 272–280, 2011, doi: 10.1111/j.1751-553X.2010.01283.x.

[101] E. Engineering, "A Portable Blood Coagulation Time Measurement Platform with Fiber-Optic Based Disposable Cartridge," no. June, 2016.

[102] E. J. Favaloro, G. Kershaw, S. Mohammed, and G. Lippi, "How to Optimize Activated Partial Thromboplastin Time (APTT) Testing: Solutions to Establishing and Verifying Normal Reference Intervals and Assessing APTT Reagents for

Sensitivity to Heparin, Lupus Anticoagulant, and Clotting Factors," *Semin Thromb Hemost*, vol. 45, no. 1, pp. 22–35, 2019, doi: 10.1055/s-0038-1677018.

[103] M. A. Laffan and R. A. Manning, "Investigation of Haemostasis 18 CHAPTER OUTLINE."

[104] "Plasma and Serum Preparation | Thermo Fisher Scientific - TR." Accessed: Nov. 29, 2023. [Online]. Available: https://www.thermofisher.com/tr/en/home/references/protocols/cell-and-tissue-analysis/elisa-protocol/elisa-sample-preparation-protocols/plasma-and-serum-preparation.html#prot4

[105] "SynthASil-0020006800." Accessed: Mar. 20, 2024. [Online]. Available: http://lexdms.werfengroup.com:1090/contentserver/contentserver.dll?get&pVersion=0046&contRep=ZDMS_LEX_01&docId=50B4F402EF8C0312E1008000C0080107&compId=303195.pdf

[106] "Dade® Innovin®", Accessed: Mar. 05, 2024. [Online]. Available: https://ec.europa.eu/tools/eudamed

[107] A. Fsl, "11528778_en Rev. 11-Outside USA", Accessed: Mar. 05, 2024. [Online]. Available: https://ec.europa.eu/tools/eudamed

[108] "HemosIL® Reagents | Werfen North America." Accessed: Mar. 05, 2024. [Online]. Available: https://www.werfen.com/na/en/hemostasis/hemosil-reagents

[109] *Point-of-Care Coagulation Testing and Anticoagulation Monitoring*. [Online]. Available: www.clsi.org.

[110] A. González-Zamora *et al.*, "Measurement of capsaicinoids in chiltepin hot pepper: A comparison study between spectrophotometric method and high performance liquid chromatography analysis," *J Chem*, vol. 2015, Jan. 2015, doi: 10.1155/2015/709150.

[111] M. Flick *et al.*, "Non-invasive measurement of pulse pressure variation using a finger-cuff method (CNAP system): a validation study in patients having neurosurgery," *J Clin Monit Comput*, vol. 36, no. 2, pp. 429–436, Apr. 2022, doi: 10.1007/S10877-021-00669-1.

[112] A. Kothari, S. Noor, C. L. Maddock, J. H. H. Vanderstappen, C. S. Bradley, and S. P. Kelley, "The lateral edge and sourcil acetabular indices for surgical decision-making in developmental dysplasia of the hip," *J Child Orthop*, vol. 14, no. 6, pp. 508–512, 2020, doi: 10.1302/1863-2548.14.200199.

[113] E. Tipton and J. Shuster, “A framework for the meta-analysis of Bland–Altman studies based on a limits of agreement approach,” *Stat Med*, vol. 36, no. 23, pp. 3621–3635, Oct. 2017, doi: 10.1002/SIM.7352.

[114] J. M. Bland and D. G. Altman, “Measuring agreement in method comparison studies,” *Stat Methods Med Res*, vol. 8, no. 2, pp. 135–160, 1999, doi: 10.1191/096228099673819272.

[115] L. Karigowda, K. Deshpande, S. Jones, and J. Miller, “The accuracy of a point of care measurement of activated partial thromboplastin time in intensive care patients,” *Pathology*, vol. 51, no. 6, pp. 628–633, Oct. 2019, doi: 10.1016/J.PATHOL.2019.05.002.

[116] Y. Teng, S. Yan, G. Liu, S. Lou, Y. Zhang, and B. Ji, “An Agreement Study Between Point-of-Care and Laboratory Activated Partial Thromboplastin Time for Anticoagulation Monitoring During Extracorporeal Membrane Oxygenation,” *Front Med (Lausanne)*, vol. 9, p. 931863, Jun. 2022, doi: 10.3389/FMED.2022.931863/BIBTEX.